

85239

**Polypropylene - Natural Zeolite Composite Films**

**By**  
**Filiz ÖZMIHÇI**

**A Dissertation Submitted to the  
Graduate School in Partial Fulfillment of the  
Requirements for the Degree of**

**MASTER OF SCIENCE**

**Department: Materials Science and Engineering**

**Major: Material Science and Engineering**

**Izmir Institute of Technology**

**Izmir, Turkey**

**September, 1999**

85239

**TC. YÜKSEKÖĞRETİM KURULU  
DOKÜMANTASYON MERKEZİ**

We approve the thesis of Filiz ÖZMIHÇI

**Date of Signature**

.....*D. Balköse*.....

**29.09.99**

**Prof. Dr. Devrim BALKÖSE**

Supervisor

Ege University, Department of Chemical Engineering

.....*Funda*.....

**29.09.99**

**Assist. Prof. Dr. Funda TIHMINLIOĞLU**

Department of Chemical Engineering

.....*Sacide*.....

**29.09.99**

**Assist. Prof. Dr. Sacide ALSOY**

Department of Chemical Engineering

.....*Muhsin Çiftçioğlu*.....

**29.09.99**

**Prof. Dr. Muhsin ÇİFTÇİOĞLU**

Head of Interdisciplinary

Material Science and Engineering Program

## ACKNOWLEDGEMENTS

I would like to thank and express my deepest gratitude to Prof. Dr. Devrim Balköse for her understanding, help, guidance and encouragement during this study and in the preparation of this thesis.

I also would like to thank Prof. Dr. Semra Ülkü, Prof. Dr. Muhsin Çiftçiođlu, and Assist. Prof. Dr. Funda Tıhmınlıođlu for their valuable comments and suggestions. I would like to thank to Cumhuriyet B y kakaıncı and  zlem Vatansever from Polinas for tensile tests and Rahim İřler, Ali  ziř, and Feridun řenol from Petkim A. ř. for performing the extrusion process.

Special thanks to Uđur  nal for help on computer problems and to research assistants for their friendship. I am indebted to Nilg n  zg l and řerife řahin for their help in the laboratory work.

Finally, I would like to thank my family for their help and support.

## ABSTRACT

In this project, preparation and characterization of polypropylene natural zeolite composites were studied. Three different series of preparation methods were performed, hot press, microscope slide, and extrusion. The composites are ranged between 0-10 wt%, 0-50 wt%, and 0-6 wt% zeolites, for hot press, microscope slide, and extrusion respectively.

Polymer matrix composites are materials which contain polymers as matrix materials surrounding very small reinforcing fibers or fillers. Polymeric composites have great potential from a manufacturing standpoint and show advantages. Such as they are inexpensive, derive from natural sources, present lower density than mineral fillers, and increases the mechanical properties of the final product.

In this research polypropylene was used as a matrix material and natural zeolite as a filler. Natural zeolite particles were modified with polyethylene glycol to break agglomerates and make a homogenous dispersion of natural zeolite in polypropylene matrix. These composites were characterized by using differential scanning calorimetry, thermal gravimetric analyzer, infrared spectrophotometer, optical microscopy, mechanical testing and by density measurement device.

It has been found that, branched shaped air pockets existed in hot pressed and extruded composites. This causes low mechanical strength, and the densities of these films also indicate the presence of voids in the composite.

## Öz

Bu projede, doğal zeolit - polipropilen kompozitlerinin hazırlanması ve karakterize edilmesi çalışılmıştır. Üç değişik metodla kompozit hazırlanmıştır; sıcak pres, mikroskop lamı, ve ekstrüzyon. Ağırlıkça ortalamaları sıcak preste % 0-10, mikroskop lamında % 0-50, ekstrüzyonda % 0-6 alınmıştır.

Anafazda polimer ve ikinci fazda liflerden yada katkı malzemelerinden oluşan malzemelere polimer matriks kompozitler denir. Malzemenin ucuz ve doğal kaynaklardan sağlanıyor olması, doğal katkı malzemelerinden daha düşük yoğunluğa sahip olması, ve nihai ürünün mekanik özelliklerini arttırıyor olması bu malzemelere olan ilgiyi giderek arttırmıştır.

Bu araştırmada polipropilen matriks, doğal zeolit ise katkı malzemesi olarak kullanılmıştır. Doğal zeolit parçacıkları, polietilen glikol ile topaklanmaları önlemek ve homojen bir dağılım sağlamak amacıyla kaplanmıştır. Hazırlanan kompozit malzemeler; termal analiz yöntemleri ve kızıl ötesi spektrometre, optik mikroskop, mekanik test ve yoğunluk ölçüm cihazı ile incelenmişlerdir.

Sonuç olarak; sıcak pres ve ekstrüzyon ile yapılmış filmlerde dallanmış hava kabarcıkları gözlenmiştir. Bu hava kabarcıkları malzemenin mekanik özelliklerini düşürmüştür. Aynı zamanda yoğunluk ölçüm sonuçlarında hava kabarcıklarının varlığını desteklemiştir.

# TABLE OF CONTENTS

LIST OF TABLES.....	VIII
LIST OF FIGURES .....	X
I. INTRODUCTION.....	1
II. POLYMER COMPOSITE MATERIAL.....	5
2.1 Polypropylene .....	6
2.1.1 Isotactic Polypropylene.....	7
2.1.2 Syndiotactic Polypropylene .....	8
2.1.3 Atactic Polypropylene.....	9
2.2 Natural Zeolite.....	10
III. SURFACE MODIFICATION OF NATURAL ZEOLITE .....	13
3.1 Coupling Agents.....	15
3.2 Dispersion Agents.....	17
IV. PREPARATION METHODS OF POLYMER COMPOSITES .....	18
4.1 Extrusion.....	18
4.2 Two-roll mill .....	20
4.3 Hot Press.....	22
4.4 Blender .....	22
V. MECHANISM OF PEARLESCENT FILM FORMATION .....	23
5.1 Stretching.....	23
5.2 Blowing .....	26
VI. CHARACTERIZATION OF MATERIALS .....	28
6.1 Characterization of Natural Zeolite .....	29
6.1.1 Characterization of Natural Zeolite by FTIR.....	29
6.1.2 Characterization of Natural Zeolite by TGA .....	31
6.2 Characterization of Polypropylene .....	31
6.2.1 Characterization of Polypropylene by FTIR Spectroscopy ..	31

6.2.2 Characterization of Polypropylene and Polypropylene composites by DSC.....	32
6.2.3 Characterization of Polypropylene by TGA .....	34
6.3 Polypropylene Composites Mechanical Behaviour .....	36
<b>VII. MATERIAL AND METHODS .....</b>	<b>38</b>
7.1 Characterization of Natural Zeolite .....	38
7.2 Polypropylene Characterization.....	38
7.3 Size Reduction ( Ball Milling ) .....	38
7.4 Fractionation of Zeolite Particles into Different Sizes .....	39
7.5 Modification of Zeolite Particles.....	40
7.6 Preparation of Zeolite-Polypropylene Composites.....	41
7.6.1 Pressing Between Microscope Slide.....	41
7.6.2 Pressing in Hot Press .....	41
7.6.3 Extrusion.....	42
7.7 Characterization of Composite Films.....	43
7.7.1 Optical Micrograph.....	43
7.7.2 Density Determination.....	43
7.7.3 Mechanical Test.....	43
<b>VIII. RESULTS AND DISCUSSION .....</b>	<b>45</b>
8.1 Characterization of Polypropylene, Natural Zeolite, Polypropylene- Natural zeolite Composite by FTIR Spectroscopy .....	47
8.1.1 Characterization of Natural zeolite by FTIR Spectroscopy.....	47
8.1.2 Characterization of Polypropylene by FTIR Spectroscopy .....	51
8.1.3 FTIR Spectrum of Polypropylene- Natural zeolite Composites Determination of Zeolite Content and Isotacticity Index.....	52
8.2 Selection of the Natural Zeolite and It's Modification for Composite Preparation .....	60

8.2.1 Selection of Natural Zeolite.....	61
8.2.2 Selection of Surface Modifier.....	62
8.2.3 Particle Size of Aldrich pp and Selection of Particle Size of Zeolite .....	63
8.2.3.1 Tensile Tested Extruded Films.....	66
8.3 Characterization of Polypropylene- Zeolite Composite by DSC.....	67
8.3.1 Characterization of Polypropylene by DSC.....	67
8.3.2 Characterization of Composite by Using DSC.....	69
8.4 Characterization of Polypropylene and Polypropylene - Zeolite Composites by TGA .....	79
8.4.1 Characterization of Polypropylene by TGA .....	79
8.4.2 Characterization of Polypropylene- Zeolite Composite by TGA.....	80
8.4.3 Kinetic Analysis of Polypropylene and Composite.....	85
8.5 Density Measurement .....	89
8.6 Mechanical Behaviour of the Composites.....	92
8.7 Comparison of Commercial Pearlescent Films and Zeolite Filled Films.....	100
CONCLUSIONS .....	102
REFERENCES .....	104



# LIST OF TABLES

Table 3.1 Additives and degree of hydrophobization of CaCO <sub>3</sub> .	14
Table 6.1 Characteristic Peaks of the Natural Zeolite.	30
Table 6.2 Characteristic Peaks of polypropylene.	31
Table 8.1 Natural zeolites and their physical properties.	45
Table 8.2 Effects of preparation techniques in polypropylene -zeolite composite.	46
Table 8.3 Intended and experimental weight fractions of extruded composites.	59
Table 8.4 Isotacticity values of polypropylene.	60
Table 8.5 Different heating rate for Petkim polypropylene.	69
Table 8.6 Gördes 1 filled polypropylene composites DSC analysis values.	70
Table 8.7 Different heating rate of DSC values for, 6% zeolite filled extruded polypropylene.	72
Table 8.8 Different heating rates for 10 % zeolite filled composites DSC values.	73
Table 8.9 1 <sup>st</sup> Melting and crystallization values of composites.	74
Table 8.10 2 <sup>nd</sup> Melting and crystallization values of composites.	76

Table 8.11 TGA values indicating weight loss %, and temperatures of 0-30 % zeolite filled microscope slide pressed composites.	80
Table 8.12 TGA values indicating weight loss %, and temperatures of 0-6 % zeolite filled extruded composites.	82
Table 8.13 Activation energy at different weight loss values and average activation energy.	86
Table 8.14 Kinetic analysis of materials.	88
Table 8.15 45 $\mu$ zeolite filled polypropylene films densities.	89
Table 8.16 2 $\mu$ zeolite filled polypropylene films densities.	90
Table 8.17 Hot pressed composites theoretical and experimental densities.	91
Table 8.18 Mechanical behaviour of hot pressed composites.	94
Table 8.19 Extruded films mechanical behaviour.	97
Table 8.20 Extruded films mechanical behaviour tested in Polinas.	98
Table 8.21 Predicted and measured elastic modulus and strength of the composite.	100
Table 8.22 Comparison of commercial pearlescent films and zeolite filled films.	101

# LIST OF FIGURES

Figure 2.1 Spatial configuration of i-polypropylene molecules.	8
Figure 2.2 Spatial configuration of s-polypropylene molecules.	8
Figure 2.3 Spatial configuration of atactic polypropylene molecules.	9
Figure 2.4 The primary building units combine to form the secondary building units which the zeolite structure is comprised of.	10
Figure 3.1 The probable reaction mechanism in the system-kaolin filler/ elastomer with $\gamma$ -mercaptopropyltrimeth - oxysilane (Domka; 1994).	16
Figure 3.2 Interaction between the titanate proadhesive agents and kaolin; chalk (Domka; 1994).	16
Figure 3.3 Surface modification of chalk with stearic acid.	17
Figure 4.1 Flow sheet of microporous polypropylene composite preparartion (Nago et al.; 1992).	19
Figure 4.2 Process line for biaxially orientation of polymer film.	20
Figure 5.1 Scanning electron micrographs of oriented toughened chalk-filled i-polypropylene films a) stretching ratio 3 b) stretching ratio 5 (Galeski et al. 1992).	21

Figure 5.2 Scanning electron micrographs of microporous polypropylene sheet. a) Surface b) Inner section at the depth of 35 $\mu$ m from surface c) At the depth of 100 $\mu$ m (Nakamura et al.; 1993).	25
Figure 5.3 Model void formation by stretching in machine direction (Nakamura et al.;1993).	25
Figure 6.1 Infrared Spectrum of Clinoptilolite.	29
Figure 6.2 Melting thermograms of i-polypropylene at a ) 110 $^{\circ}$ C b ) 120 $^{\circ}$ C.	33
Figure 7.1 Hot Press 1.upper heater 2.lower heater 3.ring 4.hydrolic part 5.pressurizing wing 6.pressure indicator 7.temperature control 8.cooling water outlet and inlet (Ulutan; 1994).	42
Figure 8.1 FTIR spectrum of Gordes 2 natural zeolite.	47
Figure 8.2 Absorbance of typical clinoptilolite peak at 609 $\text{cm}^{-1}$ and hydrocarbon peak at 2800 $\text{cm}^{-1}$ for different natural zeolite.	48
Figure 8.3 FTIR spectra of Calcium stearate, Stearic acid , PEG (4000) modified zeolites.	49
Figure 8.4 Effect of washing, modification and particle size on clinoptilolite content of Gordes 1.	49
Figure 8.5 Effect of washing on clinoptilolite and hydrocarbon content of Gordes 2.	50
Figure 8.6 Effect of washing and acid leaching on clinoptilolite content of Bigadic zeolite.	50

Figure 8.7 FTIR spectrum of Polypropylene 1. Aldrich polypropylene 2. Petkim polypropylene.	51
Figure 8.8 FTIR spectra of 10 % zeolite filled Aldrich polypropylene composites.	52
Figure 8.9 Natural zeolite and 10 % natural zeolite pp composites 609 $\text{cm}^{-1}$ peak.	53
Figure 8.10 C=O group in 10 % Kirankoy and Gordes 1 filled composite films FTIR spectra.	54
Figure 8.11 1720 $\text{cm}^{-1}$ peak in 10 % natural zeolite polypropylene composites.	54
Figure 8.12 FTIR spectra of a.Gordes 1 and b.Bigadic type natural zeolite composites.	55
Figure 8.13 Bigadic and Gordes 1 type natural zeolite filled composites clinoptilolite content, 609 $\text{cm}^{-1}$ peak.	56
Figure 8.14 3700 $\text{cm}^{-1}$ peak for Bigadic filled pp composites and Gordes 1 filled polypropylene composites.	57
Figure 8.15 FTIR spectra of a. zeolite b. polypropylene c. 20 % zeolite filled polypropylene composite 1060 and 820 $\text{cm}^{-1}$ peak.	58
Figure 8.16 b/a and b/c versus zeolite fraction.	58
Figure 8.17 Normalized peaks of FTIR spectrum for Aldrich polypropylene.	59
Figure 8.18 The Optic Micrograph of 75 times magnified a- Pure natural zeolite	

b- PEG (4000) modified natural zeolite.	62
Figure 8.19 Differential volume percent of 45 $\mu$ natural zeolite.	63
Figure 8.20 Reflected optical micrographs of extruded films with zeolite having size lower than 45 $\mu$ a) 75 times magnified composite film b) 150 times magnified composite films.	64
Figure 8.21 Transmitted optical micrograph of 2 $\mu$ size 6 % zeolite filled pp films a)100 times magnified composite film b) 250 times magnified composite film c) 400 times magnified composite film.	65
Figure 8.22 2 $\mu$ size 6 % zeolite filled pp films 75 times magnified reflected optical micrograph.	65
Figure 8.23 Tensile tested films a) 100 times magnified b) 400 times magnified taken by using transmitted optical micrograph.	66
Figure 8.24 Transmitted optical micrograph of hot press films a) 100 times magnified hot pressed Aldrich pp b) 100 times magnified 10 % zeolite filled hot pressed composite c)100 times magnified 20 % zeolite filled hot pressed composite d) 100 times magnified 40 % zeolite filled hot pressed composite.	67
Figure 8.25 DSC curves of a- Aldrich polypropylene, b- Petkim polypropylene.	68
Figure 8.26 DSC curves of microscope slide prepared composites.	70
Figure 8.27 Composite films heat of melting versus zeolite fraction.	71
Figure 8.28 6 % zeolite filled polypropylene DSC curve.	72
Figure 8.29 10 % zeolite filled polypropylene films DSC curve.	73

Figure 8.30 Hot pressed films first heating and cooling curves.	75
Figure 8.31 Hot pressed films heat of fusion versus zeolite fraction values.	77
Figure 8.32 Heat of crystallization of hot pressed films versus zeolite fraction.	77
Figure 8.33 Avrami plot.	78
Figure 8.34 TGA curve for Petkim polypropylene and Aldrich polypropylene .	79
Figure 8.35 TGA curves of 2%, 4%, 6% zeolite filled polypropylene composites.	81
Figure 8.36 TGA analysis of Aldrich polypropylene at different heating rates.	83
Figure 8.37 TGA analysis of Petkim polypropylene at different heating rates.	84
Figure 8.38 TGA analysis of 6% zeolite filled, extruded polypropylene film at different heating rate.	84
Figure 8.39 TGA analysis of 10 % zeolite filled, hot pressed composites at different heating rate.	85
Figure 8.40 Ozawa plot of Petkim polypropylene.	86
Figure 8.41 Frequency factor.	87
Figure 8.42 10 % zeolite filled hot pressed sample shaped according to ASTM D-638.	92

Figure 8.43 The stress- strain curves of a) 10 % b) 30 % zeolite filled hot pressed samples. 95

Figure 8.44 Strain -stress diagram of a) Petkim polypropylene b) 2% zeolite filled extruded films. 96

Figure 8.45 Tensile testing of a) pure polypropylene b) 4% extruded polypropylene films in Polinas. 98





# Chapter I

## INTRODUCTION

Polymer matrix composites are materials which contain polymers as matrix materials surrounding very small reinforcing fibers or fillers. The matrix materials are either thermosetting or thermoplastic polymers (Wagner and Colton;1994). Over the past several years there is an increasing interest in the use of thermoplastic as a matrix for composite materials. Thermoplastic polymers have a great potential from a manufacturing standpoint.

Polymeric composites show advantages, as they are inexpensive, derive from natural sources, present lower density than mineral fillers, and increases the mechanical properties of the final product.

The objective of this project is to prepare polypropylene (pp) natural zeolite composites. In this project, developing natural zeolite polypropylene composite film is aimed. Origin of these project is pearlescent polypropylene calcium carbonate ( $\text{CaCO}_3$ ) composite films. From the industrial point of view an alternative material to  $\text{CaCO}_3$  was sought, because industrially needed  $\text{CaCO}_3$  has been patented. Natural zeolite was chosen as a cheap alternative to  $\text{CaCO}_3$ . The rich natural zeolite beds in Aegean region and properties of natural zeolite are the other important reasons for choosing the natural zeolite as a filler.

Although, there is an increasing interest on polymer composite materials, most of the studies was made by polypropylene  $\text{CaCO}_3$  composites. Nago et al. (1992 ), made extensive studies on porous  $\text{CaCO}_3$  polypropylene composites. Polypropylene - $\text{CaCO}_3$  fillers polyester plasticiser composed of adipic acid and propylene glycol that were used as an additive surface treating agent of  $\text{CaCO}_3$  filler and antioxidant were mixed to have the base sheet. Antioxidant used was

2,6-di-*t*-butyl -4-methylphenol. Polypropylene powder, CaCO<sub>3</sub> filler and the additives were well mixed in advance and then pelletised with the aid of an extruder tandem type. The base sheet was stretched in machine direction by using two pairs of roller with different rotating speed and then stretched in transverse direction by using a biaxial stretching machine of pantogram type.

Mitsuishi et al. (1991) prepared polypropylene - CaCO<sub>3</sub> composites. Polypropylene and CaCO<sub>3</sub> particles were mixed in a two roll mill ( $180 \pm 5$  for 8 min). The polypropylene mixture prepared by mixing roll was pressed onto a moulded plate by a compression press. A pressure of 14.7 MPa was used for 1 minute (min), after preheating at a temperature of  $230 \pm 2$  for 2 min. The moulded plate was quenched by a cold press.

Galeski et al. (1993) also studied CaCO<sub>3</sub> - polypropylene composites. Chalk filled *i*-polypropylene composites were prepared from dried components. First pellets of *i*- polypropylene were wetted with liquid modifier an oligomer of ethylene oxide and precipitated chalk was added and mixed until uniform covering of the chalk particles with the oligomer of ethylene oxide was obtained. Second, chalk filled *i*-polypropylene was prepared by means of a twin screw extruder.

Surface modification of CaCO<sub>3</sub> and some other fillers were studied by Domka (1994). Modifying substances are many types of surface active substances, fatty acids and their derivatives, silane coupling agents, titanate coupling agents and other metallorganic compounds and metallocenes. Specific organic oxyethylated compounds with long chains may serve the purpose well. Due to a relatively strong hydrophobization, in particular of the surface of chalk fillers, their modification with the above compounds may lead to a considerable of polymers - CaCO<sub>3</sub> adhesion ( Domka; 1994 ).

Mitsuishi et al. (1991) used alkyl dihydrogen phosphates as modifiers for CaCO<sub>3</sub>. CaCO<sub>3</sub> particles with different particle size was modified with alkyl dihydrogen phosphates. Dried CaCO<sub>3</sub>, mixed with ethanol and modifier then put

into a round flask to modify the  $\text{CaCO}_3$  surface using rotary evaporator in vacuum. The surface modified  $\text{CaCO}_3$  particle was dried. Galeski et al. (1993) used an oligomer of ethylene oxide as a  $\text{CaCO}_3$  modifier. Mitsuishi et al. (1991) used poly(oxyethylene) oleate for modification of  $\text{CaCO}_3$  surface.

There are two explanations about formation porous polypropylene -  $\text{CaCO}_3$  composites, the first explanation is biaxially oriented film in an other words mechanical tearing of the films. The second explanation is chemical blowing.

Nakamura et al. (1993) reported the structure of biaxially oriented polypropylene. There are round filler particles with various sizes. Stretching in machine direction causes splitting of polypropylene phase at periphery of filler particles, and the increase in machine direction engenders orientation of resultant polypropylene fibrils and molecular chain along machine direction. Increase of the stretching degree makes the orientation more developed.

In technical notes of a polypropylene film producing company a similar explanation is given for pearlescent film production. In machine direction drawing unit, the molecules are oriented in the same line and form a band around  $\text{CaCO}_3$  particle and a little amounts of air diffusion occurs. In transverse direction drawing unit, as a result of the orientation of the molecules in the opposite direction the film swells around  $\text{CaCO}_3$  particles as a result of an air diffusion. These two steps of the process cause the reduction of density.

According to the second explanation polypropylene chemical blowing agent and  $\text{CaCO}_3$  are well mixed and after processing foamed polymer film with low density is obtained.

The prepared composites are oriented biaxially to formation of voids the pore sizes of voids and concentration can be controlled by the size of filler particles and their concentration (Galeski et al.1993).

Mitsuishi et al. (1991) found that the crystallization temperature of composite material increases with increase of  $\text{CaCO}_3$  content and decrease of  $\text{CaCO}_3$  size.

Nakamura et al. (1993) found that the properties of microporous polypropylene sheet depend on the particle size of the filler and stretching degree of stretching of composite material.



## **Chapter II**

### **Polymer Composites**

Composites are materials with two or more components that combine to yield characteristic superior to those of the individual constituent. Such materials must be heterogenous at least on a microscopic scale.

Composite materials may be; divided into three general classes, first one is fiber-filled composites. Second, particulate-filled materials consisting of a continuous matrix phase and a discontinuous filler phase made up of discrete particles. The last one is Skeletal or interpenetrating network composites consisting of two continuous phases (Nielsen; 1974).

Many commercial polymeric materials are composites; such as ABS materials, foams, computer sheet, sticky tape, wire coatings, cookie, soap, cake, candies, coffee, cigarette, cassette etc. packaging industries.

There are many reasons for using composite materials rather than simpler homogenous polymers. Some of the reasons are;

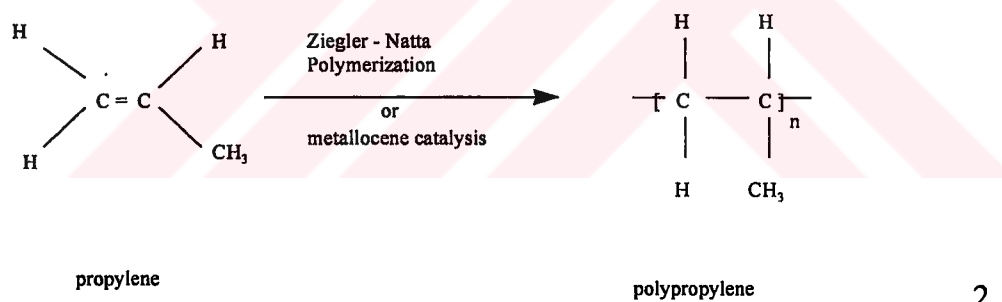
1. High stiffness and strength
2. High toughness or impact strength
3. Increased mechanical damping
4. Reduced permeability to gases and liquids
5. Modified electrical properties
6. Potential of rapid process cycles
7. Lower tooling cost alternatives
8. Reduced cost

Not all of these desirable features are found in any single composite. The properties of composite materials are determined by the shape of filler phase, by the morphology of the system, and by the nature of the interface between the phases. Thus, a great variety of properties can be obtained with composites just by alteration of the morphological or interface properties (Nielsen; 1974 ).

## 2.1. Polypropylene

Polypropylene (pp) is among the most widely exploited thermoplastic polymers and it has increasing practical importance because of its good mechanical properties, low cost, and ease of processing and recycling.

Polypropylene can be made from the monomer propylene by Ziegler - Natta polymerization and by metallocene catalysis polymerization as shown in Equation 2.



These catalysts are prepared by reacting compounds of transition metals of Groups IV-VII in lower valency states (e.g.; TiCl<sub>2</sub>, TiCl<sub>3</sub>, with metal alkyls, alkyl halides, or metal hydrides ).

The molecules constituting the crystalline fraction of polypropylene have a regular distribution of methyl side group with respect to main chain. The methyl groups in macro molecular chains of the amorphous fraction are distributed randomly. According to the Ziegler- Natta polymerization, polymers

with ordered distribution of chain links are called stereoregular, where as those with a random distribution these are called atactic. The relative content of the stereoregular and the atactic fraction of polypropylene, was determined to a large extent by the catalyst and the conditions of the polymerization. If the polymerization temperature is decreased, the content of the stereoregular fraction increases. Two kinds of stereoregular polypropylene may be distinguished, isotactic and syndiotactic.

Polypropylene is useful in a wide range of applications because of its properties.

- fairly low physical properties
- fairly low heat resistance
- excellent chemical resistance
- translucent to opaque
- low price
- easy to process

The application areas of polypropylene is fiber, filament, film, pipe, carpeting, and packaging, automotive trim pieces, hinged packaging for commodity products, i.e. soap holder, toys, bottle caps, general commodity items.

### **2.1.1 Isotactic Polypropylene ( i- polypropylene )**

The crystalline structure of i-polypropylene involves one helical conformation a three- fold helix with 6.5 Å chain axis repeat distance. The methyl (R) groups are on the same side of the carbon chain plane for i-polypropylene as seen in Figure 2.1.

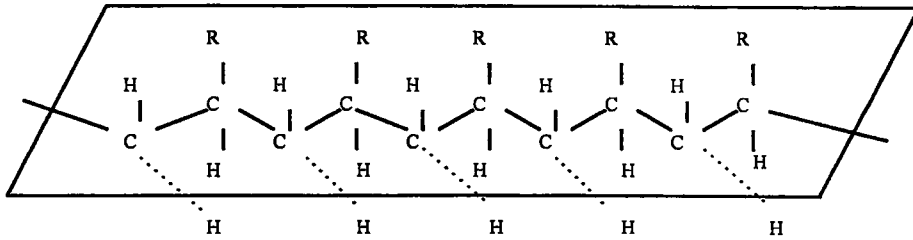


Figure 2.1: Spatial configuration of i-polypropylene molecules

The crystal structure of the most common crystal phase of i-polypropylene is  $\alpha$  phase. The overall geometry of the cell is monoclinic. The  $\gamma$  phase of i-polypropylene had remained rather elusive for many years. It is not usually observed as a different phase, but crystallises with and within the  $\alpha$  phase spherulites.  $\beta$  i - polypropylene phase produces well individualised spherulites admixed with, and therefore clearly recognizable from the  $\alpha$  i-polypropylene phase spherulites. ( Lotz et al.; 1996 )

### 2.1.2 Syndiotactic Polypropylene ( s-polypropylene )

The structure of s-polypropylene is, centred on the helical hand. The crystal structure is based on the orthorhombic cell. It is a c- centred cell composed at helices of one hand only Lotz, et al. (1996). The methyl groups are alternatively above and below the carbon chain for s-polypropylene as seen in Figure 2.2.

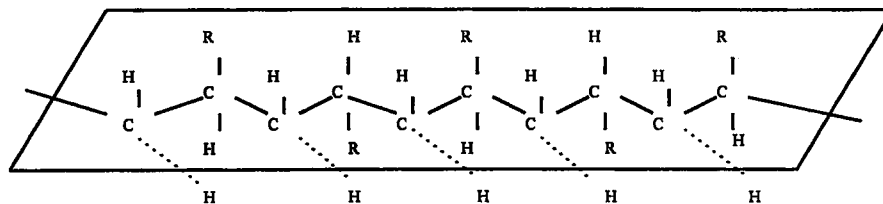


Figure 2.2: Spatial configuration of s-polypropylene molecules.



### 2.1.3 Atactic Polypropylene

Methyl groups are distributed randomly above and below the carbon chain plane as seen in Figure 2.3. The relative contents of stereoregular and the atactic fraction of polypropylene, which determine a large extent the properties of the polymer will depend the identity of the catalyst and on the basis of  $\text{TiCl}_3$  and alkyl aluminium halide, which contain electron-donating additives such as pyridine, and yield a polypropylene which is almost totally crystalline. If the polymerisation temperature is decreased, the content of the stereoregular fraction increases (Lotz et al.; 1996).

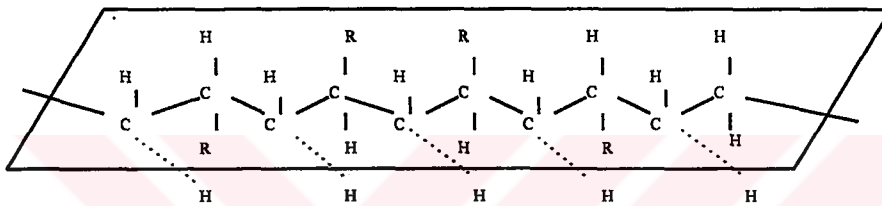


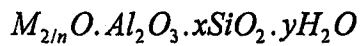
Figure 2.3: Spatial configuration of atactic polypropylene molecule

Using special metallocene catalyst, it is possible to produce block copolymers, which contain blocks of i-polypropylene and blocks of atactic polypropylene in the same polymer chain.

## 2.2 Natural Zeolite

Zeolites are crystalline, hydrated aluminosilicate of group I and II elements in particular, sodium potassium, magnesium, calcium, and barium. Structurally the zeolite are framework aluminosilicate which are based on an infinitely extending three-dimensional network of  $\text{AlO}_4$  and  $\text{SiO}_4$  tetrahedra linked to each other by shearing all of the oxygen's (Breck; 1974).

The empirical formula of zeolite is



x : generally equal or greater than 2 since  $AlO_4$  tetrahedra are joined only to  $SiO_4$  tetrahedra

n : the cation valance

Natural zeolite was found in the 18th century by a Swedish mineralogist named Cronsted, who observed upon rapidly heating a natural zeolite, that the stones began to dance about as the water evaporated.

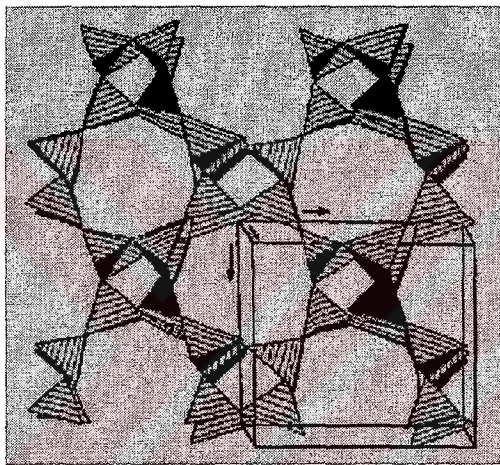


Figure 2.4: The primary building units combine to form the secondary building units which the zeolite structure is comprised of.

The primary building block of the zeolite framework is the tetrahedron, a small cation silicon (Si) or aluminium (Al) atom, in tetrahedra coordination with four oxygen at the vertices. Each oxygen atom is shared between two tetrahedra as seen in Figure 2.4. Substitution of Si or Al defines the negative charge of the framework, which is compensated by monovalent or divalent cations located together with water molecules in structural channels. Cations in the channels are substituted easily, and therefore they are termed exchange or extra framework cations, unlike Si and Al which are not exchanged under ordinary conditions Tsitsishvili et al. (1992). Positively charged metal ions and

cations, such as those of sodium, potassium, magnesium and calcium can neutralize the charge.

The voids and channels of natural zeolites are typically in the range of molecular dimensions, i.e. 3 to 10 Å. pure zeolites are colourless or white, some mineral specimens may be colored because of the presence of finely divided oxides of iron or similar impurities. The density of the zeolites range between 2 and 2.3 g/cc ( Breck; 1974 ).

Zeolites have unusual crystalline structures that give them unique chemical properties. For instance in one gram of zeolite, the channels provide up several hundred square meters of surface area on which chemical reactions can take place. The natural zeolite can absorb up to 30% of their dry weight of gases such as nitrogen or ammonia.

In Turkey the most encountered natural zeolite types are clinoptilolite and analcime. In Bahcecik - Gölpazari - Göynük, Polatli - Mulk- Oglakci - Ayas, Nallihan - Cayirhan - Beypazari, Kalecik - Candar analcime type natural zeolite is encountered; in Balikesir - Bigadic, Emet - Yukari Yoncaagac , Kutahya - Saphane, Gediz, Hisarcik, Gordes, Izmir - Urla and Kapadokya clinoptilolite type natural zeolite is encountered ( Özkan and Ülku; 1997 ).

Clinoptilolite a rare hydrothermal mineral, genesis of hydrological closed system like a saline, alkaline lake is very common and has been investigated in many times. Chemical formula of clinoptilolite is  $(\text{Na,K})_6(\text{Al}_6\text{Si}_{30}\text{O}_{72})20\text{H}_2\text{O}$  and Ca, K, and Mg also present in the clinoptilolite content. Si/Al ratio is between 4.25 - 5.25 and the density of the clinoptilolite is about 2.16 g/cc ( Gottari and Galli; 1985 ).

Ülkü and Özkan (1997) studied modification of clinoptilolite from Bigadic (west Anatolian) and water vapor adsorption of clinoptilolite was examined in detail. Clinoptilolite was used in heat pump and air drying studied by Ülkü (1986a).

Zeolites owe their value to one or more of three properties these are adsorption, ion exchange, and catalyst. Zeolite has wide range of application area; its used in odour control and in industrial gas separation processes by using the gas adsorption ability, used as a desiccation and heat storage and solar refrigeration by using its water absorption and desorption ability; in water treatment, agriculture and aquaculture by using ion exchange property. Natural zeolite is also used in paper and rubber industry as a filler and in radioactive waste water treatment.



## **Chapter III**

### **Surface Modification of the Filler**

Surfaces are the regions through which materials connect and interact with their surroundings. Surfaces are preferentially occupied by those constituents of the polymer materials that can best accommodate the constraints and interactions. Intentional chemical modification can modify portions of individual macromolecules, thus chemically also imparting different surface affinity to those segments. In either case, one finds that certain molecules, or certain portions of molecules, segregate to the surface of the material and thereby can assume a dominant role over the average bulk composition in determining how the material interacts with its surroundings. This behaviour could be thought of as the counterpart to surface reconstruction of inorganic crystalline materials (Cahn et al.; 1993).

Surface modification of  $\text{CaCO}_3$  and some other fillers were studied by Domka (1994). Inorganic fillers reveal some chemical affinity to polymer. The fillers are hydrophilic which limits their chemical affinity to polymers because polymers are hydrophobic. To avoid the agglomerations and coagulations in this heterogenous mixture fillers are modified by an inorganic material which increases its chemical affinity to polymers.

Modifying substances are many types of surface active substances, fatty acids and their derivatives, silane coupling agents, titanate coupling agents and other metallorganic compounds made on the basis of zirconium organic compounds and metallocenes. Specific organic oxyethylated compounds with long chains may serve the purpose well. Due to a relatively strong hydrophobization, in particular of the surface of chalk fillers, their modification

with the above compounds may lead to a considerable improvement of polymers-  $\text{CaCO}_3$  adhesion.

Table 3.1 lists the values of hydrophobization degree under the investigation of the filler.

Table 3.1: Additives and degree of hydrophobization of  $\text{CaCO}_3$   
( Domka; 1994 )

Type of proadhesive compounds	Amount weight parts	Degree of hydrophobization %
No adhesive compounds	—	—
Stearic acid	1	13.8
	2	20.1
	3	26.7
Magnesium stearate	1	14.8
	2	21.1
	3	28.4
Calcium stearate	1	14.4
	2	20.7
	3	28.3
p-oxyethyleneglycol PEG 4000	1	6.3
	2	9.8
	3	14.3
Oleinic acid	1	14.8
	2	21.2
	3	27.4
Aminosilane	1	3.3
	2	5.6
	3	8.7
Mercaptosilane	1	4.8
	2	8.2
	3	12.4

Precipitated  $\text{CaCO}_3$  treated with most of the proadhesive compounds decrease proportionally to the increase in the amount of the added proadhesive compounds. Only in the case of surface modification of the filler with amino silanes, polyoxyethylene glycol (PEG 4000) depending on the amount of proadhesive compounds (Domka; 1994) .

Modification of filler could be used for having a good dispersion medium between filler and matrix or for binding the filler and matrix. Figure 3.1 give schematic representation of the filler matrix relation.

### **3.1 Coupling Agent**

The coupling agent - matrix interface is a diffuse boundary where intermixing takes place because of the penetration of the matrix into the coupling agent layer and the migration of the coupling agent molecules into the matrix phase. Consequently, in addition to the enhanced adhesion, the use of coupling agent can effect the morphology of the matrix and, hence, the mechanical performance of the interphase ( Denault and Vu-Khanh;1988 ).

Titanate, zirconate, silanes and ethylene oxide are the examples of coupling agents. According to Alonso et al. (1997), organosilane coupling agents were employed for surface treatment of the talc. For surface wetting of talc; methanol, water and silane mixture was prepared. After the wetting process the mineral was dried in an oven 24 hour at 60 °C.

According to Galeski et al. (1992) the modification of mineral was made by a liquid modifier ethylene oxide. An oligomer of ethylene oxide and precipitated chalk was added and mixed until uniform covering of the chalk particles with the oligomer of ethylene oxide was obtained.

Silane coupling agents on the surface of kaolin interact according to the Figure 3.1.

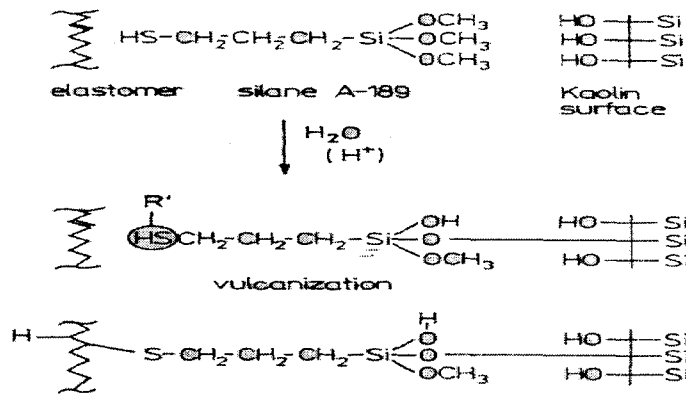


Figure 3.1: The probable reaction mechanism in the system - kaolin filler/ elastomer with  $\gamma$ -mercaptopropyltrimethoxy silane (Domka; 1994).

Interaction between the titanate coupling agents and fillers with or without hydroxyl groups are shown in Figure 3.2.

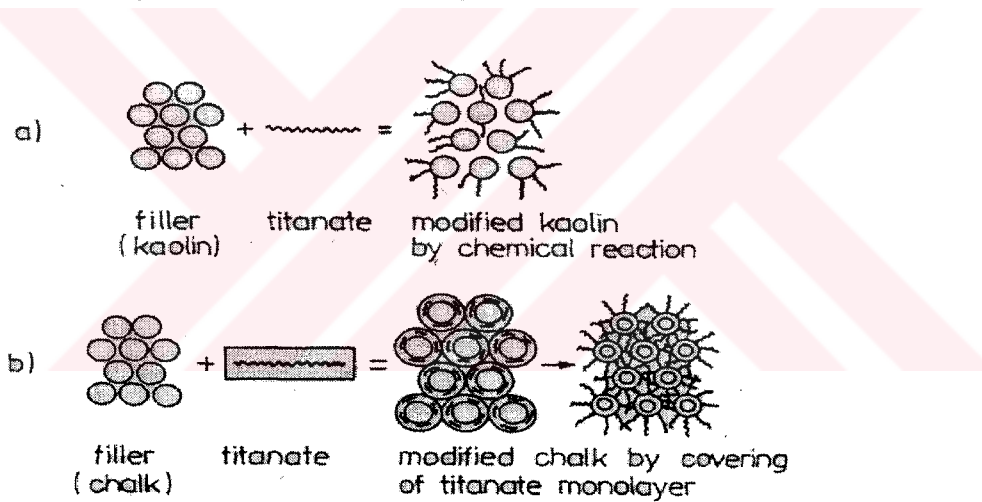


Figure 3.2: Interaction between the titanate proadhesive agents and kaolin; chalk (Domka; 1994).



### 3.2 Dispersion Agent

In dispersion, the filler- polymer interaction may have a stabilizing effect if the mechanism of uncoiling causes formation of loops on the filler surface. Chalk surface may react with stearic acid as seen in Figure 3.3. Chalk surface modification with stearic acid brings also good results, because it decreases anisotropy of its particles and at the same time increases its specific surface area ( Domka 1994 ).

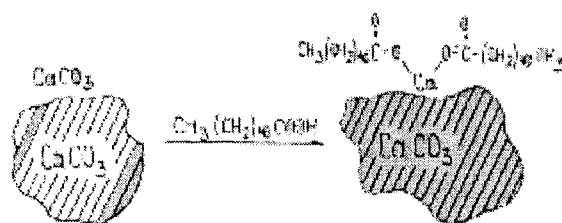
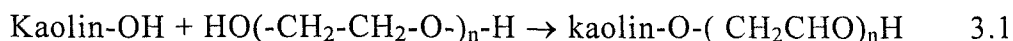


Figure 3.3: Surface modification of chalk with stearic acid

Mitsuishi et al. ( 1991 ) used alkyl dihydrogen phosphates modifier for CaCO<sub>3</sub>. First CaCO<sub>3</sub> particle was dried then ethanol and modifier were put into a round flask to modify the CaCO<sub>3</sub> particle surface using rotary evaporator in vacuum. The surface modified CaCO<sub>3</sub> particle was air dried at 105 °C.

Kaolin surface modification was made with polyethylene glycol were yielded. Non - ionic surface active compounds may be adsorbed on kaolin surface. Chemical reaction between bonded hydroxyl groups of kaolin surface and hydroxide groups of a particle of polyethylene glycol, occurs as seen Equation 3.1.



## Chapter IV

### Preparation Methods of Polymer Composite

Microporous films and sheets have so far been studying by various methods. For polypropylene composite films and sheet preparation; the common method is extrusion. At extrusion process, the molten polypropylene composite is extruded, to prepare the base sheets, and orientation of polypropylene molecules would occur to some extent. Other methods are two-roll mill, hot press and blender method. In industrial production scale, only extrusion method is used. An alternative method to prepare polypropylene composite could be solvent casting method. In solvent casting method a proper solvent is used to dissolve the polymer, the filler is added to the solution of the polymer. The mixture is placed in a shallow container and the solvent is evaporated at room temperature to obtain the films. This method is not used for polypropylene composite films, because evaporation temperature of proper polypropylene solvents is very high. Another method is microscope slide method; this method could only be used in laboratory scale, polymer and filler are mixed between two microscope slides, heated on a hot plate and pressed by fingers to obtain the films.

#### 4.1 Extrusion

Extrusion processes are concerned with the continuous delivery of a melt by means of an Archimedean screw through a die, where it acquires the required geometry. The screw has the additional task of feeding granular or powder polymer into the heated barrel and bringing it into the melt state as a uniform mass (Mascia; 1989).

Nago et al.(1992), made extensive studies on porous  $\text{CaCO}_3$ -polypropylene composites. As seen in Figure 4.1. Polypropylene,  $\text{CaCO}_3$  fillers

polyesters plasticiser composed of adipic acid and propylene glycol that were used as an additive surface treating agent of CaCO<sub>3</sub> filler and antioxidant were mixed to have the base sheet. Antioxidant used was 2,6-di-t-butyl-4-methylphenol.

Polypropylene powder, CaCO<sub>3</sub> filler and the additives were well mixed in advance and then pelletised with the aid of an extruder. The base sheet was stretched in machine direction by using two pairs of roller with different rotating speed and then stretched in transverse direction by using a biaxial stretching of pantogram type.

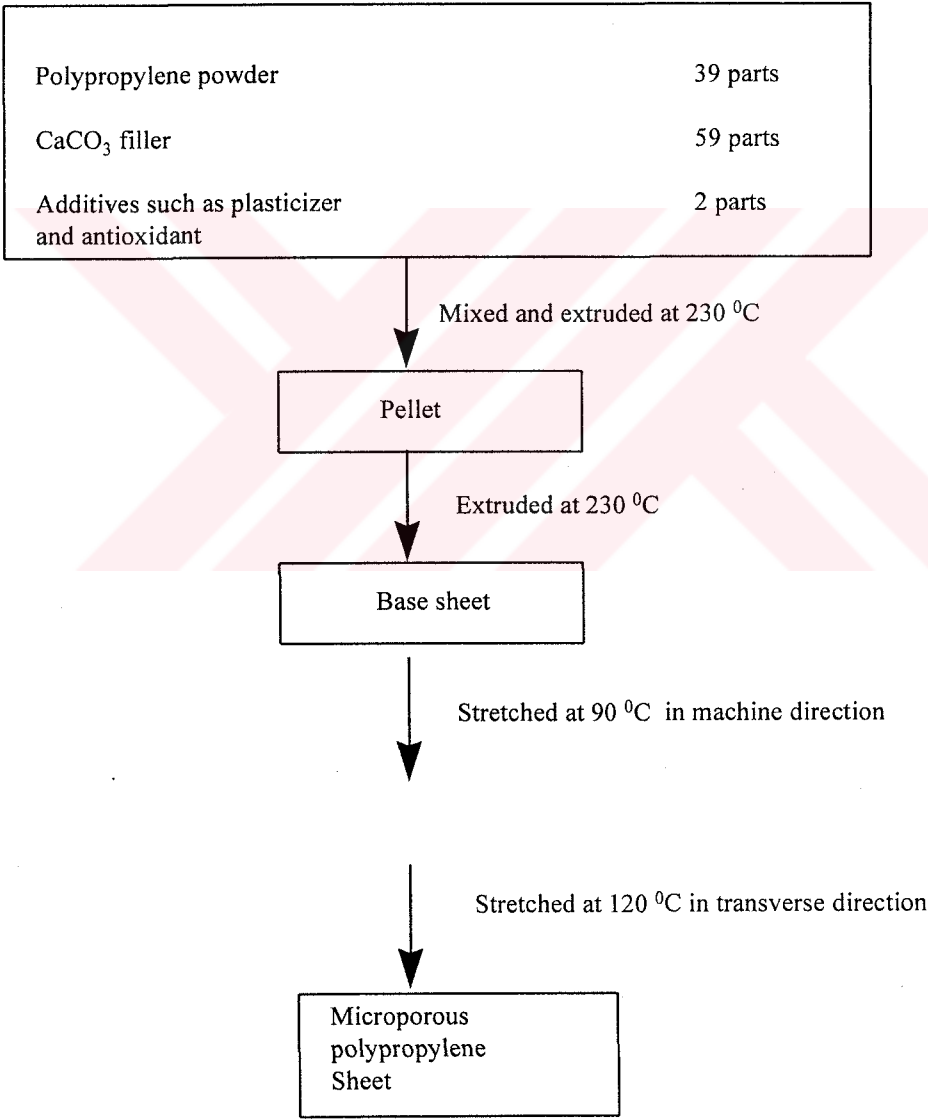


Figure 4.1: Flow sheet of microporous polypropylene composite preparation ( Nago et al.; 1992 )

Galeski et al. (1993) also studied  $\text{CaCO}_3$  - polypropylene composites. Chalk filled i- polypropylene was prepared from dried components. First, pellets of i-polypropylene were wetted with liquid modifier an oligomer of ethylene oxide and precipitated chalk was added and mixed until uniform covering of the chalk particles with the oligomer of ethylene oxide was obtained. Second, chalk filled i-polypropylene was prepared by means of a twin screw extruder, shown in Figure 4.2.

An extruder consists of two parts: the plasticisation / screw section and the shaping unit. Since the screw section is common to all extrusion processes, it can be treated independently of the type of extrudate produced. The process train usually includes a series of internally cooled rolls, a stretching device and oven enclosing the stretcher and containing a number of carefully controlled temperature zones, followed by slitting and windup equipment. For polymer composite preparation, the first step is mixing the polymer-filler and put into the extruder. After the polymer melted with the mixed filler into the base sheet comes out from the sheeting die and cooled between casting rolls. The base sheet is stretched in machine direction in preheating and web guide section. Then the film enters to the tenter section. The hot film is stretched in transverse direction. Then it is cooled between nip rolls and the biaxially stretched film is taken off by the pressure rollers.

Tjong et al. (1997) prepared polypropylene composites by twin screw extruder. Polypropylene powder premixed with  $\beta$ - nucleator in a Brabender twin screw extruder. Extrudates were pelletized.

#### **4.2 Two - roll Mill**

Ghosh et al. (1997) prepared metal filled thermoplastics by two roll mill method. Vacuum - dried i-polypropylene and treated silver were compounded on a two roll mill for 15 minutes to prepare thin sheets containing 5.6 vol % silver.

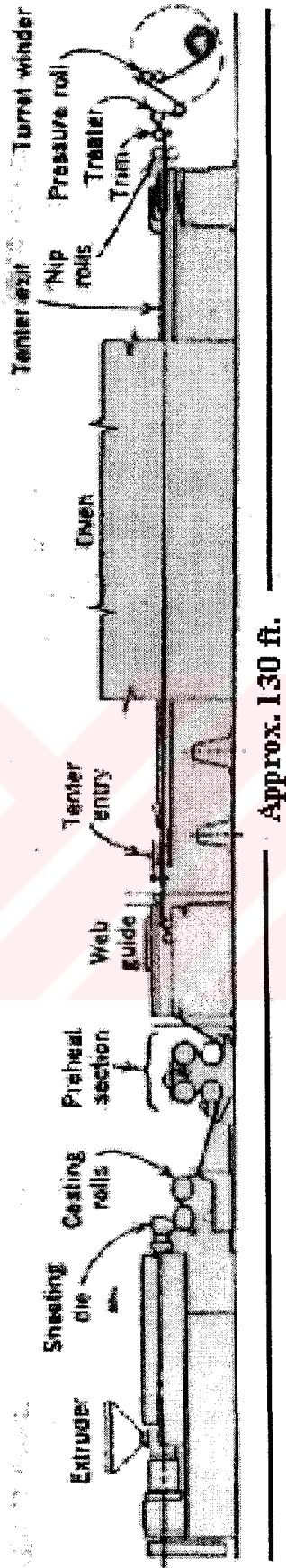


Figure 4.2: Process line for biaxially orientation of polymer film.

Mitsushi et al. (1991) mixed polypropylene and CaCO<sub>3</sub> particles in a two roll mill at ( 180 ± 5 °C ) for 8 minutes. The polypropylene mixture prepared by the mixing roll was pressed onto a moulded plate by a compression press.

#### **4.3 Blender**

Levita et al. (1989) studied the preparation of polymer composites. Polymer and heat stabiliser were first mixed in a tumbling barrel. The mixture was subsequently fed into a twin screw blender at 180 °C and thereafter milled down with a blade granulator.

#### **4.4 Hot Press**

β - polypropylene films with a thickness of 0.2 mm were prepared by cooling the hot pressed polypropylene pellets blended with β- nucleator, in air. The resultant β - polypropylene films were then subjected to biaxial drawing up to a predetermined draw ratio at a defined drawing temperature (Chu and Kimura; 1996).

## Chapter V

### Mechanism of Pearlescent Film Formation

Pearlescent film have a shining apperance. In most commercial applications polymer melts are dispersed with fillers in order to prepare pearlescent films. Pearlescent films serve a dual purpose of decreasing density and improving a microporous structure. The fillers which used in pearlescent films can be fibrous for particulate, or it can be gaseous inclusions as in polymer foams.

There are two different explanations about microporous polypropylene films in the literature. The first explanation is stretching. The base sheet is stretched in machine and transverse direction and a microporous polypropylene film with low density is obtained. The second explanation is foaming. A foaming material is put into the polymer and while the film is prepared; microbubbles are obtained by the decomposition of foaming material into gaseous products.

#### Stretching

Microporous polypropylene sheets are prepared by stretching the base sheet. The base sheet consists of uniformly dispersed filler in polypropylene continuos phase.

Galeski et al. (1992) studied chalk filled i-polypropylene and prepared the composite by using twin screw extruder. The chalk filled i-polypropylene samples were stretched in machine direction unit 3 and 5 times. Surfaces of oriented chalk filled i-polypropylene examined by scanning electron microscope, as shown in Figure 5.1. Figure 5.1 a- is stretched 3 times and b- is stretched 5 times. On the surface there are elongated pores around chalk

particles. The brighter not very sharp objects are chalk particles. The dark layer is i-polypropylene. Because of the drawing direction pores are located in the polar zones of drawing direction and generally they are open and interconnected.

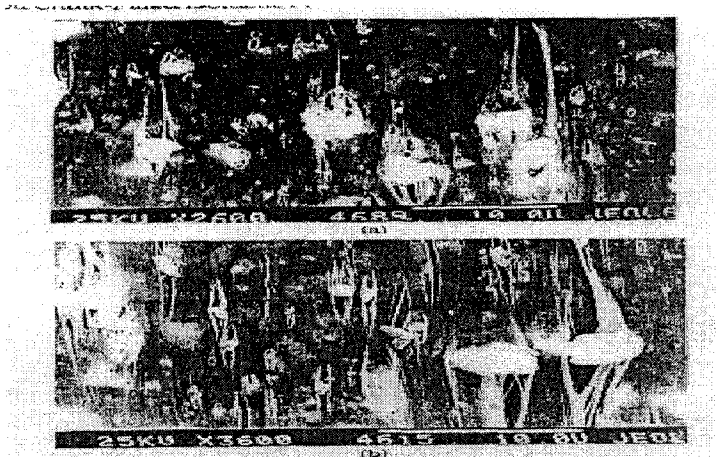


Figure 5.1 : Scanning electron micrographs of oriented toughened chalk- filled i-polypropylene films a ) stretching ratio 3 b ) stretching ratio 5 (Galeski et al.; 1992 ).

Nakamura et al. (1993) prepared microporous polymer films. The microporous polypropylene sheets were stretched biaxially in machine and transverse directions. The most common method used to orient a thermoplastic is to stretch it after it has been heated to a temperature at which it is soft. Nakamura and his coauthors were taken the scanning electron micrographs of the microporous polypropylene sheet as shown in Figure 5.2. Stretching degree in machine and transverse direction causes splitting of polypropylene phase of the base sheets at the periphery of the filler particles. Voids are enlarged and formed with increasing the stretching degrees in machine and transverse direction. As shown in Figure 5.2, there are round pores with various sizes, in which there are filler particles and the deeper under the layer is polypropylene continuous phase.



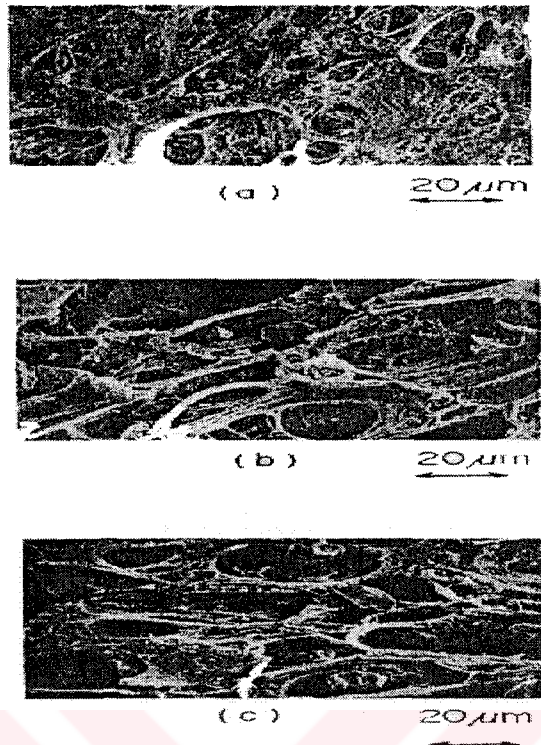


Figure 5.2 : Scanning electron micrographs of microporous polypropylene sheet. a ) Surface, b ) Inner section at the depth of 35  $\mu\text{m}$  from surface, c ) At the depth of 100  $\mu\text{m}$  ( Nakamura et al.;1993 ).

As shown from Figure 5.3 stretching in machine direction causes splitting of polypropylene phase at the periphery of the filler particles. Stretching in machine direction engenders orientation of resultant polypropylene molecular chain along machine direction (Nakamura et al.;1993).

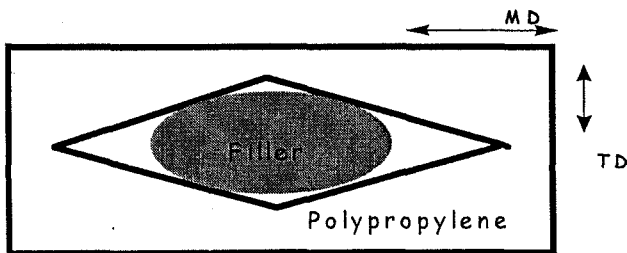


Figure 5.3 : Model void formation by stretching in machine direction (Nakamura et al.; 1993 )

According to a commercial company's technical notes; biaxially stretching of a base sheet causes formation of minute voids. In machine direction drawing unit, the molecules are oriented in the same line and form a band around  $\text{CaCO}_3$  particles and a little amount of air diffusion occurs. In transverse direction drawing unit, the molecules are oriented in the opposite direction, the film swells around  $\text{CaCO}_3$  particles as a result of air diffusion. These two steps cause to the reduction of density of the film Polinas (1990). The direction of air diffusion is not clearly explained in technical notes.

Nago et al. (1992) prepared microporous polypropylene sheet by biaxially stretching the base sheet.  $\text{CaCO}_3$  with various sizes were prepared. It is found that the decrease of particle size makes the porosity of the sheet slightly larger and the maximum pore size smaller. In another study, Nago and Mizutani (1993) prepared microporous polypropylene sheets containing polymethylsilsesquioxane as a filler. It is found that stretching in machine direction and successive stretching in transverse direction cause the thickness to decrease and increase the porosity.

## **5.2 Blowing Agent**

Blowing or foaming agents are used for the production of cellular products. These products can reduce density, lower thermal conductivity and lower dielectric losses.

Blowing agents are classified into physical and chemical types. Physical blowing agents are normally low boiling liquids or gases. Physical blowing agents exert their blowing action when brought to boiling conditions the polymer; by increasing the temperature or reducing the pressure. Ex samples of typical blowing agents; pentane, heptane, methylene chloride, trichloro fluoromethane. Properties of chemical blowing agents are; achieving in decomposition reactions. Chemical blowing agents decompose at the required rate over a fairly narrow temperature range. Typical chemical blowing agents

are azodicarbonamid, azo-bis-dibutyronitrile, p-toluene sulphonyl semicarbazide, benzene sulphonylhydrazine (Mascia; 1995 ).

Letterier and G'Sell (1994) studied formation of voids during the processing of thermoplastic composites. The composites were prepared from an aqueous slurry of polypropylene powder and glass fibers. The mixture was compacted under a pressure of 10 bars giving a sheet of an average thickness of 1 mm. Samples were used for testing the overall density. The temperature is increased to 200 °C under atmospheric pressure. It is found that at a applied pressure at 200 °C coalescence of gases predissolved in the polypropylene matrix control the polymer swelling when the temperature is raised above the melting point.

A good quality structural foam lies in the ability to dissolve in a sufficient amounts of a vapor a gas in a molten plastic, and to allow that gas to nucleate into as many fine bubbles as possible as plastic fills the mold.

The films shine because light is scattered by the small bubbles in the microporous polypropylene films. Each bubble behave as a light source when the composite is irradiated with visible light.

## Chapter VI

### Characterization of Materials

For characterisation of polymers; spectroscopic methods and thermal methods are generally used. To make the characterisation Fourier transform infra red spectroscopy (FTIR), thermal gravimetric analyser (TGA), differential scanning calorimetry (DSC) and optic micrograph are the most commonly employed instruments.

Vibrational spectroscopy in another name infra red spectroscopy (IR) gives information about the chemical composition of the materials, and in many cases can give information about the chain structure, degree of branching, stereoregularity, geometric isomerism, conformation, crystallinity and type of group present in the material. In IR spectroscopy IR radiation is passed through to a sample and certain frequencies are absorbed by the molecule that causes to vibrational changes in the molecule. There may be many IR bonds observed. Since each molecule has individual sets of energy levels, the absorption spectrum is characteristic of the functional groups that are in the molecule (Cahn et al.; 1992).

The general mode of thermal analysis is to heat or cool the sampler under determined temperature program. Thermal gravimetric analyser is used to know the extent of mass loss due to increasing temperature. Differential scanning calorimetry (DSC) is used for measurement of melting and crystallisation points, heat evolved or temperature of a phase transformation to the concentration. These two techniques are highly sensitive and quantitative analytical measurements. One of the most common applications of thermal method is to study the kinetics of various reactions and processes. In kinetic analysis method reaction rate parameters (activation energy and reaction rate)

are calculated, and then the reaction mechanism determination (frequency factor) and isothermal analysis (rate constant and reaction time) could be found.

## 6.1 Characterization of Natural Zeolites

Characterization of natural zeolites were made by using FTIR spectrum and TGA methods are used.

### 6.1.1 Characterisation of Natural Zeolite by FTIR Spectroscopy

IR spectroscopy could be useful for obtaining valuable information on the quality and relative quantity of the inorganic phases of natural minerals. IR spectroscopy has been successfully used for studying zeolite structure and properties. The observed absorption bands have been analysed.

Goryainov et al. (1995) studied the quantitative determination of clinoptilolite and heulandite natural zeolite by IR spectroscopy. Using wet grinding and dry homogenisation zeolite rocks are crushed and dried. Zeolites in the KBr pellets are prepared to perform the analysis. The IR spectra was recorded on a Specord 75 IR. A typical natural zeolite FTIR spectrum, is shown in Figure 6.1.

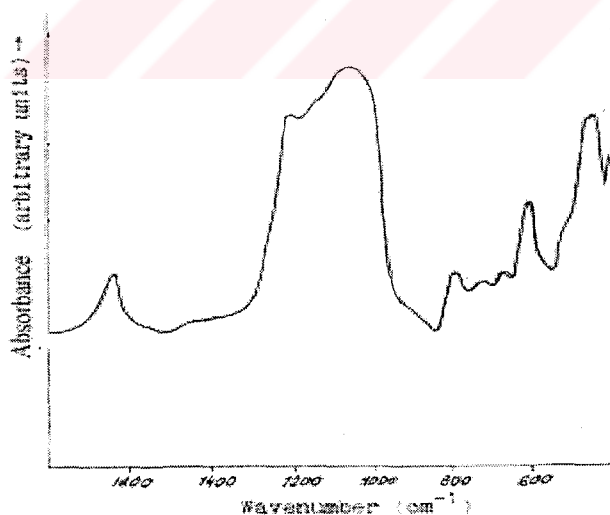


Figure 6.1: Infrared Spectrum of Clinoptilolite

Fuentes et al. (1997) were studied IR vibrations of natural zeolite. They considered two groups of frequencies for the vibrations in all zeolites. Internal

vibrations of T-O and vibrations of external linkages between tetrahedra. The internal vibrations T-O is sensitive to the Si / Al ratio of the frame work. The internal TO stretching mode is 650-820  $\text{cm}^{-1}$ . Sensitive and internal T-O bonding vibration is 420-500  $\text{cm}^{-1}$ . The characteristic peaks of the natural zeolite is given in Table 6.1.

Table 6.1 : Characteristic Peaks of the Natural Zeolite

Vibration	Wave Number ( Goryainov et al.1995)
Isolated OH stretching	3700 $\text{cm}^{-1}$
Hydrogen bonded H <sub>2</sub> O, O-H stretching	3400 $\text{cm}^{-1}$
H <sub>2</sub> O bonding	1620 $\text{cm}^{-1}$
T-O stretching ( T : Al or Si )	1065 $\text{cm}^{-1}$
External T-O ( intense symmetric stretching )	790 $\text{cm}^{-1}$
External T-O double ring	609 $\text{cm}^{-1}$
Internal T-O double ring	450 $\text{cm}^{-1}$

The 609  $\text{cm}^{-1}$  peak was chosen to determine the amounts of the clinoptilolite in the natural zeolite ( Krivacsy et al. 1992 ).

### 6.1.2 Characterisation of Natural Zeolite by TGA

Thermo Gravimetric Analysis records the weight loss of a sample heated under a determined temperature program. Most of the natural zeolites loose water during heating.

The dehydration of clinoptilolite (natural zeolite) was studied by White (1981). There are three types of water in natural zeolite; external water, loosely bond water, tightly bound water. External water is eliminated when the mineral heated to  $75 \pm 10$  °C, loosely bond water is evaporated at  $171 \pm 2$  °C and tightly bound water is removed  $271 \pm 4$  °C .According to Knowlton and White (1981)

in clinoptilolite type natural zeolite there exist 4.6 % external water, 6.6 % loosely bond water, and 2.4 % tightly bond water.

## 6.2 Characterization of Polypropylene

For characterization of polypropylene, FTIR spectrum and thermal analysis measurement devices ( TGA, DSC ) are generally used.

### 6.2.1 Characterization of Polypropylene by FTIR Spectroscopy

For characterization of polypropylene by FTIR spectroscopy, transparent polypropylene films are prepared. Characteristic peaks of polypropylene are shown in Table 6.2.

Table 6.2: Characteristic Peaks of Polypropylene

Type of Vibration	Wave Number $\text{cm}^{-1}$	
i-polypropylene	790	Polymer Handbook
	1158	Brandrup et al. (1976)
s-polypropylene	1131	Polymer Handbook
	1199	Brandrup et al. (1976)
	1230	
t-polypropylene	997	Polymer Handbook
	975	Brandrup et al. (1976)
-CH <sub>2</sub> asymmetric stretching	2930	Banwell (1983)
	symmetric stretching	2860
	deformation	1470
-CH <sub>3</sub> asymmetric stretching	2970	Banwell (1983)
	symmetric stretching	2870
	asymmetric deformation	1460
	symmetric deformation	1375

The broad peak at  $1640\text{ cm}^{-1}$  is due to the antioxidant in polypropylene.

Horrocks and D'Souza (1991) studied on quantitative analysis of transmission spectral bands. In order to find the isotacticity index or fraction the optical density ratio of the  $998$  and  $973\text{ cm}^{-1}$  bands were found. The isotacticity index of pure pp was found  $0.688$ .

### **6.2.2 Characterization of Polypropylene and PP Composites in DSC**

Differential Scanning Calorimetry is used to learn the thermal transition of a polymer when they are heated. DSC determines crystallization, melting and glass transition temperatures of a polymer.

Crystallization is a process involving the regular arrangement of chains and is consequently associated with a large negative entropy change. The alignment of polymer chains at specific distances from one another to form crystalline nuclei will be favoured when intermolecular forces are strong. The greater the interaction between chains and easier they can pack the greater the energy change will be. Thus symmetrical chains and strongly interacting chains are more likely to form stable crystals ( Rayan; 1999 ).

Kim et al. (1997) studied, multiple melting characteristics of i-polypropylene by DSC. Melting of i-polypropylene crystallized at different temperatures (  $T_c$  ) was investigated as a function of the heating rate. Figure 6.2 shows DSC melting thermograms of the i-polypropylene crystallized  $T_c$  of at  $110$  and  $120\text{ }^\circ\text{C}$ . At  $110\text{ }^\circ\text{C}$  from Figure 6.2, at a scan rate of  $32\text{ }^\circ\text{C} / \text{min}$  melting temperature (  $T_m$  ) is higher than did in  $16\text{ }^\circ\text{C} / \text{min}$ . This is due to superheating effect. At scan rate  $8\text{ }^\circ\text{C} / \text{min}$  and lower, a new melting peak at higher temperatures appeared. At  $T_c$  of  $120\text{ }^\circ\text{C}$ , from Figure 6.2 at a  $32\text{ }^\circ\text{C} / \text{min}$  heating rate melting peak is at  $163\text{ }^\circ\text{C}$ . The peak position moves to lower temperatures with scan rates of  $16$  and  $8\text{ }^\circ\text{C} / \text{min}$ . The double melting characteristics might be due to a transition of a metastable crystal form into the stable monoclinic form.



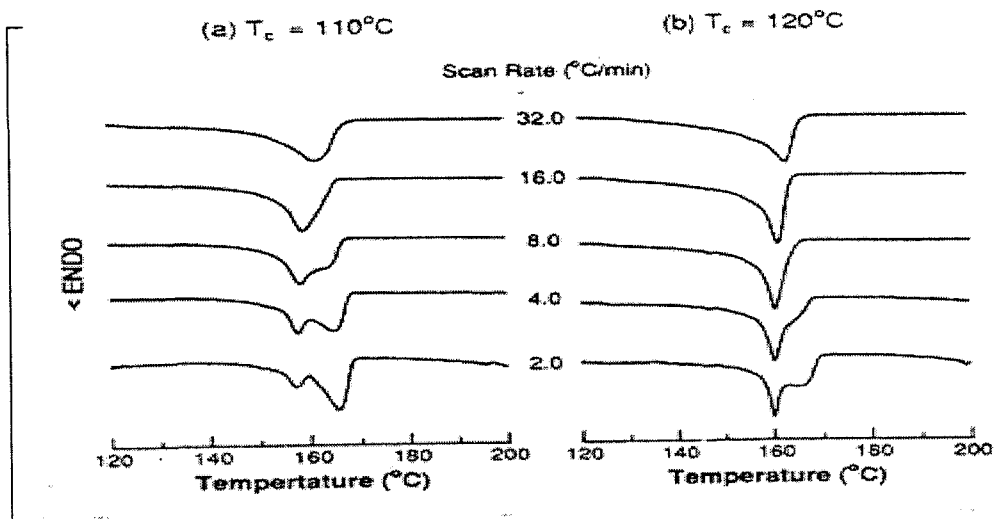


Figure 6.2: Melting thermograms of i-polypropylene at a ) 110 °C  
b ) 120 °C

According to Eder (1999) crystallization always starts from certain spots within the material or on its surface. If the average distance between nucleation sites on the wall surface is small enough a crystallization front starts at the wall.

The crystallization of polymers are generally found by using Avrami equation as seen in Equation 6.1 ( Meares; 1965).

$$\ln ( 1-\theta )= K \times t^n \quad 6.1$$

Where;

$\theta$  = Degree of crystallinity

K= Constant ( describes the rate of crystallization )

n = Exponent varying with the type of nucleation and growth process

Crystallization behaviour of filled polypropylene was studied by McGenity et al., (1982) using DSC. The samples were annealed at 230 °C for 10 min. before cooling at 200 °C / min to the crystallization temperature of 135°C. n values of 3, 2.2 and 1.5 were determined for talc, calcium carbonate, and calcium stearate coated calcium carbonate respectively.

### 6.2.3. Characterization of Polypropylene in TGA

TGA is used to determine the weight loss of polymers when they are heated.

Horrocks and D'Souza (1991) studied physicochemical changes in polypropylene films. TGA curves of 5 mg polypropylene were taken in static air under programmed 5 - 99 K/min range heating rate. Temperature, at the onset ( $T_{\text{ons}}$ ) and maximum mass loss ( $T_{\text{max}}$ ) temperatures of polypropylene are 241 and 371 °C respectively.

The TGA Kinetic analysis is based on the Ozawa method. The reaction rate parameters (activation energy and reaction rate) are calculated. Then the reaction mechanism determination (frequency factor) and isothermal analysis (rate constant and reaction time) are performed. The algorithms are described in Equation 6.2 .

According to Ozawa principle the reaction mechanism is;

$$G(x)=A*\varnothing$$

6.2

Where;

$$\varnothing = \exp(-E/RT) \times dt = \text{reduced time}$$

E= Activation energy

R = Constant

T = Temperature

t = Time

A= Frequency factor

At any temperature T the degree of thermal degradative conversion  $\alpha$ , A is the Arrhenius factor, E is the apparent activation energy of the thermal degradation, R is gas constant. Ozawa shows that this equation may be integrated and solved if A, (1-x), and E are independent of T and both A and E are independent of  $\alpha$ . Horrocks and D'Souza (1991) Equation 6.3 describes the Ozawa kinetic more clearly.

$$d\alpha/(1-\alpha)^n = A/\beta \times \exp(-E/RT) \times dT \quad 6.3.a$$

Where;

$\alpha$  = Degree of degradation conversion

$\beta$  = Rate of heating

For pp degradation n can be assumed to be 1

$$\ln (d\alpha/dT \times (1/(1-\alpha)^n)) = \ln(A/\beta) - E/RT \quad 6.3.b$$

In a TGA curve where the reaction is of the n-th order, weight loss C is equivalent to reaction percent x, but when the sample is polymer x is not necessarily equivalent to the reaction percent C. That is a product resulting from the cutting of a chain need not volatilize at the same temperature which cause the chain to broken. Accordingly, the relation between the weight loss bond ratio of main chains which are broken may be expressed in Equation 6.4, 6.5.( Shimadzu; 1999). Approximating E/RT equals 20, plot of  $\log\beta$  versus 1/T at constant  $\alpha$  given a straight line having a slope of  $-0.4567(E/R)$  (Horrocks, D'Souza; 1991).

$$1-C = (1-x)^{L-1} (1+x (N-L)(L-1)/N) \quad 6.4.a$$

Where;

N :Degree of polymerization at initial stage

L : Degree of polymerization in smallest non-volatized polymer segment

$$C = 1 - (1-x)^{L-1} (1 + (L-1)x) \quad 6.4.b$$

The Equation 6.4.b is simpler form of the Equation 6.4.a.

$$G(x) = -\log(1-x) \quad 6.5$$

The Ozawa and similar kinetic treatments cannot be applied in any case where parallel, competitive reactions occur, and this condition is likely to hold following the introduction of oxidative reaction centers within the polymeric backbone.( Horrocks and D'Souza ;1991) .

### 6.3 Polypropylene Composites Mechanical Behaviour

The properties of composite materials are determined by the properties of the components, by the shape of the filler phase, by the morphology and the nature of the interface between the phases. An important property of the interface greatly affect mechanical behaviour of the composites.

In principle fillers can modify the mechanical characteristics of a polymer in two ways. First the properties of the particles themselves for example particle size, shape and modulus have a direct effect on the properties of composite, second, can lead to changes in micromorpholgy which may give rise to differences in bulk properties ( McGenity et al.; 1992 ).

The elastic modulus and strength of the composites were calculated according to Equation 6.6 and 6.7 respectively ( Crawford; 1981 )

$$E_c = E_m(1-V_f) + E_f V_f \quad 6.6$$

Where,

$E_c$  = Young modulus of the composite

$E_m$  = Young modulus of the medium

$E_f$  = Young modulus of the filler

$$\sigma_c = \sigma_m(1-V_f) + \sigma_f V_f \quad 6.7$$

$\sigma_c$  = Stress at peak of composite

$\sigma_m$  = Stress at peak of medium

$\sigma_f$  = Stress at peak of filler

Svehlova and Poloucek (1993), studied on the mechanical properties of talk filled polypropylene. Composites were prepared by using KO-kneader and dispersing agents were added to the preparation. The mixture is injection molded and pelletized. Mechanical tests were performed by Instron TT-CM. Young modulus, yield point and ultimate tensile elongation were studied. All three mechanical quantities increase slowly with decreasing particle size. The

composite values are lower than those for unfilled polymers. Composites with a matrix being more tough have little higher toughness compared to composites having a matrix less tough. The weak dependence of toughness of talc filled polypropylene in comparison to polypropylene filled with spherical calcium carbonate is probably effected by the plate-like form of the talk particles. With increasing talc content polypropylene filling gives more than double the value growth of Young's modulus of polypropylene -talc composite. Composite ultimate elongation and tensile impact strength decrease with increasing filler content.



# Chapter VII

## Materials and Methods

### 7.1 Characterization of Natural Zeolite

In this project, five different sources of natural zeolites are studied. The zeolites were taken from Gördes 1<sup>st</sup> mine, Gördes 2<sup>nd</sup> mine, Bigadiç, Kıranköy, İncal .

For zeolite characterization Fourier Transform Infrared Spectroscopy (FTIR), Thermal Gravimetric Analyzer (TGA) techniques were used. For FTIR characterization, ground zeolite particles were mixed with KBr and compressed into 1cm pellets under 8 tons force. The IR spectra of the pellets were taken by transmission techniques using Shimadzu 8601 FTIR spectrophotometer. For TGA analysis the samples were heated at 10 °C/ min from 25 °C - 800 °C by using Shimadzu 51 TGA.

### 7.2 Polypropylene Characterization

Two different types of pp (Aldrich pp and Petkim pp) are characterized by FTIR, Differential Scanning Calorimetry (DSC), TGA, analysis were made. Films prepared by pressing molten pp between two microscope slides were studied by transmission technique. DSC curves of the films were obtained by heating the films at 5-20 °C/min heating rate in the range of 25-300 °C in Shimadzu 50. TGA analysis of the films were made by heating the films, at 5°C/min heating rate in the range of 25- 1000 °C. N<sub>2</sub> flow rate was 15 ml/min in the experiments. Aldrich and Petkim polypropylene was in powder and pellet form respectively. The particle size of Aldrich polypropylene was found by sedimentation in propanol. The Stoke's law was used in Equation 7.1 for the determination of appropriate particle size.

$$v = (\rho_s - \rho_f)gx^2 / 18\mu \quad 7.1$$

(McCabe et al.; 1985)

Where;

$\rho_s$  = Density of solid

$\rho_f$  = Density of fluid

$g = 9.81 \text{ m/s}^2$

$x$  = Particle size

$\mu$  = Viscosity of fluid

The particle size of Aldrich pp was in the range of 2.63 and 100  $\mu$ .

### **7.3 Size Reduction ( Ball Milling )**

Gordes 1 zeolite was broken into small parts, by using a hammer. Then it was placed into Multifix Ball Mill. The cylinder size was 59.5 mm in radius and 76 mm height. The particle size of zirconia balls was 9.48 mm. 50 % of the volume was filled with the balls. The 50 % of the space between the balls was filled with zeolite and ethanol. Zeolite is ground at a speed of 92 rpm for 4 hour. After ball-milling mixture was heated at 80 °C to evaporate the ethanol and then sieved to take the fraction passing through a 45  $\mu$  sieve. The natural zeolite particle size analysis was made by using Coulter particle size analyzer in Petkim A.S.

### **7.4 Fractionation of Zeolite Particles into Different Sizes**

Ground zeolite particles were put into water in a beaker. The liquid height was 10 cm in the beaker. The mixture was kept there for 25 h at 25 °C. According to Stoke' s law from Equation 7.1, 2 $\mu$  and smaller particles remain in suspension in water at the end of 25 h. The suspension is separated from the precipitate by decantation. After evaporation of water of the suspension at 80°C, zeolite particles of 2 $\mu$  or smaller size were obtained.

Some of the natural zeolites were washed by Akdeniz (1999) to remove impurities from the surface. The washing process was done for particles about 1 or 2 mm in size and was carried out at 90 °C with hot water. Dirty water was thrown away and the zeolite particles were air dried (Akdeniz; 1999).

Bigadiç zeolite was acid leached by Özkan (1996). The leaching was done using 1.6 mol/dm<sup>3</sup> HCl at 106 °C for 3 hour. The zeolite solution ratio was 1g/20 ml.

The unwashed and washed dried zeolites was ground in a ball mill and sieved to obtain particles smaller than 45µ. The unwashed zeolite was also wet milled in ethanol dried and separated into 2µ size by sedimentation in water and then the zeolites were modified.

### **7.5 Modification of Zeolite Particles**

2µ natural zeolite particles were modified with different additives. Modification was made to prepare a homogenous dispersion and to prevent the agglomeration of particles in pp film.

Modification was made by stearic acid, calcium stearate and PEG 4000. Modification was made by the method given by Domka (1982). Zeolite was mixed with 50% aqueous ethanol solution having 10% modifier. Zeolite solution ratio was taken as 1:0.3 on weight/ volume basis. The mixture was kneed at 40°C then dried in a vacuum oven at 110°C under 400 mbar pressure, for 3 h. The same method was used for stearic acid, calcium stearate and PEG 4000 modification of natural zeolite. As a result of the experiments PEG 4000 was chosen as the most appropriate modifier.



## **7.6 Preparation of Zeolite Polypropylene Composites**

For preparation of composites three different methods were performed. These are pressing between two microscope slides, hot pressing and extrusion.

### **7.6.1 Pressing Between Microscope Slide**

Aldrich pp and zeolite was mixed and melted on a microscope slide on a hot plate. The molten mixture was pressed between two microscope slides into a thin film. The films were taken from the slides after cooling down to room temperature on laboratory bench. 0.030 g pp was mixed with zeolite in the range of 0 to 50 % wt.

### **7.6.2 Pressing in Hot Press**

A hot press described by Ulutan (1994) as shown in Figure 8.1 was used for the preparation of polypropylene composite films from Aldrich polypropylene and Polinas polypropylene. 10 g polypropylene was spread evenly between two polyester films, and placed between two stainless steel plates and heated to about 200°C under 100 bar pressure. The mould was opened after cooling down to 120 °C. 0 - 40 % zeolite- Aldrich polypropylene composite films were prepared. Films having 6 % zeolite from fibers obtained in extrusion of Petkim pp were also obtained by hot pressing.

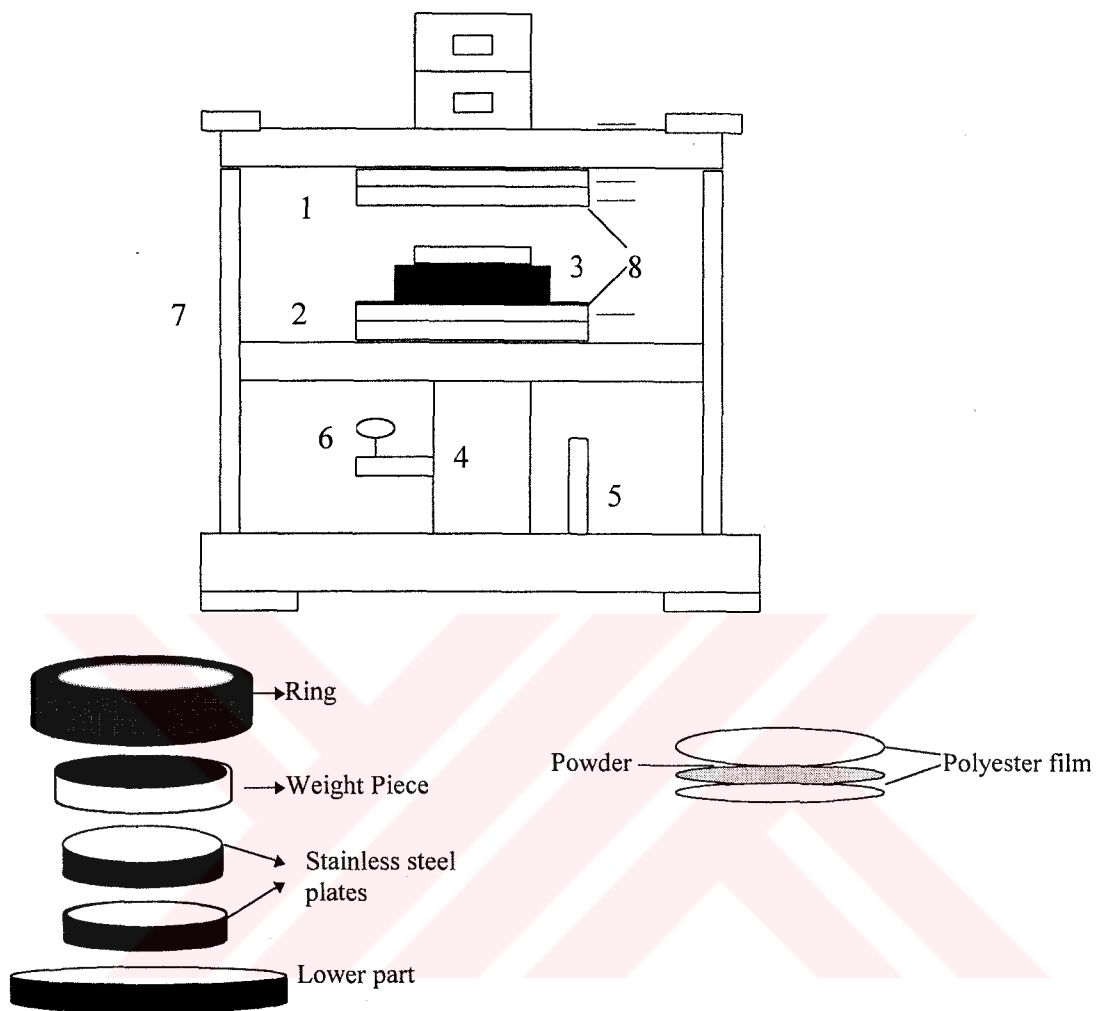


Figure 7.1: Hot Press 1. upper heater 2. lower heater 3. ring 4. hydraulic part 5. pressurizing wing 6. pressure indicator 7. temperature control 8. cooling water outlet and inlet.(Ulutan; 1994)

### 7.6.3 Extrusion

0 - 6 % zeolite Petkim polypropylene composites were prepared by extrusion in Petkim (Aliaga) using Tonaible Plastic Machinery extruder. The temperature of the extruder was 260 °C, screw control was 550 rpm. Length to diameter ( L/D) ratio was 24. 45 $\mu$  and 2 $\mu$  particle size zeolites were used. The

cast film was quenched by a polished drum cooled by tap water and was drawn by rollers with controlled speed.

## **7.7 Characterization of Composite Films**

The same experimental conditions in characterisation of pure pp films were used. Heating and cooling curves of the composites prepared in hot press were also obtained using Setaram DSC-92 at Ege University. 10 °C /min and 2 °C /min rates were used in heating and cooling respectively. Each sample was twice heated and cooled twice under the same conditions.

### **7.7.1 Optical Micrography**

Optical micrograph of zeolite, pp, modified zeolite, and composite films were taken both in transmission and reflection with optical microscope fitted with Olympus BX-60, Olympus CH40 respectively. Optical microscope is connected to fitted Olympus PM-C35B camera.

### **7.7.2 Density Determination**

Density of the 34 mm diameter films were measured by Archimede's principle using the density kit of Sartorius YDK 01 balance. The weight of the sample and the weight the water displaced by the sample were measured. The samples lighter than water were placed under a basket immersed in water in order to measure their weight in water. The samples heavier than water is placed on the basket in order to measure their density.

### **7.7.3 Mechanical Test**

Mechanical Testing of extruded and hot pressed films were performed by Testometric AX M 500. Dog bone samples were prepared according to ASTM D-638 standard. The tensile tests on these films were carried out at a speed of

300 mm/min. Extruded films were also tested using Instron 1000 tensile tester present in Polinas. Strips of 1 cm width and 30 cm length were stretched at 300 mm/min rate according to ASTM D-882.



## Chapter VIII

### Results and Discussion

In this work preparation of polypropylene-natural zeolite composite films was investigated. The effects of a number of parameters such as natural zeolite type, zeolite content, modifier, modification effect and preparation techniques were investigated in some depth.

In this thesis, five different types of natural zeolites were examined. Most proper natural zeolite for the preparation of composites was selected by characterizing of these zeolites. The selected natural zeolite was modified to prevent the agglomerations in the composite. Composites were prepared by using three different methods; pressing between microscope slide, hot press and by extrusion method. The natural zeolite types and their properties are given in Table 8.1. Table 8.2 gives the comparison of the composite preparation techniques.

Table 8.1: Natural zeolites and their physical properties

Zeolite Types	Colour	Density (g/cm <sup>3</sup> )
Kıranköy	White-light green	1.4
İncal	Brownish	2.09
Bigadiç	Greenish	2.13
Gördes 1	White-pink	1.8
Gördes 2	White-yellow	1.76

As seen in Table 8.1 Kıranköy type natural zeolite is white and light green in colour and it has the lowest density between five different type natural zeolites. The density of Kıranköy is 1.4 g/cm<sup>3</sup>. İncal is brownish and the

density of İncal is 2.09. Bigadiç type natural zeolite is greenish and has 2.13 g/cm<sup>3</sup> density. Gördes 1 is white-pink in colour and the density is 2.01 g/cm<sup>3</sup>. Gördes 2 is white yellow in colour and the density is 1.76 g/cm<sup>3</sup>.

Table 8.2: Effects of preparation techniques in polypropylene-zeolite composite

Preparation Techniques	Filler percentage	Uniformity of thickness	Distribution of filler	Thickness of the films	Tearing
Microscope slide press	0	Uniform	Uniform	20 μ	-
	5 %	Uniform	Uneven	22 μ	-
	10 %	Uniform	Uneven	24 μ	-
	20 %	Uniform	Uneven	32 μ	-
	30 %	Uniform	Uneven	22 μ	-
	40 %	Uniform	Uneven	24 μ	-
	50 %	Uniform	Uneven	15 μ	-
Extrusion	0	Non-uniform	Uniform	10-50 μ	-
	2 %	Non-uniform	Uneven	30-100 μ	-
	4 %	Non-uniform	Uneven	50-80 μ	+
	6 %	-	Uneven	30-50 μ	+
Hot Press	0	Uniform	Uniform	560 μ	-
	10 %	Uniform	Uneven	760 μ	-
	20 %	Uniform	Uneven	850 μ	-
	30 %	Uniform	Uneven	870 μ	-
	40 %	Uniform	Uneven	640 μ	-

As seen in Table 8.2, the microscope slide pressed composite films have uniform thickness and the thickness of the films are between 15-32 μ. In the microscope slide pressed composites, filler distribution is uneven. In extruded films all films have non-uniform thickness and the thickness of the films are

distributed in a large scale. They are between 10-100  $\mu$ , and also the distribution of the fillers are uneven. Due to large particle size uneven thickness and non uniform distributions of the fillers, tearing is observed in some of the films. Other preparing method was hot press method. The distribution of the filler was also uneven thickness of the film prepared by hot press method was very thick (560-870  $\mu$ ). This was the main problem of this method.

## 8.1 Characterization of Polypropylene, Natural Zeolite, Polypropylene - Natural Zeolite Composites by FTIR Spectroscopy

For having information about the chemical composition of the materials and chain structure FTIR spectroscopy were used. As discussed in chapter 6, the FTIR spectra of the polymers were analyzed by preparation of transparent films. The same technique was used for polymer composite samples. Natural zeolites FTIR spectra were taken by preparation of KBr pellets as discussed in chapter 6.

### 8.1.1 Characterization of Natural Zeolite by FTIR Spectroscopy

FTIR spectrum of a Gördes 2 natural zeolite is given in Figure 8.1 and all characteristic peaks of the natural zeolite given in Table 6.1 are observed in the spectrum.

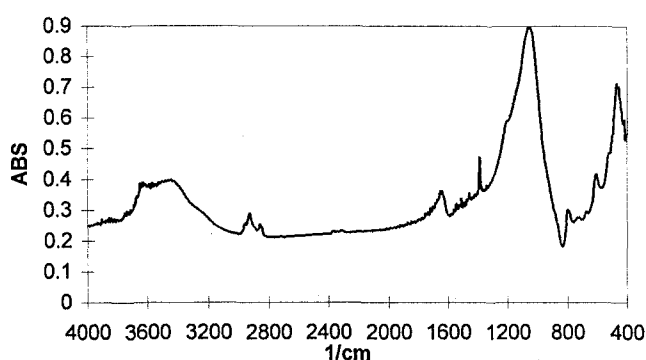


Figure 8.1: FTIR Spectrum of Gördes 2 natural zeolite

There are small peaks related with C-H stretching vibration of organic impurities at 2800  $\text{cm}^{-1}$  in Gördes 2 and İncal zeolites.

The  $609\text{ cm}^{-1}$  peak was chosen to determine the amount of the clinoptilolite in the natural zeolite (Krivacsy et al.;1992). To make a decision about choosing the most proper natural zeolite, the absorbance of  $609\text{ cm}^{-1}$  peaks in FTIR spectra of zeolites were normalized to the same absorbance scale by dividing the peak height in mm to the maximum absorbance of the axis and are shown in Figure 8.2.

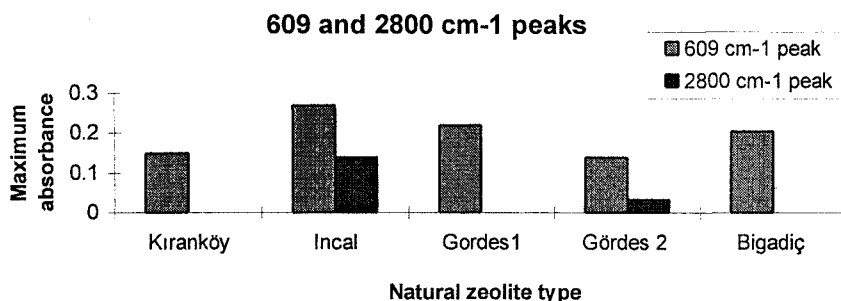


Figure 8.2: Absorbance of typical clinoptilolite peak at  $609\text{ cm}^{-1}$  and hydrocarbon peak at  $2800\text{ cm}^{-1}$  for different natural zeolite.

As seen in Figure 8.2 İncal and Bigadiç zeolites have higher absorbance values, that indicates higher clinoptilolite content. The higher hydrocarbon contents are in İncal and Gördes 2.

Effect of modification was indicated by FTIR spectroscopy. Modification of zeolite was made to prepare a homogenous dispersion and to prevent the agglomerations of particles in polypropylene films. To modify the ground zeolite particles three different modifiers (calcium stearate, stearic acid and PEG (4000)) 3 percent modifiers were used in all modifiers. The FTIR spectra of modified zeolites are shown in Figure 8.3. The C-H symmetric peaks were observed in FTIR spectra of the modified composites.  $-\text{CH}_2$  asymmetric stretching at  $2930\text{ cm}^{-1}$  and symmetric stretching at  $2970\text{ cm}^{-1}$ .



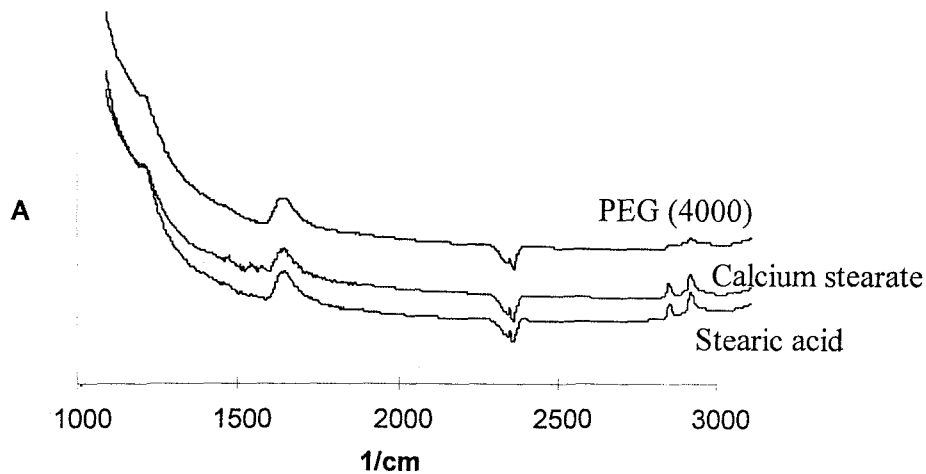


Figure 8.3: FTIR spectra of Calcium stearate, Stearic acid, PEG ( 4000 ) modified zeolites.

Some of the natural zeolites were washed to remove impurities from the surface of the natural zeolite. The washing process for particles about 1 or 2 mm in size was carried out at 90<sup>0</sup>C. Natural zeolite particles were put into a 90 <sup>0</sup>C hot water and washed, then the hot dirty water was thrown away by decantation. The effects of washing, modification and particle size on the clinoptilolite content of Gördes 1 which was dried at 85 <sup>0</sup>C under 200 mbar pressure is shown in Figure 8.4. The 609 cm<sup>-1</sup> peak was normalized for this purpose.

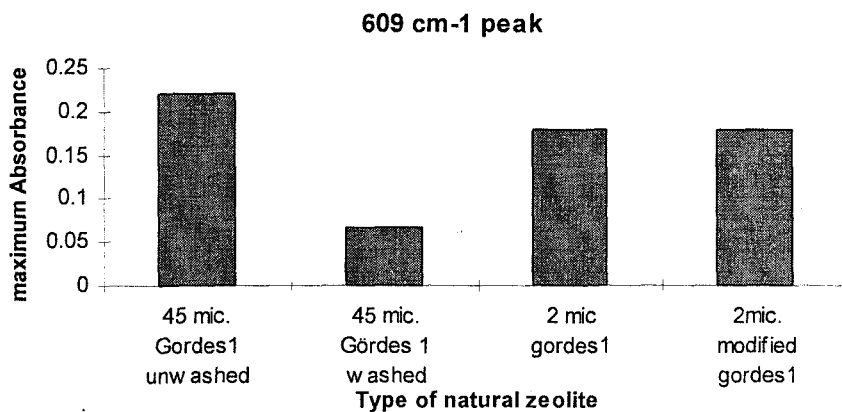


Figure 8.4: Effect of washing, modification and particle size on clinoptilolite content of Gördes 1.

As seen in Figure 8.4 impurities and some of the clinoptilolite were thrown away by the way of washing process for Gördes 1 natural zeolite. Modification does not effect the clinoptilolite content of Gördes 1 natural zeolite.

Effect of washing on clinoptilolite and hydrocarbon content of Gördes 2 is shown in Figure 8.5. From Figure 8.5 it is understood that the washing process decreased in a small extent the clinoptilolite content and appreciably hydrocarbon content of Gördes 2 zeolite. For zeolite the impurities from the surface of the Gördes 2 zeolite are removed mainly by the washing effect.

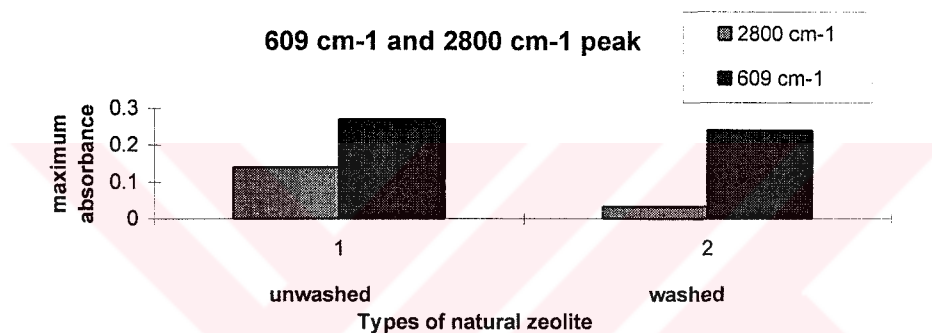


Figure 8.5: Effect of washing on clinoptilolite and hydrocarbon content of Gördes 2.

Effect of washing and acid leaching on Bigadiç zeolite was investigated. The comparison is shown in Figure 8.6.

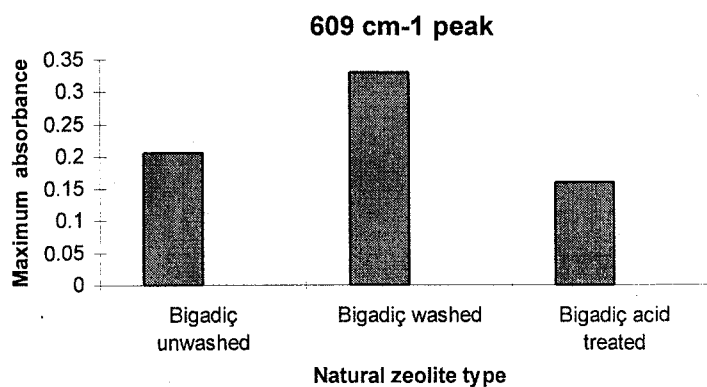


Figure 8.6: Effect of washing and acid leaching on clinoptilolite content of Bigadiç zeolite.

Bigadiç zeolite was treated by HCl (1.6 N) ( Özkan; 1998 ) . Normalized absorbance values are given in Figure 8.6.

Washing process has different effects on clinoptilolite of Gördes 1, Gördes 2 and Bigadiç zeolites. These effects may due to the natural zeolite mines. Each zeolite sample was taken from different zeolite rocks. They may contain different chemicals and impurities. These notable changes may effect the clinoptilolite content of zeolites.

### 8.1.2 Characterization of Polypropylene by FTIR Spectroscopy

For characterization of polypropylene, 10-100  $\mu$  transparent films were prepared from Aldrich and Petkim polypropylene and were used in FTIR spectroscopy. The FTIR spectrum of the polypropylene is shown in Figure 8.7. Characteristic peaks of polypropylene seen in Table 6.2 were all present in the spectrum of polypropylene.

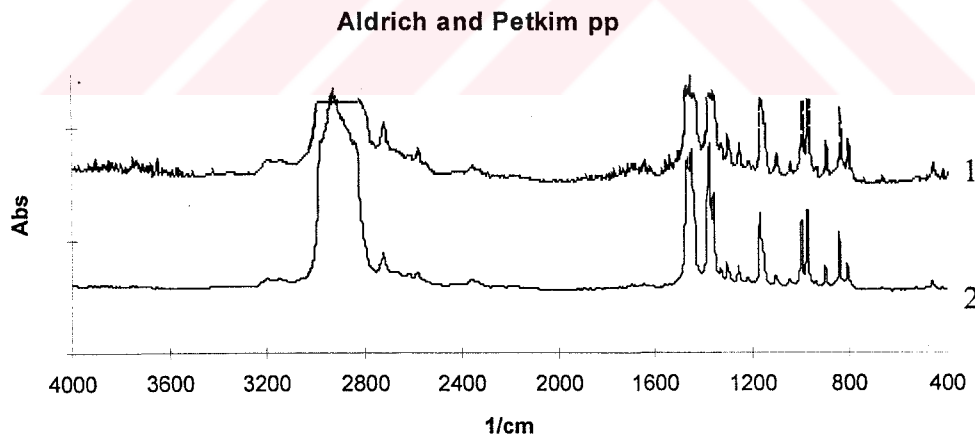


Figure 8.7: FTIR Spectrum of Polypropylene 1: Aldrich polypropylene  
2: Petkim polypropylene

The broad peaks at  $3100\text{ cm}^{-1}$  and  $1640\text{ cm}^{-1}$  are due to the antioxidant in polypropylene.

### 8.1.3 FTIR Spectrum of Polypropylene-Natural Zeolite Composites, Determination of Zeolite Content and Isotacticity Index

Polypropylene and 10% wt zeolite composites were prepared by heating the mixture on a glass slide on hot plate and compressing the molten mixture between two microscope slides. Some of the polypropylene zeolite composites blackened during this process. The FTIR spectra of these composites are given in Figure 8.8. Normalized clinoptilolite contents of composites found from the absorbance of  $609\text{ cm}^{-1}$  peak are given in Figure 8.9.

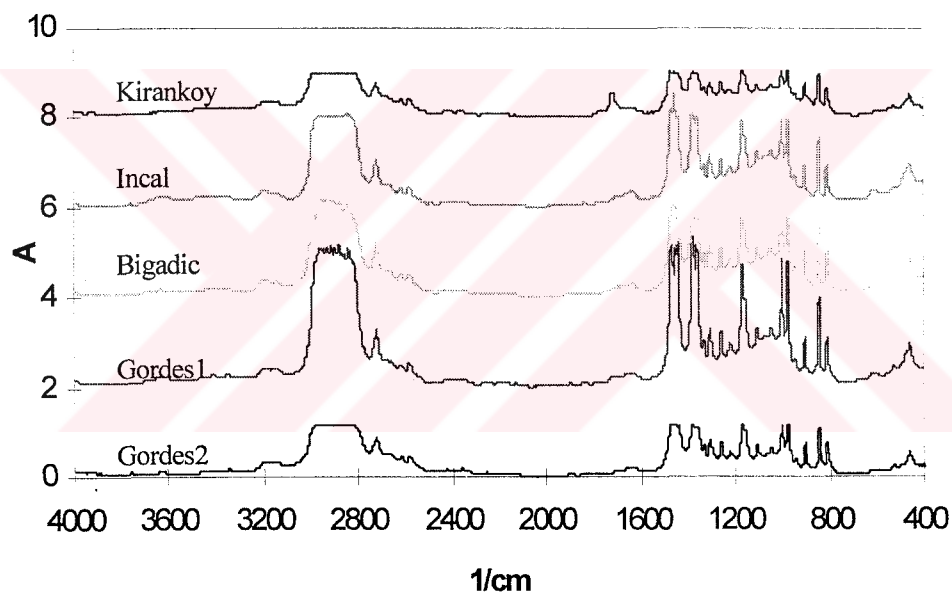


Figure 8.8: FTIR Spectra of 10 % zeolite filled Aldrich polypropylene composites.

As seen in Figure 8.8 the zeolite filled composites FTIR spectra are already the same. The differences are observed because of the difference in

zeolite fraction. As it was mentioned before in section 6.1.1 and 6.2.1 all characteristic zeolite and polypropylene peaks were observed in composite films.

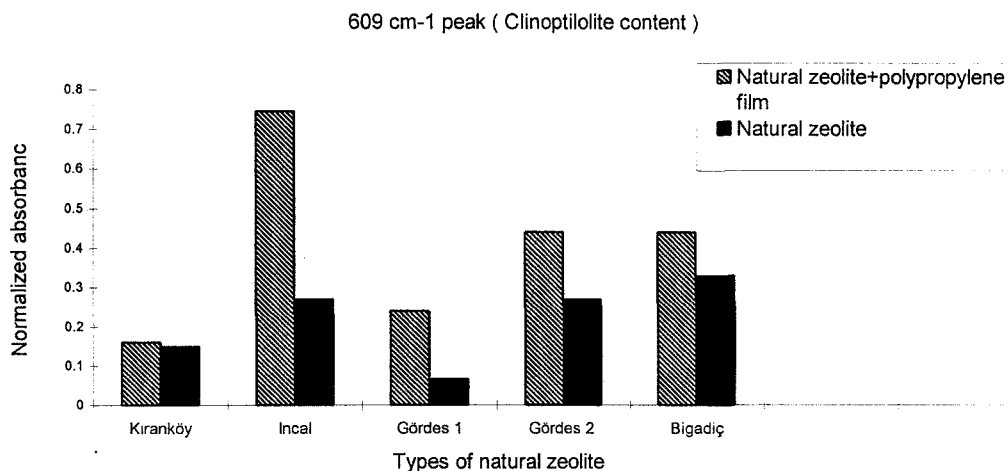


Figure 8.9: Natural zeolite and 10 % natural zeolite polypropylene composites 609 cm<sup>-1</sup> peak

As seen in Figure 8.9 the 609 cm<sup>-1</sup> peak is greater in polypropylene natural zeolite composites than that of in pure natural zeolite. Since KBr pellets have 1 mg. zeolite / 200 mg KBr and polypropylene films have 10 % zeolite, the films have higher zeolite content. The biggest natural zeolite content is in İncal filled polypropylene composite.

The blackening of the composites may be due to either oxidation of polypropylene or metal ions in zeolites. Iron in zeolites oxidizes the composites and give dark coloured products. The hydrocarbon present in zeolites may also blacken when heated. When polypropylene is oxidized carbonyl groups form as seen in Equation 8.1. The oxidation of polypropylene is prevented by antioxidants added to polypropylene during production. Since zeolites are good adsorbents for small molecules, antioxidants may be adsorbed on zeolites and do not prevent oxidation of polypropylene. The carbonyl group (C=O) formed in polypropylene has a stretching vibration at 1720 cm<sup>-1</sup>. FTIR spectra of

composites seen in Figure 8.10 shows the presence of C=O groups in some samples. The intensity of carbonyl peak of composites are shown in Figure 8.11.

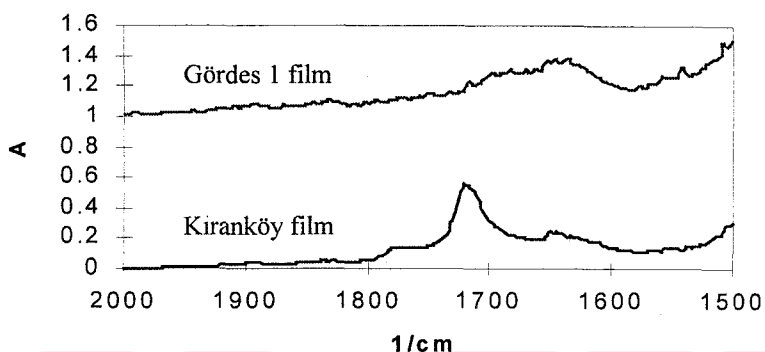
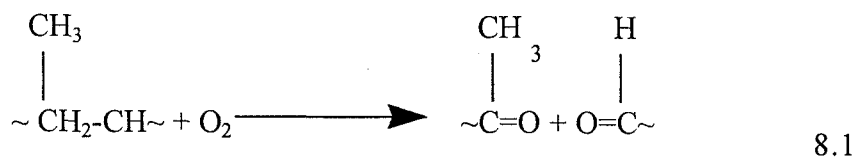


Figure 8.10: C=O group in 10 % Kiranköy and Gördes 1 filled composite films FTIR spectra.

As seen from Figure 8.10 the C=O peak of Gordes 1 zeolite filled composite is smaller than that of in Kiranköy zeolite filled composite.

1720 cm<sup>-1</sup>

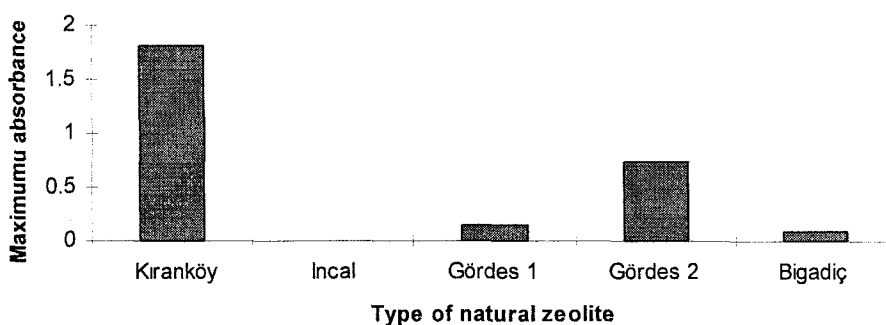
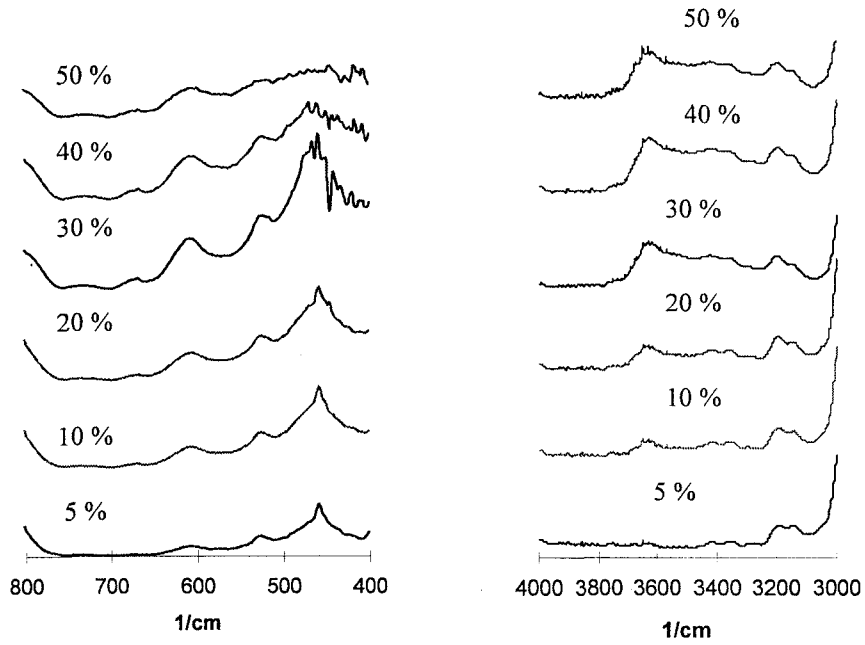


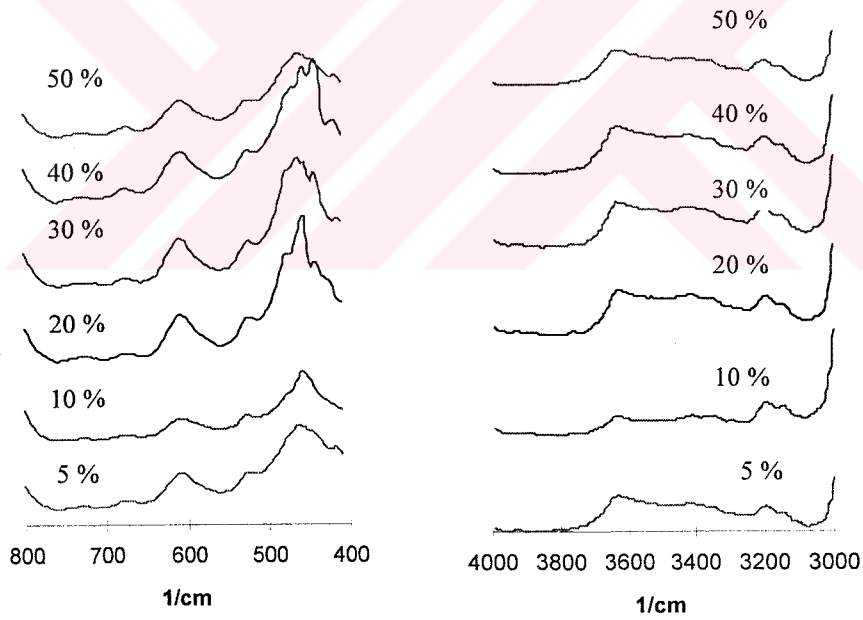
Figure 8.11: 1720 cm<sup>-1</sup> peak in 10 % natural zeolite polypropylene composites.

As seen in Figure 8.11 the biggest C=O group concentration is in Kiranköy type zeolite filled polypropylene composites.



a.1 Gördes 1 609  $\text{cm}^{-1}$  peak

a.2 Gördes 1 3700  $\text{cm}^{-1}$  peak



b.1 Bigadiç 609  $\text{cm}^{-1}$  peak

b.2 Bigadiç 3700  $\text{cm}^{-1}$  peak

Figure 8.12 : FTIR spectra of a. Gördes 1 and b. Bigadiç type natural zeolite composites

Composites with different zeolite content were prepared by using Bigadiç and Gördes 1 type natural zeolite. The concentrations of zeolites in these composites were 5, 10, 20, 30, 40, 50 percent by weight. 609  $\text{cm}^{-1}$  clinoptilolite content peak was investigated on Bigadiç and Gördes 1 type natural zeolite composites. Figure 8.12 shows the FTIR spectra of some of these composites.

In Figure 8.12 the Gördes 1 and Bigadic type natural zeolites 609 and 3700  $\text{cm}^{-1}$  peak is shown. From Figure 8.12 a.1 the 5% zeolite filled composite shows the smallest peak at 3700  $\text{cm}^{-1}$  absorbance value and the largest isolated OH bond content is seen in 50% zeolite filled composite. The same explanation can be made for 609  $\text{cm}^{-1}$  peak and for Bigadic type natural zeolite 3700 and 609  $\text{cm}^{-1}$  peaks. Normalized clinoptilolite content of composites is as shown in Figure 8.13.

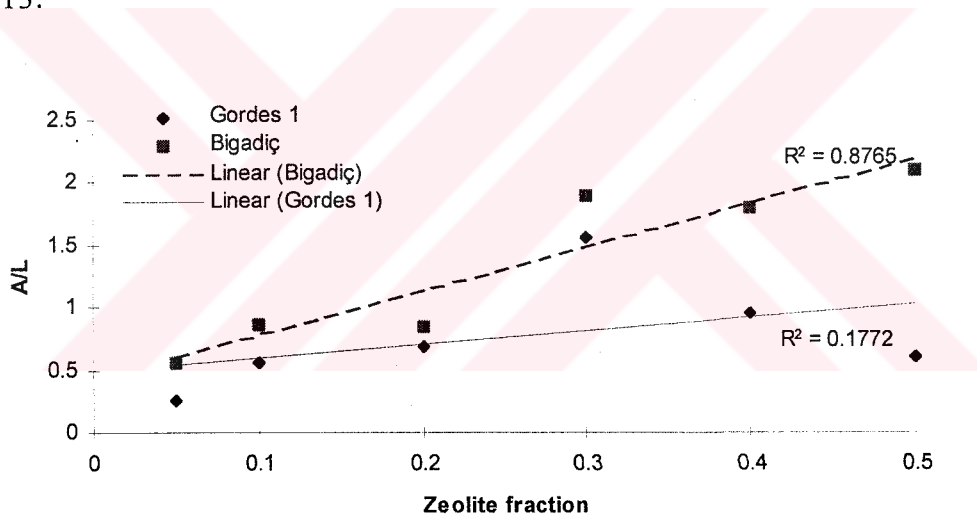


Figure 8.13 : Bigadiç and Gördes 1 type natural zeolite filled composites clinoptilolite content, 609  $\text{cm}^{-1}$  peak.

As seen in Figure 8.13 Bigadiç zeolite filled composites have higher clinoptilolite content as seen in Figure 8.4. Because of the non-homogenous dispersion of zeolites in composites the linear regression coefficients of lines



for Bigadic filled composites is 0.865 and for Gördes 1 filled composites it is 0.1772. The linear regression coefficient of Gördes 1 filled is smaller than Bigadic filled composite.

Isolated OH stretching bond at  $3700\text{ cm}^{-1}$  is a characteristic natural zeolite peak as indicated in Table 6.1.  $3700\text{ cm}^{-1}$  peak is examined for Bigadiç and Gördes 1 type natural zeolite filled composites. A/L ratio versus zeolite fraction for  $3700\text{ cm}^{-1}$  peak is given in Figure 8.14.

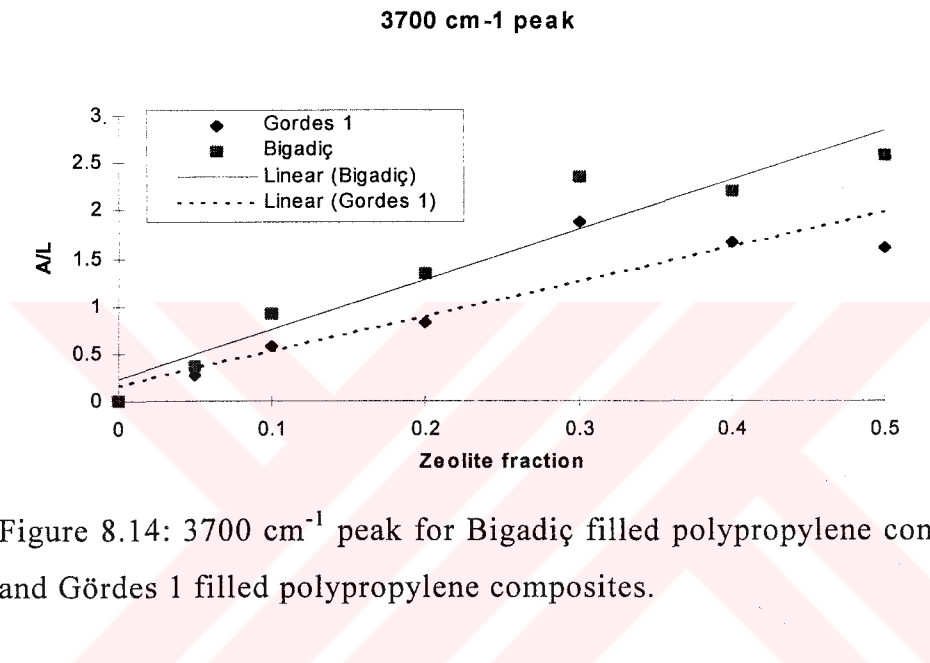


Figure 8.14:  $3700\text{ cm}^{-1}$  peak for Bigadiç filled polypropylene composites and Gördes 1 filled polypropylene composites.

As shown in Figure 8.14 Bigadic zeolite filled composites have higher -OH stretching values than Gördes 1. From Table 6.1 and 6.2 at  $1060\text{ cm}^{-1}$  zeolite has a peak which is small and sharp and also at the same absorbance values polypropylene has a wide peak. Figure 8.15 shows characteristic of pp peak at  $1060\text{ cm}^{-1}$  and  $820\text{ cm}^{-1}$  are characteristic of pp and the peak at  $1060\text{ cm}^{-1}$  for zeolite. In determination of zeolite/pp ratio in composites, the absorbance of  $1060\text{ cm}^{-1}$  peak of the composite is resolved into zeolite (b) and pp (a) fraction as indicated in Figure 8.15. The b/a versus zeolite content is linear as seen in Figure 8.16. The ratio of b and c; (the absorbance of  $820\text{ cm}^{-1}$  peak characteristic of pp) versus zeolite content was also linear as seen in Figure 8.16.

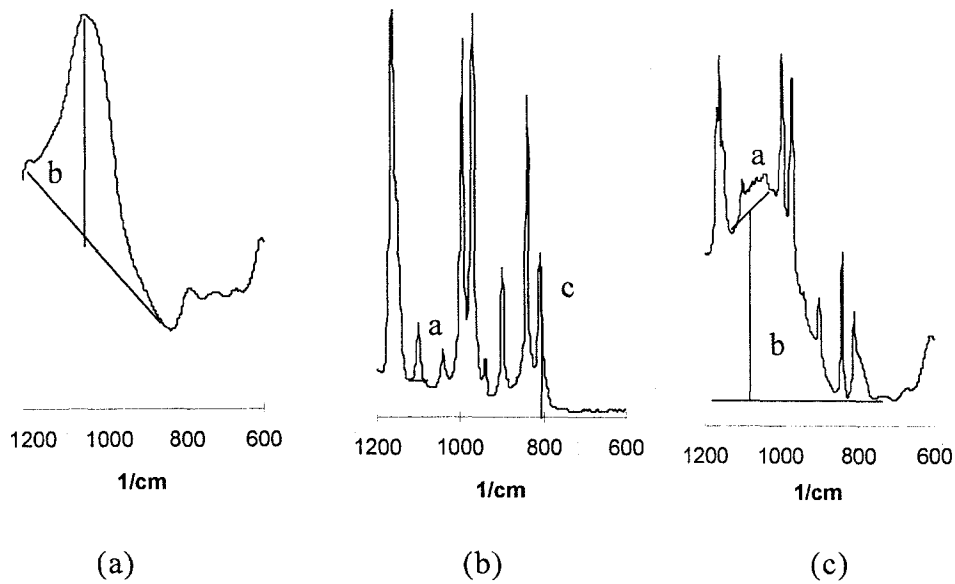


Figure 8.15 : FTIR spectra of a) zeolite, b) polypropylene, c) 20 % zeolite filled polypropylene composite 1060 and 820  $\text{cm}^{-1}$  peak.

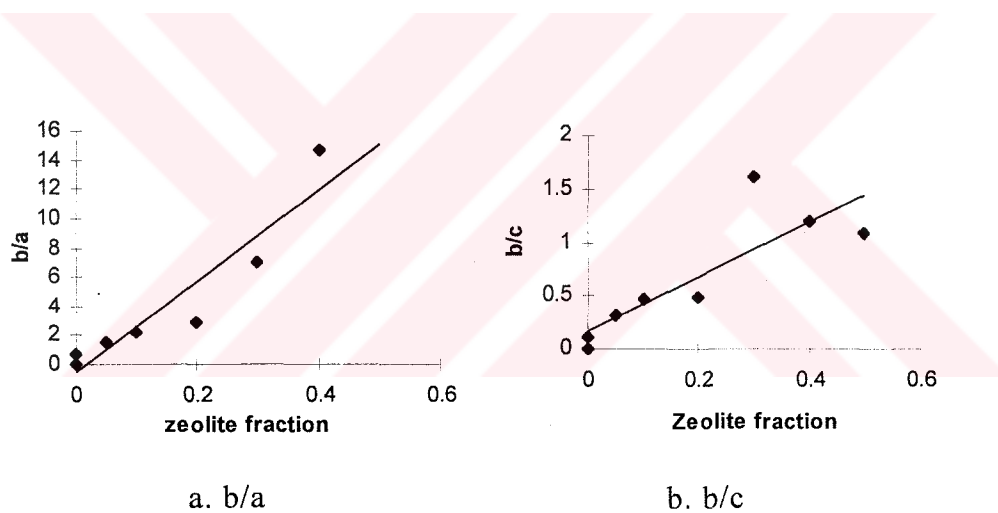


Figure 8.16: b/a and b/c versus zeolite fraction

Since absorbance of  $3700 \text{ cm}^{-1}$  and  $609 \text{ cm}^{-1}$  peaks were very small for thin films prepared by extrusion, the b/a or b/c versus zeolite fraction calibration curves in Figure 8.16 were used to determine their zeolite content. These films had agglomerates and uneven dispersion of zeolite composites. By using the calibration curve extruded films intended to have 2, 4 weight percent zeolite actual weight fractions were found and given in Table 8.3.

Table 8.3: Intended and experimental weight fractions of extruded composites.

Intended content of zeolite	1060 cm <sup>-1</sup> normalized values ( found )	820 cm <sup>-1</sup> normalized values ( found )
2 %	27 %	15 %
4 %	23 %	7 %

From Table 8.3 intended and found values of extruded films are very different from each other. Zeolite fraction values for 2 % and 4 % zeolites were found 27 and 23 % respectively from Figure 8.16.a. The values are disconnected from each other and they are very big than expected values. This difference between intended and found values was because of the non-homogenous dispersion in extruded films as it was mentioned before. For 2 and 4 % intended actual content zeolite was found 15 and 7 % respectively from Figure 8.16.b. Especially the 4 % extruded films value ( 7 % ) could be accepted.

Another study on FTIR spectroscopy was made to find the isotacticity index of polypropylene as it is mentioned before in section 6.2.3 the isotacticity index found from dividing the 998 cm<sup>-1</sup> peak to 974 cm<sup>-1</sup> peak ( Horrocks and D'Souza; 1991 ). The typical 998 and 974 cm<sup>-1</sup> peaks are shown in Figure 8.17.

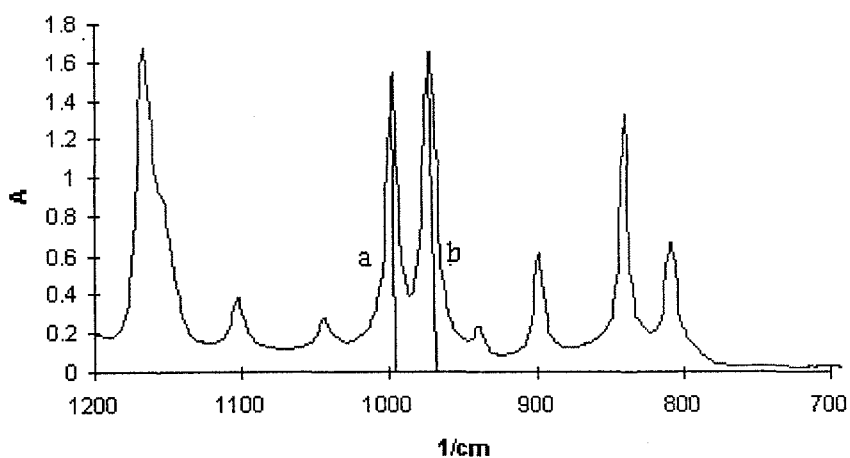


Figure 8.17: Normalized peaks of FTIR spectrum for Aldrich polypropylene.

By normalizing the 998  $\text{cm}^{-1}$ / 974  $\text{cm}^{-1}$  peaks for Petkim, Aldrich polypropylene and microscope slide pressed composites the isotacticity index of polypropylene is found. The a/b isotacticity values are given in Table 8.4.

Table 8.4: Isotacticity values of polypropylene

	a/b
Petkim polypropylene	0.75
Aldrich polypropylene	0.94
5 % zeolite+polypropylene	0.98
10% zeolite+polypropylene	0.81
20% zeolite+polypropylene	0.98
30% zeolite+polypropylene	0.98
40% zeolite+polypropylene	-
50% zeolite+polypropylene	-

As shown in Table 8.4 petkim polypropylene isotacticity is found 0.75 and Aldrich polypropylene isotacticity index is 0.94. Aldrich polypropylene isotacticity is greater than that of Petkim pp. The isotacticity of the polypropylene is used in this study is higher than the isotacticity ( 0.688 ) of the polypropylene used by Horocks and D'Souza ( 1991 ). For composite materials containing 5, 10, 20, 30 % zeolite filled composites isotacticity values are 0.98, 0.81, 0.98, 0.98 respectively. Since the 998 and 975 peaks are not measured for 40 and 50 % zeolite composites, isotacticity of these composite are not calculated.

## **8.2 Selection of the Natural Zeolite and it's Modification for Composite Preparation**

As mentioned before, five different types of zeolites, Kıranköy, İncal, Bigadiç, Gördes 1 and Gördes 2 were characterized for choosing the most appropriate natural zeolite. Gördes 1 was chosen as the proper natural zeolite. For modification of natural zeolite PEG (4000), calcium stearate, and stearic

acid were used. These modifiers and modification effects were mentioned in chapter 3. After modification of natural zeolite by each modifier; PEG (4000) was chosen as the best modifier.

### **8.2.1 Selection of Natural Zeolite**

FTIR spectra of natural zeolites and clinoptilolite content were direct attention to selection of the proper zeolite. İncal and Bigadic zeolites have the highest clinoptilolite content. Gördes 1 and Gördes 2 and Bigadic type natural zeolites were washed. The washing increased the zeolite content of Bigadic zeolite. Washing changes the clinoptilolite content, but it may give extra cost to composite preparation process.

Beside clinoptilolite, hydrocarbon contents in natural zeolite are also important. From Figure 8.2 İncal and Gördes 2 type natural zeolites have higher hydrocarbon content than the other zeolites.

Zeolite filled pp film IR spectra showed that the carbonyl (C=O) groups formed from degradation of pp was the highest for Kıranköy zeolite filled composite.

10 % zeolite filled polypropylene films were prepared and it was observed that some of the composites were blackened during heating. They were blackened may be because of oxidation of hydrocarbon present in natural zeolite. As it's mentioned before in the highest hydrocarbon content was in İncal and Gördes 2 types zeolite and highest carbonyl content was in Kıranköy filled composites. These three types of natural zeolites are eliminated for preparation of composites. Other types of natural zeolites Gördes 1 and Bigadiç types did not have any direct effect on blackening, but Bigadiç type natural zeolite is Greenish and Gördes 1 is pink- white. Since these polypropylene composite films will be used in packaging industry the white coloured one namely Gördes 1 is selected as the most appropriate natural zeolite for composite preparation.

## 8.2.2 Selection of Surface Modifier

Stearic acid, calcium stearate, PEG (4000) were used in surface modification of zeolites. Natural zeolites were modified as discussed in chapter 7.

The aim of surface modification is to obtain homogenous dispersion and to break the agglomerates of zeolites in polypropylene. In dispersion the filler polymer interaction may have a stabilizing effect. Modification of filler could be used for having a good dispersion medium between filler and matrix.

Calcium stearate, stearic acid and PEG (4000) modified natural zeolites were examined by using optical micrography. According to optical micrograph of modified natural zeolites, PEG (4000) was chosen as the appropriate modifier. In Figure 8.18 the optic micrographs of pure natural zeolite and PEG (4000) modified natural zeolite are given.

As seen in Figure 8.18a- the natural zeolite was agglomerated, and after modification by PEG (4000) the agglomerates were broken.

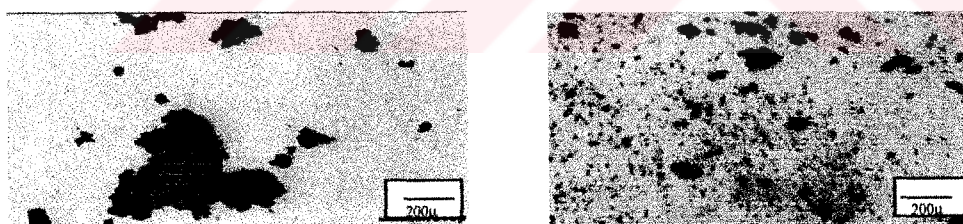
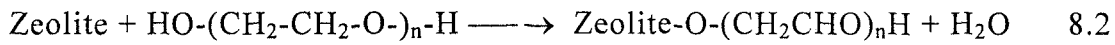


Figure 8.18: The Optic Micrograph of 75 times magnified a- Pure natural zeolite b- PEG (4000) modified natural zeolite.

The maximum agglomerate size was 700 $\mu$  and 150 $\mu$  before and after PEG (4000) treatment. The same effect was not observed under the same conditions for stearic acid and calcium stearate modified natural zeolite. The chemical reaction between PEG (4000) and natural zeolite occurs as seen in Equation 8.2.



As a result, PEG (4000) was chosen as the modifier of natural zeolite.

### 8.2.3 Particle Size of Aldrich pp and Selection of Particle Size of Zeolite

The particle size of Aldrich pp was found by sedimentation rate measurement in water and by using Stoke's law ( Equation 7.1 ). The smallest particle size of pp found as 2.63  $\mu$  and the biggest size found as 100  $\mu$ .

Natural zeolite rocks were ground by using wet grinding technique. Natural zeolites were ground first into small parts of 1 or 2 mm in size. Then they were put into wet milling part. The critical speed of the ball mill calculated from Equation 8.3 ( Reed; 1995) as 92 rpm.

$$W_{CR} = 1/2 R^{1/2} \quad 8.3$$

Where;

R : Mill radius in meter ( m )

After ball milling, ground natural zeolite particles were sieved as discussed in section 7.3. The particle size distribution of zeolite passing through 45  $\mu$  sieve is as seen in Figure 8.19.

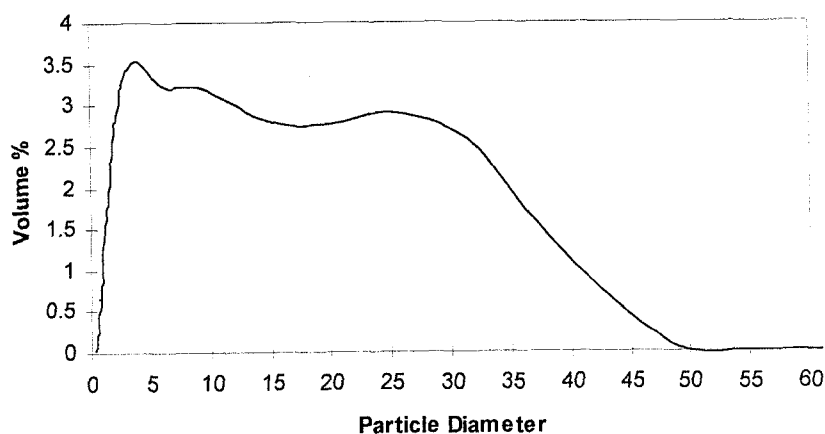


Figure 8.19: Differential volume percent of 45 $\mu$  natural zeolite

As seen from Figure 8.19 all particles are below  $45\mu$ . The mean particle size of the zeolite is found  $10\mu$ .

Zeolite- pp films were obtained first by mixing  $45\mu$  sized zeolite and Petkim pp by extrusion. The zeolite content was intended to be 2 and 4 %. The extruded films were stretched in machine direction. Void formation similar to the voids shown in Figure 5.3 and suggested by Nakamura et al. (1993) occurred by stretching the films in machine direction. The extruded films have non-uniform thickness and have agglomerates of zeolites and tearings. The optic micrographs of these films can be seen in Figure 8.20.

As seen in Figure 8.20 voids were formed around the natural zeolite particles. Expansion of air from pores of zeolites during heating in extruder and entrapment of them on quenching is another reason for void formation in the films. As long as the films are stretched void formation occurs and voids are growing around the particles. When the zeolite particles were large tearing of the film occurred. If the natural zeolite particles were smaller no tearing would occur while stretching.

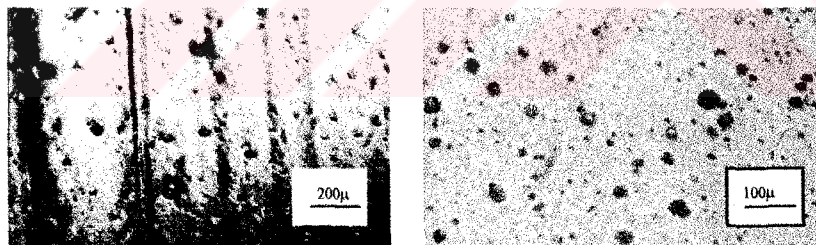


Figure 8.20: Reflected optical micrographs of extruded films with zeolite having size lower than  $45\mu$  a) 75 times magnified composite film b) 150 times magnified composite films.

$2\mu$  natural zeolite and polypropylene were also extruded. The films were non-homogenous, non-uniform thickness and agglomerations were observed, but no tearing occurred for 2 to 4 % zeolites. For 6 % zeolite the films were thorn during extrusion. Fibers of composites rather than films were obtained. The



transmitted and reflected optical micrographs of 6 % zeolite filled pp composites are seen in Figure 8.21 and 8.22 respectively.

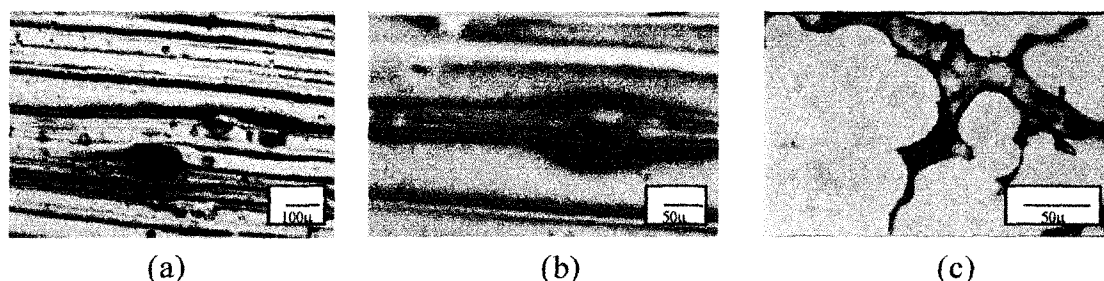


Figure 8.21: Transmitted optical micrograph of 2µ size 6 % zeolite filled polypropylene films a) 100 times magnified composite film b) 250 times magnified composite film c) 400 times magnified composite film.



Figure 8.22: 2µ size 6 % zeolite filled pp films 75 times magnified reflected optical micrograph.

As seen from Figure 8.21 (a) the spherical dark particles are zeolite particles. The brighter under the layer is pp. While the composite was stretched in machine direction the drawing direction could be seen as a layer. Figure 8.21 (b) was magnified 250 times and the drawing direction and air spaces around zeolite could be seen. In Figure 8.21 (c) the composite was magnified 400 times and zeolites could not be seen but the air bubbles are seen from the figure.

Figure 8.22 was taken by using a reflected optical micrograph. The sample was magnified 75 times and zeolite particles and three-dimensional pp layer in the direction of drawing unit could be seen.

### 8.2.3.1 Tensile tested extruded films

The optical micrographs of the tensile tested films can be seen in Figure 8.23. The films were elongated 3.37 times in stretching direction.

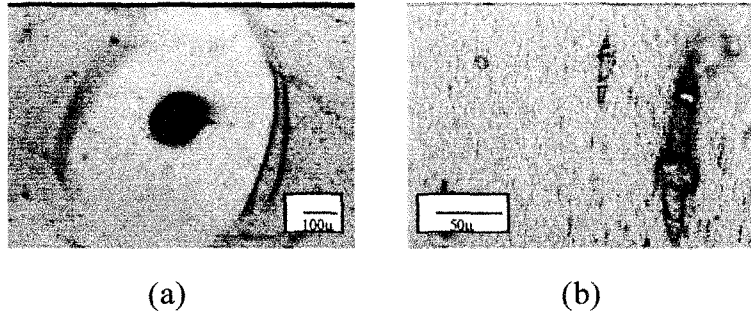


Figure 8.23: Tensile tested films a)100 times magnified b) 400 times magnified taken by using transmitted optical micrograph.

Extruded 4 % zeolite filled pp composite film were stretched in machine direction while the extrusion process was applied. Then the film stretched in transverse direction in tensile testing and the drawing size could be seen from Figure 8.23a. The zeolite particle is dark and in the middle of the cavitations and these are seen brighter than the zeolite. The brighter part represents air bubbles.

The optical micrographs of hot pressed films were taken by using transmitted optical micrograph and these are given in Figure 8.24.

As seen from Figure 8.24 the hot pressed films were magnified 100 times. Figure 8.24(a) shows for the Aldrich pp composite, there are some particles seen in the Figure. The range of particle size of pp 2.6-100 µ. Since the powder was not mixed in hot press during pressing at 200 °C, they were melted and fused to each other keeping their identity. Figure 8.24 (b), (c) and (d) shows zeolite filled pp composites; the dark objects are zeolites and the brighter are pp. As seen in Figure 8.24 the zeolite particles were agglomerated and did not disperse in the pp medium. Entrapped air with branched structure was also present in the films as seen in Figure 8.24 b, c, and d.

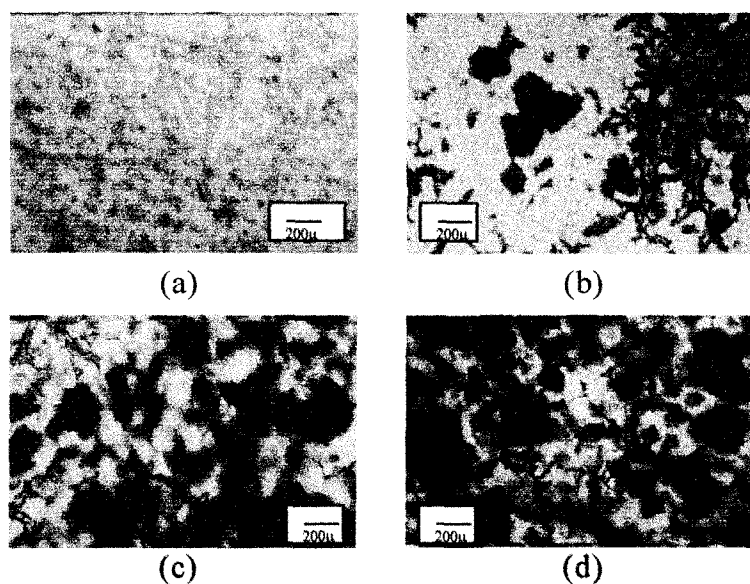


Figure 8.24: Transmitted optical micrograph of hot press films a) 100 times magnified hot pressed Aldrich pp b) 100 times magnified 10 % zeolite filled hot pressed composite c) 100 times magnified 20 % zeolite filled hot pressed composite d) 100 times magnified 40 % zeolite filled hot pressed composite.

### 8.3 Characterization of Polypropylene - Zeolite Composites by DSC

In this project, DSC was used to analyze the melting and crystallization behaviour of polypropylene and polypropylene-natural zeolite composites.

#### 8.3.1 Characterization of Polypropylene by DSC

Two types of polypropylene were used for composite preparation. They are Aldrich and Petkim polypropylene. The DSC curves of Petkim and Aldrich polypropylene are shown in Figure 8.25. The experiment was carried at a rate of  $10\text{ }^{\circ}\text{C} / \text{min}$  until  $300\text{ }^{\circ}\text{C}$ , under nitrogen inert gas flow with a rate of  $15\text{ ml/min}$ .

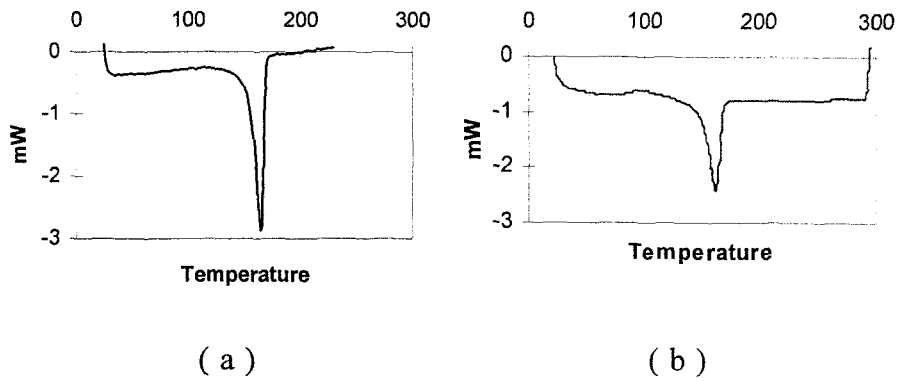


Figure 8.25: DSC curves of a- Aldrich polypropylene , b- Petkim polypropylene.

From the melting curves of Aldrich and Petkim polypropylene in Figure 8.25 the heat of fusion, was found as 71.5 kJ/kg, and 61.5 kJ/kg for Aldrich and Petkim polypropylene, respectively. The difference is observed because of the different crystallinities of the two polypropylenes. The % crystallinity changes with the rate of cooling of molten pp. The faster the pp is cooled, the lower the degree of crystallinity. Aldrich pp has higher heat of fusion, thus higher crystallinity than Petkim pp.

The heating rates, peak temperatures, and heat of fusion ( $\Delta H_f$ ) and % crystallinity values are given in Table 8.5.  $\Delta H_f$ , 209 kJ/kg for 100 % crystalline pp ( Horrocks and D'Souza 1991) is used to find the crystallinity of composites using Equation 8.4.

$$\% \text{ Crystallinity} = \frac{\text{Heat of fusion of sample}}{\text{Heat of fusion of 100 \% crystalline sample}} \quad 8.4$$

Table 8.5 : Different heating rate for Petkim polypropylene

Heating Rate °C / min	Peak Temperature °C	$\Delta H_f$ kJ/kg	% Crystallinity
5	161	54.58	0.26
10	162	61.52	0.29
20	161	52.71	0.25

From Table 8.5 for different heating rates the heat of melting values changed but the peak temperatures did not. As it was mentioned before in section 6.2.2 Kim et al.(1997) studied on the effect of melting thermograms of *i*-polypropylene and found that a new peak observed if the heating rate is lowered. In Petkim polypropylene the peak temperature did not change while the heating rate is changed. This means that the Petkim polypropylene is in a stable crystalline form. Heat of melting values are slightly different from each other. The crystallinity values does not change with heating rate. Degree of crystallinity of Petkim pp are within the range of 0.25 -0.29.

### 8.3.2 : Characterization of Composites by Using DSC

As explained before in section 7.6 three different composite preparation techniques were used. The films which were prepared between two microscope slides were analyzed in first sight. These composites were prepared by using Aldrich polypropylene. DSC curves of these are given in Figure 8.26.

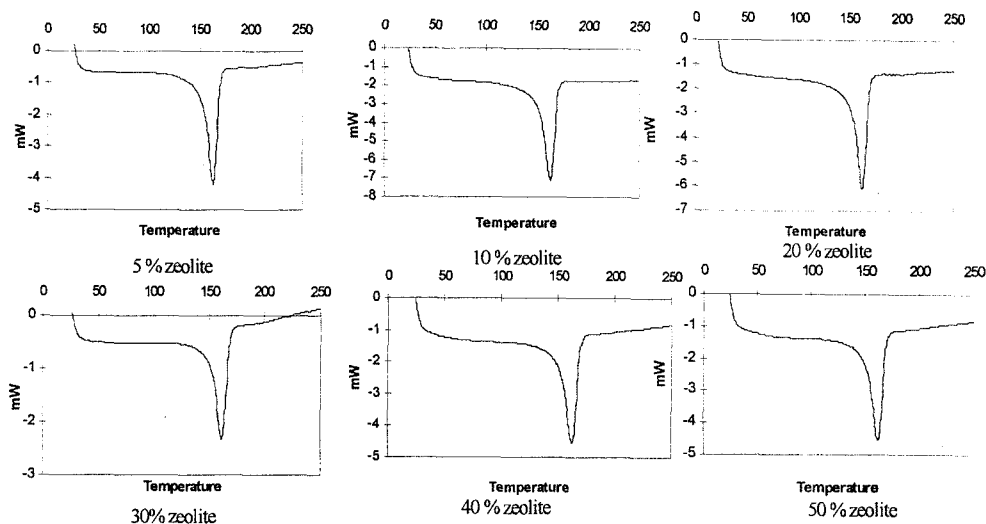


Figure 8.26 : DSC curves of microscope slide prepared composites

As seen from Figure 8.26 all samples melt about 160 °C. Information obtained from these curves are given in Table 8.6.

Table 8.6 : Gordes 1 filled polypropylene composites DSC analysis values.

Zeolite fraction	Peak temperature	$\Delta H_f$ (kJ/kg)	% Crystallinity
polypropylene film	163.8	71.5	0.34
5 %	162.7	99.3	0.47
10 %	163.7	98.7	0.47
20 %	162.7	83.0	0.39
30 %	161.6	50	0.24
40 %	163.8	64.6	0.31
50 %	162.2	67.9	0.32

As seen in Table 8.6 the peak values are not so different from each other it is about 162 °C but heat of melting found from the area of the peak is different from each sample. Aldrich pp film has lower crystallinity than composite with 5 %zeolite. This may be due to faster rate of cooling of pp film. Degree of crystallinity values are with in the range of 0.24 - 0.47. Heat of

melting versus zeolite fraction values gave a linear relation ship as shown in Figure 8.27.

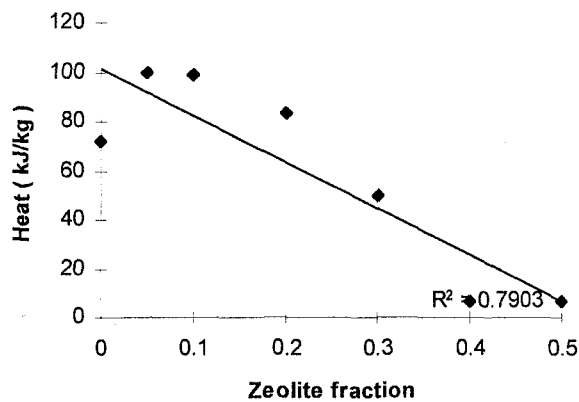


Figure 8.27: Composite films heat of melting versus zeolite fraction.

From Figure 8.27 the linearity of curve is not good. Regression coefficient is 0.7903. Some of the heat of melting values are different than predicted. The difference and nonlinearity comes from the non-homogeneity of zeolite particles in composites as mentioned before. From Table 8.6 and Figure 8.27 the heat of melting values are not expected values because films have different zeolite fractions and distribution of zeolite.

The other preparation technique was extrusion. In DSC only the 6 % zeolite filled extruded composite were characterized. The composite were heated 5, 10, 20 °C/min heating rates. The peak temperature, the heat of melting values were investigated. The DSC curve of 6 % zeolite filled Petkim pp at 5, 10, 20 °C/min heating rates from 25-300 °C under inert N<sub>2</sub> gas flow is shown in Figure 8.28.

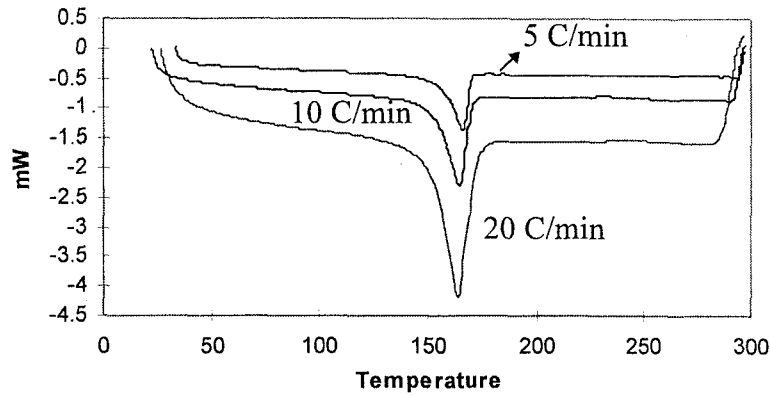


Figure 8.28: 6 % zeolite filled polypropylene DSC curve.

From Figure 8.31 the onset value of the curves is  $146^{\circ}\text{C}$  and the endset value is  $172^{\circ}\text{C}$ . These two values are same as for Aldrich and Petkim pp and other composites'; onset and endset values. The peak temperature is also the same  $162^{\circ}\text{C}$ . The heat of melting value is  $60.59\text{ kJ/kg}$ . The peak temperature and heat of melting values for  $5, 10, 20^{\circ}\text{C} / \text{min}$  heating rate are given in Table 8.7.

Table 8.7 :Different heating rate of DSC values for, 6 % zeolite filled extruded polypropylene.

Heating rate $^{\circ}\text{C}/\text{min}$	Peak Temperature $^{\circ}\text{C}$	$\Delta H_f$ $\text{kJ/kg}$	% Crystallinity
5	162	55.75	0.27
10	162	60.59	0.29
20	162	55.66	0.27

As seen in Table 8.7 the peak temperature for 6 % zeolite filled polypropylene did not change. The crystallinity degree does not change deeply by changing the heating rate.

Other prepared composites are hot press films with 10 % zeolite filled Aldrich polypropylene composites DSC curve is given in Figure 8.29. The experiment was carried under  $\text{N}_2$  inert gas and at a rate of  $10^{\circ}\text{C} / \text{min}$  until  $300^{\circ}\text{C}$ .



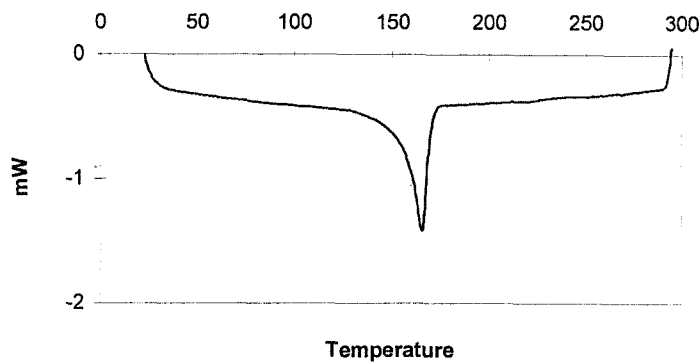


Figure 8.29: 10 % zeolite filled polypropylene films DSC curve

From Figure 8.29 the onset value is 122 and the endset value is 170 °C. The melting peak temperature is 164 °C and the heat of melting value is found 38.69 kJ/kg. Heat of melting values of extruded and microscope slide pressed films are different. The difference is observed because the sample which were analysed contain more zeolite than predicted. The hot press films examined at different heating rates at DSC; the peak temperature values and heat of melting values are given in Table 8.8.

Table 8.8 : Different heating rates for 10 % zeolite filled composites  
DSC values

Heating rate °C/min	Peak Temperature °C	Heat of melting kJ/kg	% Crystallinity
5	162	66.78	0.32
10	162	38.69	0.19
20	162	55.43	0.27

As seen in Table 8.8 the peak temperature values are the same like in all polypropylene composites. The same explanation for extruded polypropylene composite film could be made for hot press polypropylene composite.

In hot press method the films were prepared with 0, 6, 10, 20, 30, 40 % zeolite by weight. All of these samples were heated at 10 °C / min until 250 °C and cooled until 30 °C at a heating rate of 2 °C/min. The same heating - cooling order is repeated for a second time for each sample using Setaram DSC 92.

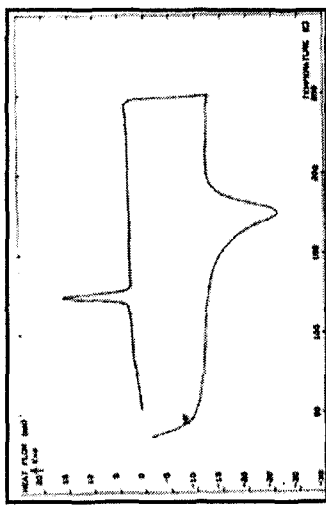
Figure 8.30 shows the hot pressed Aldrich pp, 10 %, 20 %, and 40 % zeolite filled composite melting and crystallization curves. These experiments were done to get the crystallization and melting information of composites given in Table 8.9 and 8.10.

As seen from Figure 8.30.a for Aldrich pp the composite melts at 168.2 °C and the heat of melting is 83.4 J/g. The crystallization temperature of pure pp is 117.1 °C and heat of crystallization is 79.7 J/g. For 10 % zeolite filled composite, the composite melts at 179 °C and the heat of melting is 75.9 J/g. The crystallization temperature of composite is 119.9 °C and heat of crystallization is 65.5 J/g. 20 % zeolite filled composite melts at 179 °C and the heat of melting is 74.2 J/g. The crystallization temperature of composite is 122.8 °C and heat of crystallization is 64.8 J/g. 30 % zeolite filled composite melts at 171.4 °C and the heat of melting is 69.9 J/g. The crystallization temperature of composite is 123.7 °C and heat of crystallization is 58.3 J/g.

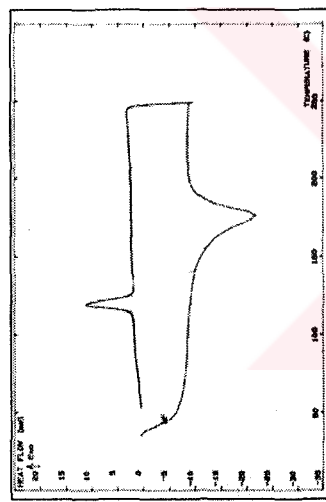
The 40 % zeolite filled composite melts at 171.4 °C and the heat of melting is 69.9 J/g. The crystallization temperature of composite is 123.7 °C and heat of crystallization is 58.3 J/g.

Table 8.9: 1<sup>st</sup> Melting and crystallization values of composites.

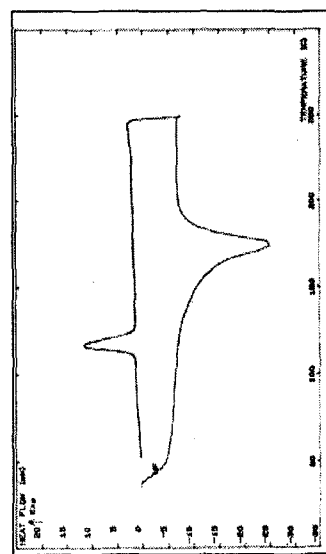
Zeolite Fraction	Melting T <sub>max</sub> °C	Crystallization T <sub>max</sub> °C	ΔH <sub>m</sub> J/g	ΔH <sub>cry</sub> J/g	% Crystallinity
Aldrich pp	172.5	113.6	59.39	84.5	0.40
0 % film	168.2	117.1	83.36	79.7	0.38
6 % film	174.2	122.7	79.19	72.9	0.34
10 % film	179.0	119.9	75.90	65.6	0.31
20 % film	179.0	122.8	74.25	64.8	0.31
30 % film	171.4	123.7	69.90	58.3	0.27
40 % film	174.7	124.4	68.77	59.1	0.28



c) 20 % zeolite



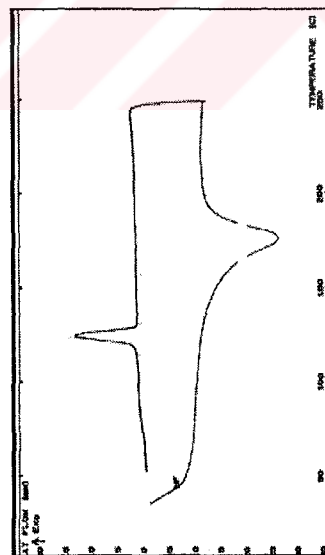
b) 10 % zeolite



a) Aldrich pp



e) 40 % zeolite



d) 30 % zeolite

Figure 8.30. Hot pressed films first heating and cooling curve

From Table 8.9 and 8.10 melting 1 value is for the first heating of material and melting 2 shows the second heating step values. The 1 and 2 values are different from each other especially the  $\Delta H$  values. The heat of fusion values for the first and second heating of composites reflects the state of crystallinity obtained in press and in DSC respectively.

As zeolite fraction increases, the polypropylene fraction decreases and if zeolite has no effect on crystallinity a linear decrease of heat of fusion is expected with increasing zeolite content. On the other hand, the zeolite may act as nucleating agent in crystallization of polypropylene and may lead high degree of crystallinity than pure polypropylene. The linear relation between heat of fusion and zeolite fraction seen in Figure 8.31 and 8.32 indicated zeolite had no effect on crystallization of pp.

Table 8.10: 2<sup>nd</sup> melting and crystallization values of composites

Zeolite Fraction	Melting $T_{max}$ °C	Crystallization $T_{max}$ °C	$\Delta H_m$ J/g	$\Delta H_{cry}$ J/g	% Crystallinity
Aldrich polypropylene	172	114.9	81.2	84.20	0.40
0 % film	173	117.4	79.6	79.47	0.38
6 % film	172.5	124.0	77.2	72.85	0.34
10 % film	173.6	120.5	73.4	67.00	0.32
20 % film	172.5	125.2	68.8	65.19	0.31
30 % film	175.2	124.6	61.9	58.67	0.28
40 % film	173.1	125.5	62.2	59.78	0.28

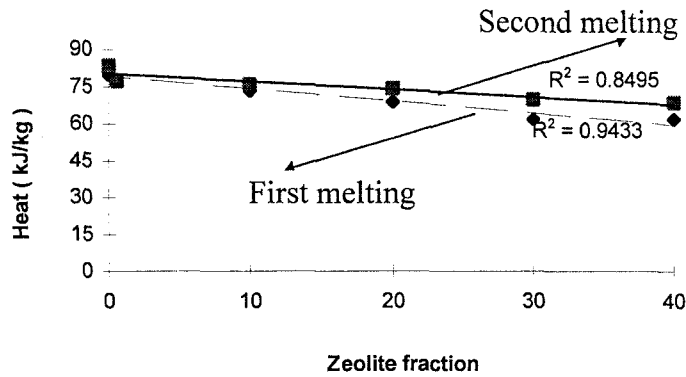


Figure 8.31: Hot pressed films heat of fusion versus zeolite fraction values

Figure 8.31 gives approximately a linear relationship because the linear regression coefficient of the line is 0.9. The linearity means the samples that were taken, contain the actual zeolite fraction and also the zeolites were good dispersed in the polypropylene medium. For 2<sup>nd</sup> heat of fusion values the same linear relation is also valid. The linear regression coefficient of the line in Figure 8.32 is 0.8.

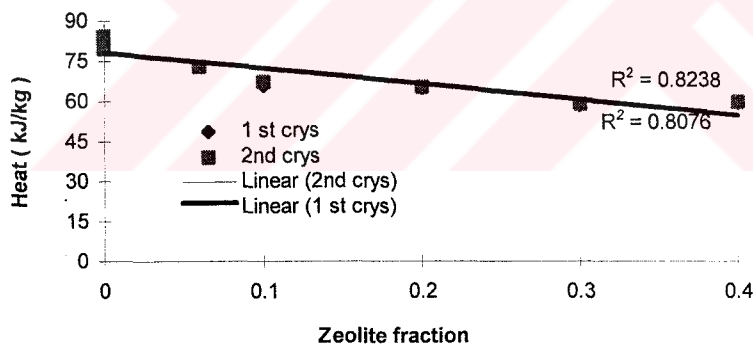


Figure 8.32: Heat of crystallization of hot pressed films versus zeolite fraction values.

Since, the same cooling program was used in first and second crystallization, pp was crystallized to the same extent. Thus the same degree of crystallinity were obtained when composites were cooled in the same manner. The film obtained in extruder by quenching lower crystallinities (27 - 29 %) were obtained than that of films prepared by pressing and air cooling (40 %) as expected.

For studying the crystallization behaviour of the composites Avrami plot was used. The Avrami Equation was given in section 6.2 as Equation 6.1. The Avrami plot for Aldrich pp and for composite with 20 % zeolite is given in Figure 8.33.

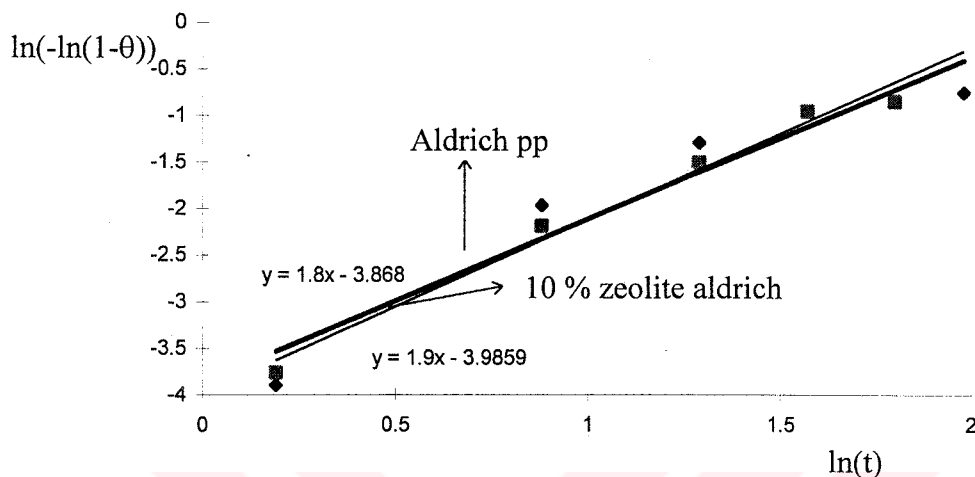


Figure 8.33: Avrami plot

The degree of crystallinity ( $\theta$ ) versus time of crystallization were computed using the crystallization peak of the films. Even if crystallization were not done at constant temperature, it occurred in a small temperature range of 120-110 °C. Thus the use of the Avrami equation valid at constant temperature was justified. In section 6.2.3 according to the Equation 6.2 the  $\ln(-\ln(1-\theta))$  versus  $\ln(t)$  graphs slope should give  $n$  ( crystallinity value ) and the intercept should give  $k$  ( rate of crystallization ). As seen from Figure 8.33 the  $n$  value as for hot pressed pp and 10 % zeolite filled pp were found 1.8 and 1.9 respectively. Since very close  $n$  values were obtained for pure and zeolite filled pp, zeolite did not effect appreciably the crystallization behaviour of pp.  $n$  values between for calcium carbonate (2.2) and for calcium stearate coated calcium carbonate filled (1.5) pp composites made by McGenity et al. (1982). The  $K$  values were found for pp and hot press composite 3.8 and 3.9 respectively.

## 8.4. Characterization of Polypropylene and Polypropylene-Zeolite Composites by TGA

In this study by using TGA of the polypropylene and natural zeolite-polypropylene composites weight losses by the increase of temperature were examined. Generally all samples were studied until 600 °C under 15 ml/min N<sub>2</sub> inert gas. The temperature of 600 °C is enough for polypropylene. Ulku et al. studied Gordes 1 zeolite used in composite preparation. In this project at 500 °C Gordes 1 zeolite kept in 75% relative humidity at 25 °C lost 11.2 % water.

### 8.4.1: Characterization of Polypropylene by TGA

In polypropylene characterization both Aldrich and Petkim polypropylene were used. Figure 8.34 shows the TGA curves for Aldrich and Petkim polypropylene.

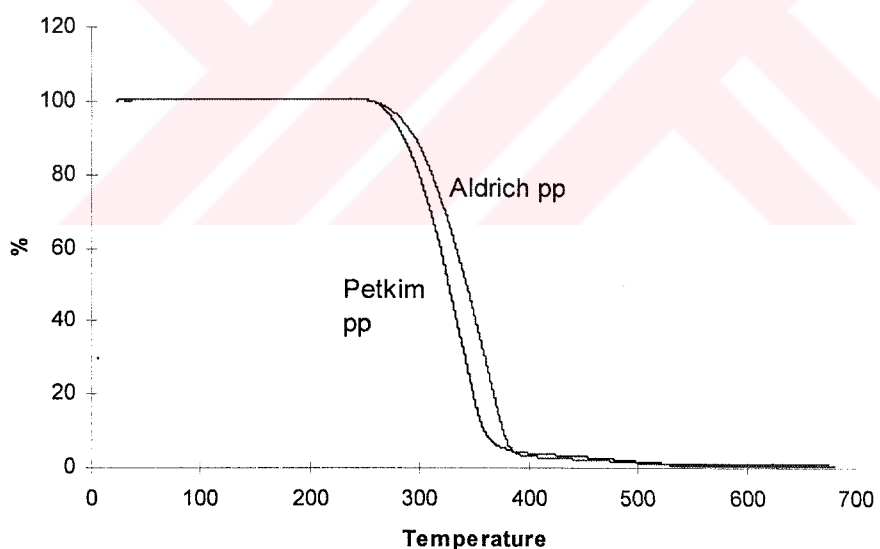


Figure 8.34: TGA curve for Petkim polypropylene and Aldrich polypropylene .

From Figure 8.34 for Petkim polypropylene the weight loss started at 220 °C and at about 390 °C 95.9 % polypropylene lost. TGA gives information

about degradation of polypropylene as explained in 6.2.3. Second and slow mass loss step was observed in the range 390-600 °C the material loss was 3.906 %. Totally mass loss for 600 °C was 99.8 %. For Aldrich polypropylene weight loss started at about 208 °C and 100 % weight loss occurred at about 500 °C in one step.

#### 8.4.2 Characterization of polypropylene - zeolite composites by TGA

Microscope slide pressed composites were examined in TGA. Zeolite filled composites ranged between 0 and 30 percent zeolite were analyzed. All of the composites show the same environment and start to degrade about 200 °C and degradation was completed about 550 °C. Depending on the zeolite content the percentage of weight loss was not 100 % as for polypropylene's. The remained mass percent at the end of degradation should be nearly equal to zeolite percent, since zeolite is not volatile. Temperatures of the starting and termination of the degradation, weight losses and percentage of the remained mass are given in Table 8.11.

Table 8.11: TGA values indicating weight loss, %, and temperatures of 0-30 % zeolite filled microscope slide pressed composite.

Zeolite fraction	Temperature °C		Weight loss %	Remained mass
	Starting of degradation	Termination of degradation		
0 % Aldrich pp	208	500	100	0
10 %	200	580	88.5	4.5
20 %	190	560	83.1	16.9
30 %	190	550	84.6	15.4

As seen in Table 8.11 the starting degradation temperature of all composite lower than that of polypropylene. The weight loss of Aldrich polypropylene is 100 % , that is all of the polypropylene is degraded by heating process. For zeolite filled composites it was expected that the zeolites would not



undergo to degradation and only the polypropylene would be degraded. Starting from this idea 10 %, 20 %, and 30 % zeolite filled polypropylene composite should loose weight 90 %, 80 %, and 70 % respectively. On the other hand for 10, 20, 30 % zeolite filled composite 88.5, 83, 84 % weight loss occurred. These values are different that expected weight loss values because the samples that were analyzed, were not in the desired zeolite percent due to uneven dispersion of zeolite in composites.

The other examined composites were extruded materials. These samples are heated until 1000 °C at a heating rate of 10 °C/min. Figure 8.35 gives the extruded composites TGA curves.

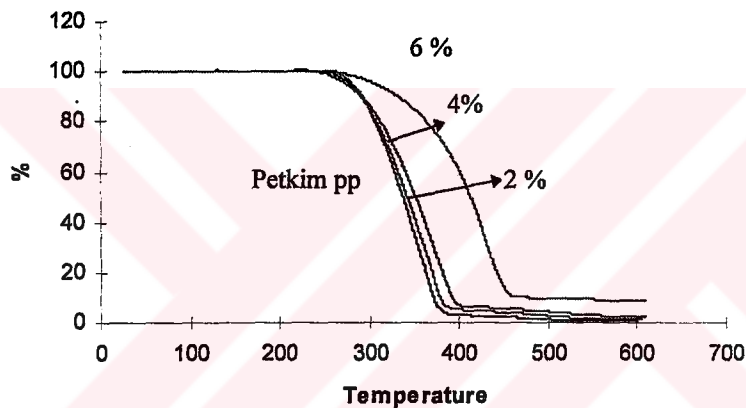


Figure 8.35: TGA curves of 2%, 4%, 6% zeolite filled polypropylene composites.

As seen from Figure 8.35 all samples starts degradation about 220 °C. Petkim polypropylene loose 100 % of the weight and 2, 4, and 6 % zeolite composite did not loose all of the weight, remaining weight should give the information about zeolite content in the composite. Table 8.12 gives the temperatures of the starting and termination of degradation, weight losses and percentage of the remained mass.

Table 8.12: TGA values indicating weight loss %, and temperatures of 0- 6 % zeolite filled microscope slide pressed composite.

Zeolite fraction	Temperature °C		Weight loss	Remained mass
	Starting of degradation	Termination of degradation		
0 % Petkim pp	220	550	100	0
2 %	230	575	99	1
4 %	230	575	98	2
6 %	240	575	91	9

From Table 8.12 Petkim polypropylene started degradation at 220 °C but the composites started 10-20 °C later. Termination of degradation for Petkim polypropylene is at 550 °C and for the zeolite filled composites were at 575 °C. The degradation temperature of composites shifts to higher values due to zeolite content in the composite. Remaining mass losses for composites for 2, 4, and 6 % zeolite filled composite are 1, 2, and 9 respectively. These values are not the desired values. The expected values for 2, 4, and 6 % should be the same as their values. The TGA results are different than expected values, this means uneven dispersion in the extruded films are observed in TGA results. Because of uneven dispersion the analyzed samples gives different results.

Aldrich polypropylene, Petkim polypropylene, 6 % zeolite filled extruded film, and 10 % zeolite filled hot pressed films were analyzed at different heating rates to obtain the effect of heating rate. Aldrich polypropylene TGA curves at different heating rates are given in Figure 8.36.

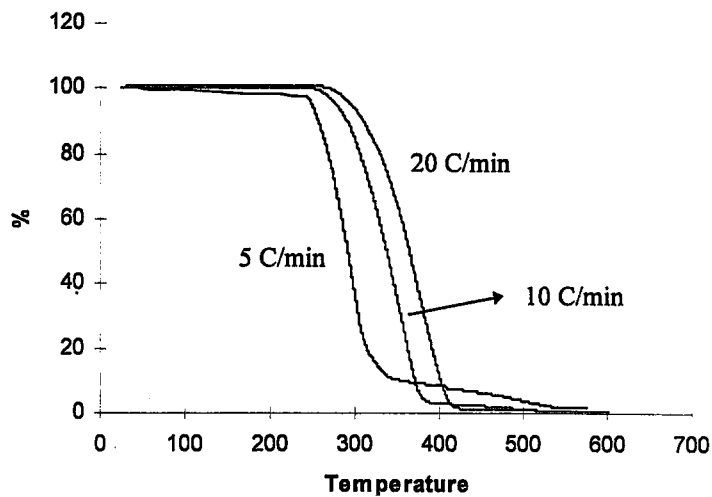


Figure 8.36: TGA analysis of Aldrich pp at different heating rates.

As seen from Figure 8.36 changing the heating rates effects the degradation temperature. Increasing the heating rate also increases the degradation temperature. The temperatures that degradation started for 5 °C/min, 10 °C/min, and 20 °C/min were found 220 °C, 240 °C and 260 °C respectively. Heating rate influences the termination of degradation temperature. As the heating rate increases the termination of degradation values decrease, such as at 5 °C/min, 10 °C/min, and 20 °C/min heating rates termination temperatures were 540 °C, 510 °C, and 420 °C respectively. At the end of 600 °C all of the sample were degraded.

In Figure 8.37 Petkim polypropylene TGA curves were given. As seen in Figure 8.37 for Petkim pp degradation starts at about 220 °C. At different heating rates the starting degradation temperature did not changed. The same explanation is true for the termination degradation temperature and it was 550 °C. From Figure 8.37 the sample which was heated at a rate of 10 °C/min did not exhibit the expected one. This curve must be between the curves for 5 and the 20 °C/min heated samples. The weight loss of the Petkim pp at the end of 600 °C was 100 %.

6% zeolite filled extruded film was heated at different heating rates and the curves are given in Figure 8.38.

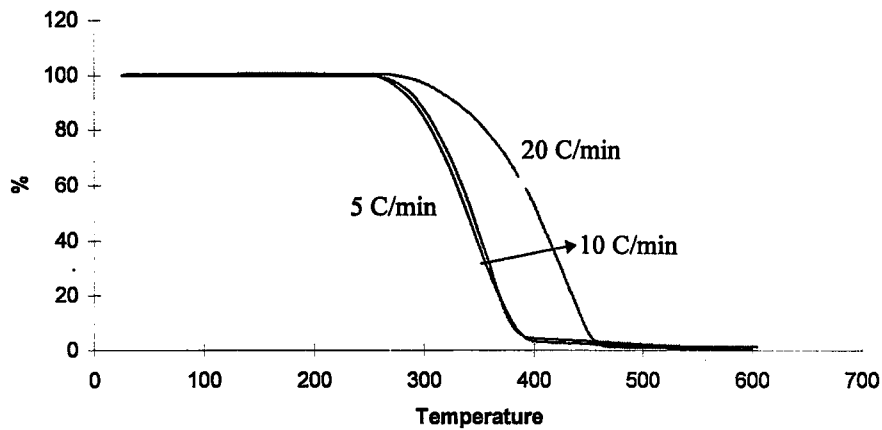


Figure 8.37: TGA analysis of Petkim pp at different heating rates.

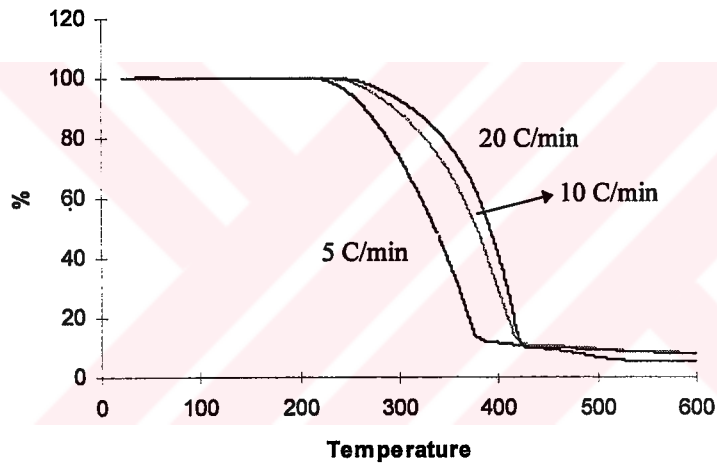


Figure 8.38: TGA analysis of 6 % zeolite filled, extruded polypropylene film at different heating rates.

From Figure 8.38 all samples were started degradation at about 220 °C at different heating rates. The termination of degradation value for 5 °C/min heating rate was 520 °C for 10 °C/min and 20 °C/min it was found 550 °C. This difference is because of at high heating rates the samples are exposed to high temperatures for shorter times.

10 % zeolite filled hot pressed film was heated at different heating rates and the curves are given in Figure 8.39.

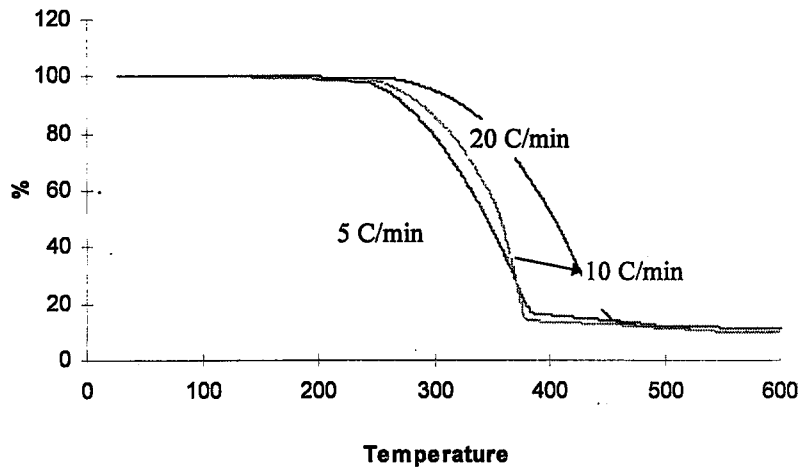


Figure 8.39: TGA analysis of 10 % zeolite filled, hot pressed composite at different heating rates.

As seen in Figure 8.39, for all heating rate the starting temperature did not change and it was found 220 °C. Termination of degradation temperature of composite was for 5, 10, 20 °C/min 550 °C. The 10 °C/min heated sample's TGA curve was not between the 5 and 20 °C/min heated samples TGA curve. This may due to uneven dispersion of zeolite in the samples used in TGA analysis.

#### 8.4.3 Kinetic Analysis of polypropylene and composites

Aldrich, Petkim pp and 6 % zeolite filled extruded pp and 10 % zeolite filled composites kinetic analysis were made by using TGA kinetic analysis software of Shimadzu 51 TGA. The kinetic analysis software can be described by Ozawa principle as explained before in section 6.3. Three different heating rates 5, 10, and 20 °C/min were used to analyze the materials. Figure 8.40 and Figure 8.41 give the Ozawa plots.

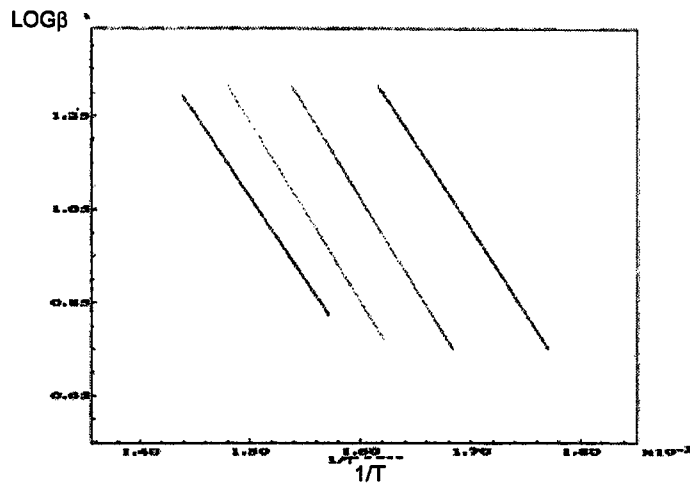


Figure 8.40: Ozawa plot of Petkim pp

The Ozawa plot, which is the logarithm of heating rate versus  $1/T$  at constant  $x$  values is seen for 20, 40, 60 and 80 % conversions in Figure 8.40. From the slopes of the lines activation energy,  $E$  is found for different weight losses and tabulated in Table 8.13.

Table 8.13: Activation energy at different weight loss values and average activation energy

Type of pp	Weight Loss				Average
	80	65	40-49	27-33	
Petkim pp	59.3	53.0	51.9	50.5	53.57
Aldrich pp	56.7	52.7	51.2	50.3	52.7
6 % extruded	42.9	45.2	49.8	55.5	48.3
10 % hot pressed	67.2	70.6	69.5	63.8	67.8

$C$  ( mass loss ) read from the graphs  $x$  is found from the Equation 6.4.b. giving  $L= 4.9$  and  $5.0$   $G(x)$  is found from Equation 6.5. Reduced time  $\theta$  is found from Equation 6.2. In Figure 8.41  $G(x)$  versus reduced time is plotted. The slope of the line gives  $A$  according to Equation 6.2.

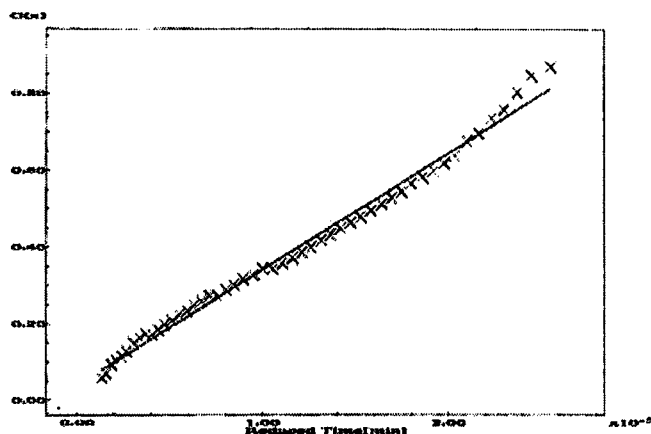
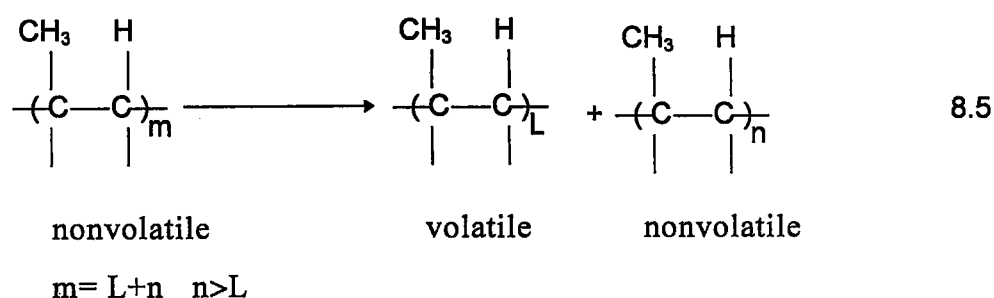


Figure 8.41: Frequency factor

For Petkim, Aldrich pp and 6 % zeolite filled extruded film, 10 % zeolite filled hot pressed films; the activation energy 'E', order 'L', frequency factor 'A', and reaction rate 'k' values at 250 °C were found from their Ozawa and frequency factor plots and are given in Table 8.14.

According to Ozawa principle volatilization is an important property, and order value 'L' gives information about volatilization of pp. Equation 8.5 shows degradation of pp by heat and the difference between volatile and nonvolatile materials.



If the degree of polymerization of degraded polymer is lower than a critical L value, it is volatile. For pp L is around 5. k is rate constant of the first order degradation reaction calculated at 250 °C from Arrhenius Equation 8.6.

$$k = A e^{-E/RT} \quad 8.6$$

Table 8.14: Kinetic analysis of materials

	E (kcal/mol)	n	A 1/min	$k \times 10^3$ 1/min
Petkim polypropylene	59.34	4.9	$2.39 \times 10^3$	3.4
Aldrich polypropylene	56.35	4.9	$3.57 \times 10^3$	8.4
6 % zeolite filled extruded film	42.90	5.0	$5.88 \times 10^2$	30
10 % zeolite filled hot presses film	67.18	5.0	$3.03 \times 10^2$	5.9

As seen from Table 8.14 for Petkim pp, and for 6 % zeolite filled extruded pp film the activation energy found as 59.34 and 42.90 kcal/mol respectively. The extruded films were prepared from Petkim pp and as seen from Table 8.14 the zeolite decreases the activation energy. For Aldrich pp and 10 % zeolite filled hot pressed film the kinetic energy was found as 56.35 and 67.18 kcal/mol respectively. Zeolite increases the activation energy of Aldrich pp.

Degree of polymerization of volatile polymer. L were nearly the same for pure pp (4.9) and zeolite added pp (5.0).

While zeolite accelerated the degradation of Petkim pp, it decelerated the degradation of Aldrich pp at 250 °C. Since the reaction rate constant at 250 °C was  $3.4 \times 10^{-3}$  and  $8.4 \times 10^{-3} \text{ min}^{-1}$  respectively for extruded Petkim pp and composite made of Petkim pp and 6 % zeolite. The reaction rate constant at 250 °C was  $3.0 \times 10^{-3}$  and  $5.9 \times 10^{-3} \text{ min}^{-1}$  respectively for Aldrich pp and composite from Aldrich pp and 10 % zeolite.



## 8.5 Density Measurements

Microporous polypropylene sheets have pores around the filler particles as mentioned before in section 5.1. The pores are lowering the density of the composites. The density of the polypropylene and zeolite is 0.89 and 1.8 respectively. The most important property of the pearlescent films is lowering the density by obtaining pores while stretching the films; this property causes to decrease the manufacture cost of the composites. The density was measured by using Sartorius YDK 01 balance as it was explained in 7.7.c. Extruded films were stretched in machine direction so only the densities of the extruded films with zeolites should be lower than that of the films without zeolite. The densities of the 45 $\mu$  and 2 $\mu$  zeolite filled polypropylene composites are as given in Table 8.15 and 8.16 respectively. For 45 $\mu$  zeolite filled composites with 2 % and 4 % zeolite, the samples were taken from the beginning and the end rolls of the films. The same method were applied for 2 $\mu$  zeolite filled composites having in 2, 4, and 6 % zeolite.

Table 8.15: 45 $\mu$  zeolite filled polypropylene films densities.

Zeolite fraction	Thickness ( mm )	Density ( g/cm <sup>3</sup> )
0 % ( polypropylene)	0.01	0.88
2 % ( beginning )	0.07	0.86
2 % ( end )	0.06	0.9
4 % ( beginning )	0.07	0.89
4 % ( end )	0.03	0.88

The density of polypropylene is 0.88 and the composites densities are about the same; namely the composite fraction value and stretching did not cause great differences in the density of 45  $\mu$  composites.

Table 8.16: 2 $\mu$  zeolite filled polypropylene films densities.

Zeolite fraction	Thickness ( mm )	Density ( g/cm <sup>3</sup> )
2 % ( beginning )	0.01	0.87
2 % ( middle )	0.02	0.82
2 % ( end )	0.04	0.77
4 % ( beginning )	0.05	0.73
4 % ( middle )	0.02	0.87
4 % ( end )	0.03	0.73
6 % ( beginning )	0.05	0.83
6 % ( middle )	0.03	0.78

From Table 8.16 the density values of composites are lower than the polypropylene's density. For 2% middle sample the density was found as 0.82 and for end sample it was found as 0.77. For 4% beginning and end samples the density was found as 0.73. For 6% end sample it was found as 0.78.

Table 8.15 and 8.16 show that the densities of 2 $\mu$  zeolite filled composites were lower than the density of 45  $\mu$  zeolite filled composites. But these values are not in the desired level. The desired level in the commercial meaning is 0.6 g/cm<sup>3</sup>. Generally in industry the composites are firstly mixed to prepare masterbatches. Masterbatch means polypropylene and the filler material mixed evenly in the desired filler fraction and pelletized in an extruder. Then the prepared masterbatch pellets are put into the film extruder. In these project the filler in powder form and polypropylene in pellet form were mixed and were put into the extruder. The zeolite particles were smaller and had higher density than the polypropylene particles so; in extrusion process first the zeolites are introduced into the extruder and composites mixed un-homogenously while extrusion process is continued. The composites could not be stretched in the machine direction because tearing was observed when the zeolite content was high and the air bubbles were not entrapped in the desired level. Thus the density of the composites was not find low desired.

Hot pressed composites theoretical densities were calculated from Equation 8.7. The experimental densities were measured, by using density kit of Sartorius YDK 01 balance and also from sample mass and volume. The experimental and theoretical densities are given in Table 8.17.

Table 8.17: Hot pressed composites theoretical and experimental densities

Zeolite Fraction	Thickness ( mm )	Density g/cm <sup>3</sup>			ε
		Theoretical Density	Experimental		
			Sartorius	Sample geometry	
0 %	0.56	0.89	1.0	0.90	-
6 %	0.39	0.95	1.08	0.98	-
10 %	0.71	0.98	0.96	0.93	0.05
20 %	0.60	1.1	1.04	0.97	0.11
30 %	0.63	1.2	1.02	1.03	0.15
40 %	0.83	1.3	1.09	1.01	0.16

$$d_c = \sum M_i / \sum (M_i/d_i) = (M_1+M_2)/(M_1/d_1+M_2/d_2) \quad 8.7$$

Where;

$d_c$ : Density of composite

M: Mass

d : Density

1 : Zeolite

2 : pp

Taking density of zeolite as 1.8 g/cm<sup>3</sup>.

From Table 8.17 the theoretical values are greater than the pure polypropylene's density. The experimental values are smaller than the theoretical's. Indicating the presence of voids in composites. Indeed, in Figure

8.24 the branched shaped air pockets are observed. The void volume of fractions composites are found from Equation 8.8 and are given in Table 8.17.

$$d_{c,e}=(1-\varepsilon)\times d_{c,t} \quad 8.8$$

Where;

e: experimental

t: theoretical

d: density

$\varepsilon$ : void volume fraction

In hot pressed films void volume fraction was maximum at 0.16.

### 8.6 Mechanical Behaviour of the Composites

Hot pressed and extruded pp composites mechanical tests were performed by using Testometric AX M 500. Instron 1000 ( Polinas ) were used for repeating only extruded films mechanical tests. The samples were shaped for Testometric AX M 5000 according to ASTM D-638 standard as seen in Figure 8.42 and for Instron 1000 ASTM D-882 standard as it was mentioned before in section 7.7.d.

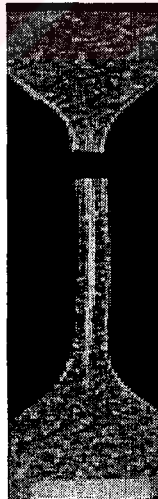


Figure 8.42: 10 % zeolite filled hot pressed sample shaped according to ASTM D-638 standards.

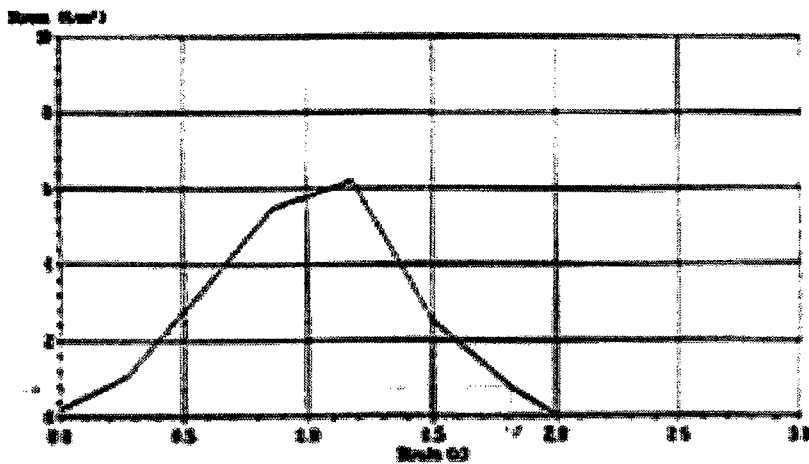
The hot pressed samples mechanical tests were performed and the mechanical behaviour of hot pressed composites are given in Table 8.18. The samples were prepared and tested three times and mean values of the tests were given in the same Table.

As seen in Table 8.18 for pure pp, which was prepared in hot press, the stress at peak value found 25.9 N/mm<sup>2</sup>. For composites the stress at peak value was decreasing by the increasing zeolite content. Strain at peak values showed also the same property. While the pure pp strain at peak is 4.7 %, the composites strain percentage at peak were decreasing by increasing zeolite fraction in the range 0.42-4.42. The stress at break and strain at break points from Table 8.17 were also decreasing with increasing zeolite fraction. In hot pressed films, for some of the films it was not possible to measure any strain and stress at break points, due to uneven zeolite dispersion in the films. Some of the samples were more brittle because of excessive zeolite content. In Testometric AX M 500 young modulus of the samples were calculated from the recorded data. Some of the samples strain - stress diagrams did not give necessary values to calculate the young modulus. Only Aldrich pp and 6 % zeolite filled composite's young modulus were calculated. These are found as 569 and 885 N/mm<sup>2</sup> respectively. The young modulus of 6 % zeolite filled composite was greater than that of pp's.

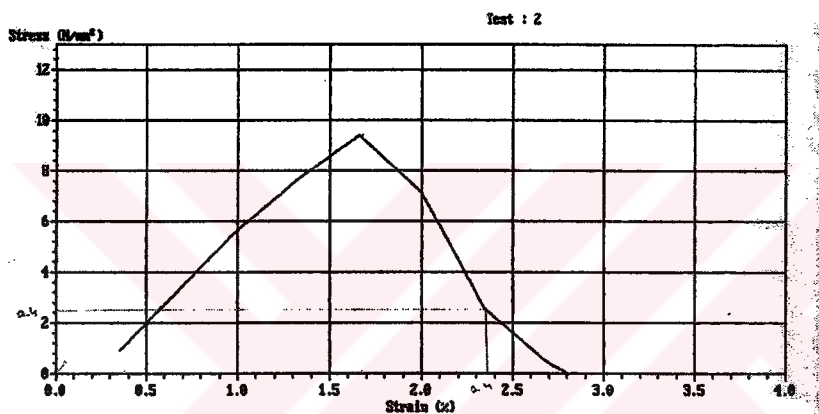
The strain - stress diagrams of hot pressed samples are given in Figure 8.43.

Table 8.18: Mechanical behaviour of hot pressed composites

Zeolite fraction	Stress at peak N/mm <sup>2</sup>		Strain at peak %		Stress at break N/mm <sup>2</sup>		Strain at break %		Young modulus Mean	
	Mean		Mean		Mean		Mean		Mean	
Pure pp	27.1		4.1		4.0		6.3		716.3	
		25.9		4.7		4.1		5.9		569.0
	24.9		5.3		4.2		5.4		421.8	
6%	20.6		2.4		4.1		3.6		-	
	19.2	20.7	2.5	2.5	1.2	3.2	3.8	3.6	837	885.8
	22.3		2.6		4.3		3.4		934.5	
10%	13.7		2.3		2.9		3.1		-	
	8.9	9.8	1.2	4.4	4.4	3.5	1.3	2.1		
	6.8		0.9		3.2		1.9			
20%	3.5		0.9		0.3		1.7		-	
	2.0	3.76	0.9	0.9	-	1.5	-	1.5		
	5.7		0.9		2.7		1.2			
30%	9.4		1.7		3.8		1.8		-	
	2.6	6.1	0.5	1.1	2.4	3.1	2.4	2.1		
	6.2		1.2		-		-			
40%	0.9		0.35		-		-		-	
	1.9	1.4	0.57	0.42	-	0.7	-	1.0		
	-		0.35		0.7		1.0			



(a)



(b)

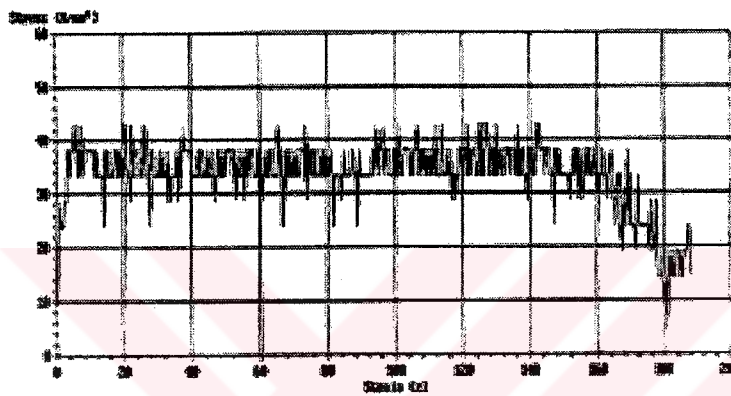
Figure 8.43: The stress strain curves of a)10 % b) 30 % zeolite filled hot pressed samples.

As seen from Figure 8.43 the stress - strain diagrams of the hot pressed samples have neither elastic nor plastic region. Stress and strain values at the break points was very small and the samples were broken easily when the tension was applied.

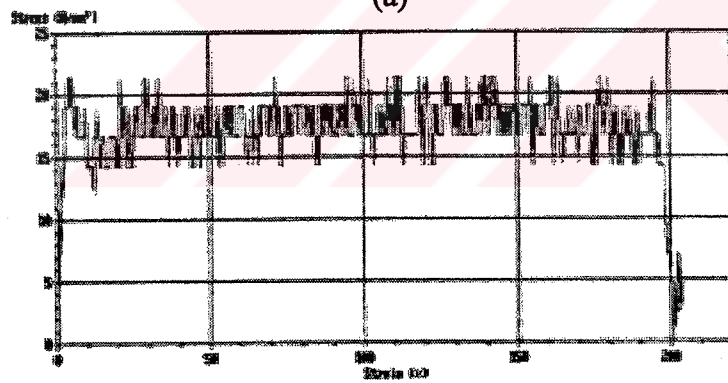
The optical micrographs of hot pressed films in Figure 8.24 showed the presence of branched shaped air pockets in composites indicating incomplete fusion of pp particles in filled films. Since it was not possible to evacuate the air emitted from the pores of zeolite particles in hot press, cohesion of pp the

particles did not occur properly. Thus unless an evacuated die is developed, it is not proper to use hot press for composite preparation.

Extruded films mechanical test were performed in Testometric AX M 500 and Instron 1000 mechanical testing device. The samples were shaped rectangular according to ASTM standart D-882. For the mechanical tests which were performed in Testometric AX M 500 stress- strain diagrams are given in Figure 8.44 and the values are given in Table 8.19. Measured values with the Instron 1000 mechanical testing device are given in Table 8.20.



(a)



(b)

Figure 8.44: Strain - stress diagram of a) Petkim pp b)2 % zeolite filled extruded films.

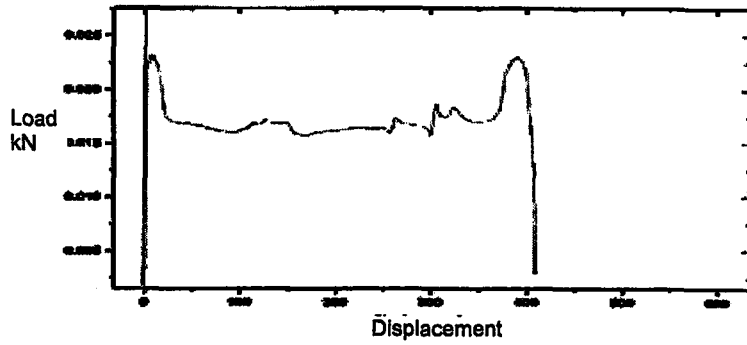


Table 8.19: Extruded films mechanical behaviour

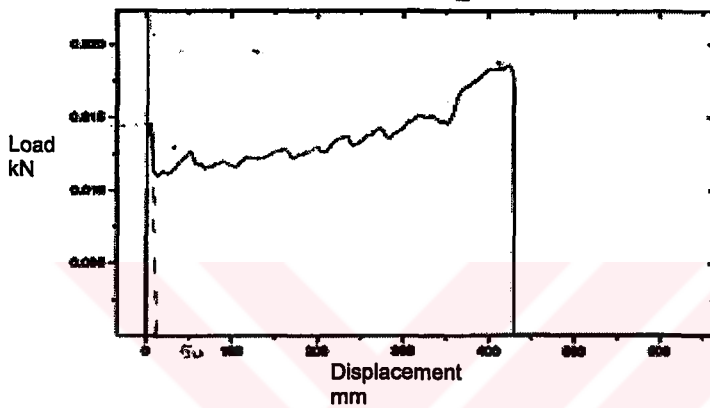
Zeolite Fraction	Stress at peak N/mm <sup>2</sup>		Strain at peak %		Stress at break N/mm <sup>2</sup>		Strain at break %		Young modulus	
	Mean		Mean		Mean		Mean		Mean	
Petkim	52.4		196.7		14.3		260		-	
pp	57.1	50.8	3.7	68.6	22.1	17.5	52	164	1117.1	806
	42.9		5.4		16		180		494.6	
2%	21.2		4.3		3.5		203.5		374.8	
	30.9	26.1	275.3	94.2	7.1	6.3	310	204.5	-	406.2
	26.2		3.0		8.2		100		437.5	
4%	21.4		290.0		2.9		320		-	
	25.7	27.6	3.85	159.1	8.5	7.1	95	205	493.3	493.3
	35.7		183.3		10		200		-	

As seen in Table 8.19 the pure pp' s stress at peak value find 50.8 N/mm<sup>2</sup>. Stress at peak values were decreasing by increasing zeolite content. The percent strain at peak value for pp is 68.6 and for increasing zeolite content the strain value is also increasing. This means that the increasing zeolite content increases elongation. For stress at break points the values were decreasing and for strain at break increasing while the zeolite content increases. The young modulus of the materials were found 805.9, 406.2, and 493.3 for pp, 2 % zeolite filled pp, and 4 % zeolite filled pp respectively. The young modulus of the samples decreases by increasing the zeolite fraction.

Tensile test diagram obtained in Polinas are shown in Figure 8.45.



(a)



(b)

Figure 8.45: Tensile testing of a) pure pp b) 4 % extruded pp films in Polinas

Table 8.20: Extruded films mechanical behaviour tested in Polinas.

Zeolite fraction	Stress at Peak $N/mm^2$	Strain at Peak %	Stress at Break $N/mm^2$	Strain at Break %	Young Modulus $N/mm^2$
Petkim pp	18.1	9.1	6.9	409	706.1
2 %	11.5	3.3	3.8	49.5	603.5
4 %	14.6	423.1	13.7	428.9	470.3

As seen in Table 8.20 the stress at peak values of Petkim pp is  $18.1 N/mm^2$  and the zeolite filled pp films stress at peak values were smaller than pp. The strain at peak values were changing disorderly this may be due to even

distribution of zeolites in the composite. The largest elongation is observed in 4 % zeolite filled composite. Stress at peak and strain at peak values were also changing disorderly and the same explanation because of uneven zeolite dispersion the values were disordered. Young modulus of the Petkim pp, 2 % zeolite filled pp, and 4 % zeolite filled pp were found 706.1, 603.5, and 470.3 respectively. The young modulus values were decreasing by increasing zeolite fraction. For prolongation of 4 % and 2 % zeolite filled films less tension is necessary for 4 % zeolite filled composite.

Extruded films mechanical test values which was tested in Testometric AX M 500 and in Instron 1000 model instruments were found different from each other as shown in Tables 8.19 and 8.20 and 8.21. The stress at peak, strain at peak and stress at break points were different from each other when measured in different instruments. The difference may observed due to the heterogenous structure of the films.

For extruded films theoretical young modulus and stress at peak values were calculated from Equation 6.6 and 6.7.

For extruded films theoretical young modulus and stress at peak values were calculated from Equations 6.6 and 6.7. The young modulus found 351.2 for 2 % zeolite filled pp composite. The calculated value is (684) higher than measured value (406). The stress at peak value from theoretical calculations found as 43.3 the measured value is (26.1) lower than theoretical value. For 4 % zeolite filled pp composite the predicted young modulus was found as 652.

The Equations 6.6 and 6.7 are valid when the filler and the matrix adhere to each other perfectly well. For the case of zeolite filled composites, microphotographs seen in Figure 8.24, indicated zeolite particles in spherical air bubbles in the pp matrix. Thus no adhesion between pp and zeolite exists.

For this case for  $V_f$ , volume fraction of voids ( $\epsilon$ ) should be taken. Volume fraction of voids is found from experimental densities of the films in Table 8.16, using Equations 8.6 and 8.7.

Table 8.21: Predicted and measured elastic modulus and strength of the composite

Zeolite fraction	$\epsilon$	Predicted $E_c$	Measured $E_c$		Predicted $\sigma_c$	Measured $\sigma_c$	
			Testometric AX C 500	Instron 1000		Testometric AX C 500	Instron 1000
2 %	0.13	686	406	603	43.3	26.1	11.5
4 %	0.18	652	493	470	41.14	27.6	14.6

The  $\epsilon$  values predicted and experimental  $E_c$  and  $\sigma_c$  for the composites are as reported in Table 8.21. Lower experimental  $E_c$  and  $\sigma_c$  values than predicted the presence of structural faults other than the void space created by zeolites.

### 8.7 Comparison of Commercial Pearlescent Films and Zeolite Filled Films

It was not possible to obtain biaxially oriented films in this study. The drawing in machine direction was possible but the temperature and drawing ratio was not controllable. The transverse direction drawing was done using tensile tester by cold drawing the extruded films test pieces.

The properties of the film given in Table 8.22 belong to extruded films.

Table 8.22: Comparison of commercial pearlescent films and filled films.

	Commercial	Zeolite filled film
Thickness, $\mu$	35-70	30-100
Filler type	CaCO <sub>3</sub>	Gordes 1 zeolite
Filler %	8	4
Colour	White yellow	Yellow
Appearance	Shiny	Shiny
Density, g/cm <sup>3</sup>	0.63	0.78
Tensile Strength, N/mm <sup>2</sup>	85 Machine direction 176 Transverse direction	26 Transverse direction

Further experiments for biaxial drawing under identical conditions with plant are required to obtain the pearlescent film from Gordes 1 zeolite and pp.



## Conclusions

The selection of suitable zeolite, modifier and preparation method of zeolite filled pp composites were made in this study. The effect of zeolite on thermal degradation behaviour in air and in N<sub>2</sub> atmosphere were studied. In air thermooxidative behaviour is observed in zeolite containing pp causing blackening of the films. Gördes 1 zeolite was chosen as the proper filler since, it did not cause oxidation of pp. In N<sub>2</sub> atmosphere Gördes 1 zeolite accelerated the degradation of Petkim pp and decelerated the degradation of Aldrich pp at 250 °C. At the processing temperature, 200 °C of pp no effect on degradation was observed with zeolite addition to pp.

The crystallization behaviour of pp did not changed with presence of zeolite. Very similar Avrami equation constants were found for pure and 10 % zeolite filled composite.

The composites were prepared by pressing between microscope slide, hot press and by extrusion. Branched shaped air pockets existed in hot press and by extrusion. Branched shaped air pockets existed in hot press films causing low mechanical strength. Zeolite particles in spherical air bubbles in pp matrix existed in extruded films with 2 to 6 % zeolite. The films which were elongated 3.37 times in tensile tester contained zeolite particles in rhombus shaped voids and they were pearlescent. The densities of the hot press and extruded films also indicating the presence of voids in composites. The voids formed by the release of air in pores of zeolite and splitting of pp phase at the periphery of the filler particles caused by stretching films in machine direction.

Even if the PEG (4000) modification were made agglomerations and uneven distribution of the zeolite particles were observed both in extruded and

hot pressed films. Uneven distribution of the zeolites were determined by DSC, FTIR and TGA and optical micrograph.

Gördes 1 zeolite is a promising material for pearlescent film preparation, since it did not effect chemical decomposition and crystallization behaviour of pp. The tensile strength 26-27 N/mm<sup>2</sup> of the films with 2-4 % zeolite was sufficient for most of applications of films. Void volume fraction of the films were in the range 0.13-0.18.

Adding a small amount of liquid plasticizer to obtain more even distribution of the filler in pp in extruder is suggested for future work. The wetted zeolite particles with plasticizers will stick to pp granules on mixing. Thus the mixture fed to the extruder will have the same composition at every point, and films will be obtained with even zeolite distribution. Water vapor adsorption characteristics of the composites should also be determined since zeolites have great affinity for water.

## References

1. Akdeniz Y., Characterization of Natural Zeolites and Structure Modification by Using Microwave, *MS thesis*, 1999.
2. Alanso M., Velasco J.I, Soja J.A.; Constrained Crystallization and Activity of Filler in Surface Modified Talc polypropylene Composites; *European Polymer Journal*, Vol.33, No 3, 1997, 255-262.
3. Bayer G., Hoffmann W., Siesler H. W., characterization of Deformation Phenomena in Polymers by rapid-scanning FTIR and mechanical measurements: 1 Orientation of i-polypropylene during uniaxial deformation, *Polymer*, Vol 21, February 1980, 235-239.
4. Brandrup J., Immergut E.H. *Polymer Handbook* Second Edition, 1976, Newyork.
5. Breck D.W., *Zeolite Molecular Sieves, Structure Chemistry and Use*, A Wiley Interscience Publication, 1974, Newyork.
6. Busfield W. K., Blake C. S., Low Temperature Annealing of i-Polypropylene by DSC, *Polymer*, Vol.21, January 1980, 37-40.
7. Cahn R.W., Hoasen P., Kramer E.J., *Material Science and Technology*, Edited Thomas E.L.; Vol. 12, 1993, Newyork.
8. Chu F., Kimura Y., Structure and Gas Permeability of Microporous Films Prepared by Biaxial Drawing of  $\beta$ -form Polypropylene, *Polymer*, Vol. 37, N.4, 1996, 573-579.
9. Countinho F.M.B., Costa T.H.S., Corvolho D.L., Polypropylene-Wood, Fiber Composites: Effect of Treatment and Mixing Conditions on Mechanical Properties, *Journal of Applied Polymer Science*, 65, 1997, Pq 1227-1235.
10. Crowford R.J., *Plastic Engineering*, Pergamon Press, 1981, page 69, Exeter Great Britain.
11. Denault J. and Vu-Khanh T., Role of Morphology and Coupling Agent in Fracture Performance of Glass - Filled Polypropylene, *Polymer composites*, October, Vol. 9, No. 5, 1988, 360-367.



12. Domka L., Modification at Kaolin, Chalk and Precipitated Calcium Carbonate as Plastomer and Elastomer Fillers, *Colloid and Polymer Science*, 272, 1994, 1190-1202.
13. Eder G., Non-Isothermal Crystallization, *Nato/ASI Advanced Study Institute*, May 1999, Portugal.
14. Fuad M.Y.A., Ismail Z., Ishak Z.A.M., Omar A.K.N.; Application of Rice Husk Ash as a Fillers in Polypropylene: Effect of Titanate, Zirconate, and Silane Coupling Agents, *European Polymer Journal*, Vol. 31, No:9; 1995; 885-893.
15. Fuentes G. R., Ruiz-Salvador A. R., Mir M., Picazo O., Quintana G., Deldago M., Thermal and cation influence on IR vibrations of modified natural clinoptilolite, *Microporous and Mesoporous Materials*, 20, 1998, 269-281.
16. Galeski A., Kryszewski M., and Kawolewski T., High Orientation of Toughened Chalk-Filled i-Polypropylene: Preparation and Properties; *Polymer Engineering and Science*, September, Vol.32, No.17, 1992, 1217-1227.
17. Gensler R., Plummer C., Kousch H.H., *Physical and Structural Phenomena Influencing the Long Term Stability of Polypropylene*, Laboratoire de polymeres, 1998, Ciba-Geigy Limited, Basle, Switzerland.
18. Ghosh K., Maiti S.N., Melt Rheological Properties of Silver Powder-Filled Polypropylene Composites, *Polymer-Plastic Technology Engineering*, Vol.35, No.5 ; 1997, 700-722.
19. Goryainov S. V., Stolpovskaya V. N., Likhacheva A. Y., Belitsky I. A., Fursenko B. A., Quantitative Determination of Clinoptilolite and Heulandite in Tuffaceous Deposits by Infrared Spectroscopy, *Natural Zeolites*, Ming D. W., Mumpton F. A., eds., 1995, 245-255.
20. Gottardi G., Galli E., *Natural Zeolites*, Brühlsche Universitätsdruckerei, 1985, Giesen.
21. Horrocks A. R., D'Souza J. A., Physicochemical Changes in Stabilized, Oriented Polypropylene Films during the Initial Stages of

- Thermal Oxidation, *Journal of Polymer Science*, Vol. 42, 1991, 243 - 261.
22. Jançar J., Dibenedetto A. T., Effect of Morphology on the Behaviour of Ternary Composites of Polypropylene with Organic Fillers and Elastomer Inclusion, *Journal of Material Science*, 30, 1995, 1601-1608.
  23. Kim Y. C., Ahn W., Kim C. Y., A Study on Multiple Melting of Isotactic Polypropylene, *Polymer Engineering and Science*, Vol. 37, No 6, June 1997, 1003-1011.
  24. Krivacsy Z., Hlavay J., A simple method for the determination of clinoptilolite in natural zeolite rocks, *Zeolites*, 15,1995, 551- 555.
  25. Leterrier Y., G'Sell C., Formation and Elimination of Voids During the Processing of Thermoplastic Matrix Composites, *Polymer Composites*, April, Vol. 15, No.2, 1994, 101-105
  26. Levita G., Marchetti A., Lazzeri A., Fracture of Ultrafine CaCO<sub>3</sub> / polypropylene composites, *Polymer Composites*, February Vol. 10, No. 1, 1989, 39-43.
  27. Lotz B., Withmann J.C., Lovinger A.J., Structure and Morphology of Polypropylene a Molecular Analysis, *Polymer*, Vol 37, N: 22, 1996, 4979 - 4992.
  28. Mascia L., *Thermoplastics (Material engineering)*, Second Edition, Elsevier Science Publishers, 1982, NewYork
  29. McGenity, Hooper J.J., Paynter C.D., Riley A.M., Nutbeem C., Elton N.J. and Adams J.M., Nucleation and Crystallization of pp by Mineral Fillers: Relation Ship to Impact Strength, *Polymer*, 1992,Volume 33, Number 24.
  30. Meares P., *Polymer Structure and Bulk Properties*, D. Van Nostrand Company Ltd.;1965, London.
  31. Mitsuishi K., Veno S., K. Sanji K., Kawasaki H., Crystallization Behaviour of Polypropylene Filled with Surface- Modified Calcium Carbonate, *Journal of Applied Polymer Science*, Vol. 43, 1991, 2043-2049.

32. Nago S., Mizutani Y., Microporous Sheets Containing Polymethylsilsesquioxane Filler, *Journal of Applied Polymer Science*, Vol. 50, 1993, 1815-1822.
33. Nago S., Mizutani Y., Preparation of Microporous Polypropylene Sheets Containing CaCO<sub>3</sub> Filler: Effect of Draft Ratio, *Journal of Applied Polymer Science*, Vol 61, 1996, 31-35.
34. Nago S., Nakamura S., Mizutani Y., Structura of Microporous Polypropylene Sheet Containing CaCO<sub>3</sub> Filler, *Journal of Applied Polymer Science*, Vol. 45, 1992, 1527-1535.
35. Nakamura S., Kaneko S., Mizutani Y., Microporous Polypropylene Sheets Containing CaCO<sub>3</sub> Filler, *Journal of Applied Polymer Science*, Vol.49, 1993, 143-150.
36. Nielsen L. E., *Mechanical Properties of Polymers and Composites*, 1974 , Marcel Deker Inc. , Newyork
37. Özkan F., Adsorbent yatakların dinamik davranışının incelenmesi ve doğal kaynakların adsorbent olarak değerlendirilmesi, *PhD thesis*, Izmir, 1996.
38. Özkan F. Ç., Ülkü S., Ambalaj sanayiinde nem tutucu olarak doğal zeolit ( klinoptilolit ) kullanılması, *Ambalaj Kongresi ve Yan Sanayii Kongresi ve Sergisi*, Izmir, 1997, 277-285.
39. Rayan A.J, Terrilli N.J., Patrick J., Fairclough A., A Scattering Study of Nucleation Phenomena in Homopolymer Melts, *Nato/ASI Advanced Study Institute*, May 1999, Portugal.
40. Reed J.S., *Principles of Ceramic Processing*, John wiley and sons, Inc., 2<sup>nd</sup> Edition, Canada, 1995.
41. Svehlva V., Poloucek E., Mechanical Properties of Talc-Filled pp, *Die Angewandte Makromolekulare Chemie*, 1994, 91-99.
42. Thermal Analysis Systems TA-50WSI TGA Kinetic Analysis Program (Ozawa Method ) *Instruction Manual*, Shimadzu, Japan.
43. Tjong S.C., Li R.K.Y., Cheung T., Mechanical Behaviour of CaCO<sub>3</sub> Particulate-Filled  $\beta$ -crystalline Phase Polypropylene Composites, *Polymer Engineering and Science*, January, Vol. 37, 1997, No. 1, 166-172.

44. Tsitsishuili G. V., Andronikashvili T.G., Kirov G. N., Filizova L. D., Natural zeolites, Ellis Harwood Limited, 1992, England.
45. Ulutan S. PhD thesis, PVC-Silika Kompozit Malzemelerinin Gelistirilmesi, Ege Universitesi, Bornova,1994.
46. Ülkü S., Balköse D., Ozmihci F., Akdeniz Y., and Negis F., Study of water vapour Adsorption to Sepiolite, Clinoptilolite and Tinkal Minerals, *MTA Symposium*, Izmir,1999.
47. Ülkü S., Natural Zeolites in Energy Storage and Heat Pumps, Studies in Surface Science, 2, Catalysis, Kodansia-Elsevier Pub., 28, 1047-1054.
48. Ülkü S., Özkan F., Water Vapor Adsorption on Local Clinoptilolite, *Zeolite 97*, 1997, Italy.
49. Vaillant D., Lacoste J., Lemaire J., Stabilization of i-Polypropylene Problems Bound to the Interactions of Stabilizers with Pigments and Fillers, *Journal of Applied Polymer Science*, Vol 65, 1997, 703- 722.
50. Wagner P. and Colton, On-line Consolidation Thermoplastics Towpreg Composites in Filament Winding, *Polymer Composites*, December, No.6, Vol. 15, 1994, 436-440.
51. Whaley P. D., Kulkarni S., Ehrlich P., Stein R. S., Winter H. H., Canner W. C., Beaucage G., Isotactic Polypropylene Foams Crystallized from Compressed Propane Solutions, *Journal of Polymer Science*, Part B, Polymer Physics. Vol. 36, 1988, 617-627.
52. Wool R. P., Boyd R. H., Molecular Deformation of Polypropylene, *Journal of Applied Physics*, 51, 10, October, 1980, 5116 - 5124.